

University of Montana

ScholarWorks at University of Montana

Graduate Student Theses, Dissertations, &
Professional Papers

Graduate School

2010

Using Airborne Laser Altimetry to Characterize Surface Fuels in Western Montana

Tim E. Wallace
The University of Montana

Follow this and additional works at: <https://scholarworks.umt.edu/etd>

Let us know how access to this document benefits you.

Recommended Citation

Wallace, Tim E., "Using Airborne Laser Altimetry to Characterize Surface Fuels in Western Montana" (2010). *Graduate Student Theses, Dissertations, & Professional Papers*. 1156.
<https://scholarworks.umt.edu/etd/1156>

This Thesis is brought to you for free and open access by the Graduate School at ScholarWorks at University of Montana. It has been accepted for inclusion in Graduate Student Theses, Dissertations, & Professional Papers by an authorized administrator of ScholarWorks at University of Montana. For more information, please contact scholarworks@mso.umt.edu.

USING AIRBORNE LASER ALTIMETRY TO CHARACTERIZE SURFACE FUELS

IN WESTERN MONTANA

By

Timothy Erin Wallace

Bachelor of Arts, Graceland College, Lamoni, Iowa, 1999

Thesis

presented in partial fulfillment of the requirements
for the degree of

Master of Science
in Forestry

The University of Montana
Missoula, MT

May 2010

Approved by:

Perry Brown, Associate Provost for Graduate Education
Graduate School

Dr. Carl A. Seielstad
Department of Forest Management

Dr. LLoyd P. Queen
Department of Forest Management

Dr. Charles Palmer
Department of Health and Human Performance

Using Airborne Laser Altimetry to Characterize Surface Fuels in Western Montana

Chairperson: Carl Seielstad

Abstract.

Quantifying surface fuels in forests is problematic for land managers due to the difficulty in measuring fuels of different sizes and spatial variability. Estimating fuel loads is important for identifying departures from historical fire regimes, predicting fire behavior and effects, and prioritizing parcels for fuels reduction. Current field methods of estimation are not always cost-effective nor can they be practical for full coverage at landscape scales. Several studies have examined remote sensing techniques for estimating fuel loads. One of the most promising is Light Detection and Ranging (LiDAR), which thus far has been applied primarily to forest canopies. Metrics derived from LiDAR include canopy base height, canopy bulk density, biomass, crown height, basal area, and tree stem location. This study focuses on the surface fuel bed, defined as the two meter stratum above ground. The relationships between LiDAR-derived surface roughness and fuels were explored in mixed-conifer forest using a relatively sparse LiDAR dataset (~ 1 point/m²). Surface roughness was imputed as the standard deviation of ground height distribution of laser pulse returns. Field data were derived from the nationally-scoped Fire-Fire Surrogate Study for 432 plots using two opposing azimuth Brown's transects at each sample point. Fuel loading and surface roughness were both highly variable at plot level across the study area.

Total biomass could be predicted at a nine ha resolution ($R^2 = 0.73$). Relationships for total biomass in the fuelbed, analyzed at 2.25 ha and 0.07 ha resolutions, showed less correlation ($R^2 = 0.56$ and 0.094 , respectively). Individual surface fuel components were analyzed for correlation with surface roughness. A combination of forest floor mass and 1-hour fuels produced the highest correlation ($R^2 = 0.86$). Additionally, LiDAR-derived data were used to derive fire behavior fuel models. Fuel models were classified by decision tree, CART analysis, and unsupervised classification using LiDAR-derived inputs. Results were validated using 101 gridded forest inventory plots. While LiDAR consistently characterized the plots at fine scale, the subjective nature of fuel model designation made statistical validation difficult.

Dedication, Vita, Acknowledgements

First and foremost, I would like to thank my advisor, Dr. Carl Seielstad for continued support and guidance through this project. I would like to thank my committee, Dr. Carl Seielstad, Dr. LLOYD Queen, and Dr. Charles Palmer as committee members but more importantly as fellow firefighters and as fellow scientists. A Master's of Science in Forestry would not be a possibility for me without the encouragement and support of these individuals. I want to thank Eric Rowell, Dr. Agus Suratno, Dr. Jim Riddering, and Dr. Matt Jolly for technical help and discussions about advanced science that furthered my understanding of science's role in my chosen field. I also would like to acknowledge the efforts of Edmund Ward, Mike Fritsen, and John Kovalicky for working with me to promote higher standards within the smokejumper program and within the Forest Service. On a personal note, I want to thank Ann Hadlow for her consistent support and accommodation throughout this project, science is for nought if there's no home to return to. Lastly, I owe a great deal of gratitude to the University of Montana's National Center for Landscape Fire Analysis for investing resources and time into me with the hope that it would pay dividends in the future, 'For the Greater Good...'

Table of Contents

CHAPTER 1. INTRODUCTION	1
1.1 Importance of Quantifying Fuels for Fire Management	3
1.2 Resulting challenges for fire managers	4
CHAPTER 2. BACKGROUND	5
2.1 Introduction	5
2.3 Fire regimes	7
2.4 Effects of fire suppression on fuels and fire management	8
2.5 Describing Individual Fuel Components in the Fire Environment	9
2.5.1 Surface fuels and ground fuels	9
2.5.2 Aerial/Crown fuels	12
2.5.3 Quantifying Fuels	12
2.6 Methods for estimating fuel loads	13
2.6.1 Fixed Plot Method	13
2.6.2 Planar Intercept Method	13
2.6.3 Fuel Load Method (Lutes)	13
2.6.4 Photo Series Methods	14
2.7 Fuel Models	14
2.7.1 Classic 13	15
2.7.2 NFDRS (20)	15
2.7.3 New Classics (40)	15
2.7.4 Fuel Characteristic Classification System	16
2.8 Mapping of fuels	16
2.8.1 Field and passive forms of remote sensing	16
2.8.2 Active Forms of Remote Sensing	17
2.8.3 Why LiDAR presents a different option	17
2.8.4 Laser Altimetry and forestry applications	19
2.8.5 Shortcomings of LiDAR	19
CHAPTER 3. METHODS	21
3.1 Introduction	21
3.2 Study Area	21
3.3 Field Data and Resource Inventory Plots at Lubrecht	22
3.3.1 Field Data of the Fire/Fire Surrogate Study	22

3.3.2 Resource Inventory Plots	24
3.4 Acquisition	24
3.5 Data Pre-processing	25
3.5.1 TerraScan Surface Model	26
3.5.2 Validation	27
3.5.3 Error Points	27
3.5.4 Mosaicking and Generating Canopy Height (CH)	27
3.5.5 Generating Surface Roughness	28
3.6 Data Analysis	28
3.6.1 Analysis of Surface Roughness on FFS	28
3.6.2 Mapping Roughness for Fuels	30
3.7 Total Biomass and a Fuels Map	31
3.8 Classification of Fuel Models	32
CHAPTER 4. RESULTS	35
4.1 FFS Roughness Analysis	35
4.2 LiDAR-derived Surface Roughness Values	42
4.3 Fuel Model Classification	46
4.3.1 RIP Photo Series classification	46
4.3.2 Landfire as an independent fuels assessment	48
4.3.3 Decision Tree	51
4.3.4 Decision Tree and LANDFIRE comparison	51
4.3.5 CART Analysis	52
4.3.6 Unsupervised Classification	55
4.4 Classification method summaries	59
4.4.1 Fuel model prediction methods and RIP Photo Series	59
4.4.2 Fuel model prediction methods and LANDFIRE	60
CHAPTER 5. DISCUSSION	62
5.1 Data/Acquisition	62
5.1.1 Integrity of BE/CAN Classification	62
5.1.2 Transformations Applied to Data	63
5.2 Surface Roughness	63
5.2.1 Fuel Bed Parameters	64
5.2.2 Other Causes of Roughness	65
5.2.3 Variability of Surface Roughness	68
5.2.4 Sidelap/ Data Density Biases	68

5.2.5 Mosaicking	69
5.2.6 Validation of Roughness Map	70
5.3 FFS Plot Data	71
5.3.1 Brown's Transects	72
5.3.2 Positional Accuracy and Precision	73
5.3.3 General Sparse Nature of Fuels at Lubrecht	73
5.4 Regression Analyses	74
5.4.1 Linear Regression	75
5.4.2 Appropriate Scale	75
5.4.3 Stepwise Regression	75
5.4.4 Contributions from Fuel Types	76
5.5 Biomass Map	78
5.5.1 Scale	79
5.5.2 Validity	80
5.6 Fuel Models	80
5.6.1 RIP Plots	80
5.6.2 Problems with Human Subjectivity When Classifying from Photos	80
5.6.3 Decision Tree Approach	81
5.6.4 Issues with Decision Tree	84
5.6.5 CART Analyses	85
5.6.6 Unsupervised Classification	86
5.7 Project Summary	87
CHAPTER 6. BIBLIOGRAPHY	90

List of Tables and Figures

Table 1. Linear regression of CWD Sound and Rotten vs roughness (9 ha scale).....	35
Table 2. Pearson correlation and significance between individual fuel components.	36
Table 3. Stepwise regression (roughness – fuels) results at three scales.	37
Table 4. Regression Analysis for Aggregated Fuels Estimates vs. Roughness.....	41
Table 5. LANDFIRE confusion matrix of four fuel models using RIP photo classification...	48
Table 6. Confusion Matrix of Decision Tree vs. RIP Photo Series.	51
Table 7. Cross-reference of LANDFIRE and Decision Tree Output.....	52
Table 8. Confusion Matrix of RandomForest Analysis on RIP Photo Series using percentage splits. Correctly identified classes marked in Red.	53
Table 9. Confusion Matrix of RandomForest Analysis on RIP Photo Series using 10-fold cross-validation. Correctly identified classes marked in Red.....	53
Table 10. Confusion Matrix of RandomForest Analysis on LANDFIRE using 10-fold cross-validation. Correctly identified classes marked in red.....	54
Table 11. Confusion matrix of RandomForest Analysis on LANDFIRE using percentage splits. Correctly identified classes marked in red.	55
Table 12. Confusion matrix of LANDFIRE vs. Unsupervised classification.....	59
Table 13. Summary of Decision Tree, CART, Unsupervised Classification, and LANDFIRE methods used to classify RIP Photo Series.....	60
Table 14. Summary Table of Decision Tree, CART, and Unsupervised Classification methods used to classify LANDFIRE.....	61
Figure 1. NFDRS 1978 change in relative moisture of various sizes of dead fuels over time (h) (Bradshaw et al., 1984).	11
Figure 2. Scan map with tile scheme overlaid for Lubrecht Experimental Forest.	25
Figure 3. Linear regression plot of the highest correlation between fuel components and surface roughness.....	39
Figure 4. Color coded regression showing different treatment structures and loads with corresponding roughness values.	39
Figure 5. Linear regression of Biomass vs. Roughness at 150m X 150m scale (n= 48).	40
Figure 6. Linear regression analysis of roughness vs. plot level fuels data. Plot is heavily heteroskedastic, indicating high variance of fuels and roughness.	40
Figure 7. Surface roughness for 2006 acquisition at 1 meter cell size. Blue to red gradient with low roughness as blue, high roughness as red.	43
Figure 8. Histogram of Surface Roughness for the Lubrecht Acquisition.	44
Figure 9. Total fuel bed biomass estimates for 2006 acquisition at 300m cell size	45
Figure 10. Representative fractions of fuel models in Lubrecht Experimental Forest for Resource Inventory Plots and Landfire classifications.....	47
Figure 11. LANDFIRE coverage of Lubrecht showing six fuel models at 30 meter cell size. Open areas were classified as non-forested areas.....	49
Figure 12. Decision Tree output showing four fuel models within the Lubrecht Experimental Forest at 10 meter cell size.....	50
Figure 13. Unsupervised classification of five LiDAR-derived layers resulting in six fuel model classes.	56
Figure 14. Fractional percentages of fuel models for Lubrecht using Unsupervised Classification.....	58

Figure 15. Digital photo of RIP plot 81, identified by the Unsupervised Classification as FM10.....	66
Figure 16. Block 3 of the FFS study site showing roughness raster. Areas of high roughness are coded red with areas of low roughness blue	69
Figure 17. Color coded linear regression of mean surface roughness vs. mean biomass at 9 ha resolution.....	70
Figure 18. Showing roughness (top), CIR imagery(middle), and overlay (bottom) where roughness identified individual downed tree boles.....	72
Figure 19. Percentages of single fuel components' contribution to Total Biomass estimate at 300m X 300m scale.	77
Figure 20. Surface roughness of 2005-2006 Lubrecht LiDAR acquisition.	78
Figure 21. Predicted fuel loads (Mg) for Lubrecht at 300m cell size.....	79

CHAPTER 1. INTRODUCTION

Fuels are an ever-present facet of land management in a range of disciplines—from fire suppression to wildlife habitat, from restoration treatments to watershed hydrology. Wherever vegetation can gain a foothold, the detritus of previous generations of species continuously accumulate as part of ecosystem dynamics. This accumulation has been kept in check by a series of natural disturbance cycles that promote a balance between species-specific adaptations and succession regimes to provide biodiversity at many scales (Arno et al., 1995). The encroachment of civilization into forested and range landscapes and the boon of natural resources these landscapes represent has sired many different management aims than the natural ecosystem mechanics produce. In the West, the disturbance most threatening to public safety, human-made infrastructure, and potential resources is wildfire. Damage assessments of wildfires inherently include acres burned, structures lost, and at their worst, casualties of fire events. The past 100 years have seen fire control efforts and management strategies evolve through lessons learned. Management has drawn upon scientific research and field observations to provide the necessary information needed for long-term planning and decisions that address the problems at hand.

Changing weather patterns (Westerling et al., 2006), fuels accumulation (Reinhardt et al., 2008), and an expanding wildland urban interface (WUI) (Cohen, 2008) have been accounted as factors for increased fire damage which puts greater pressure on land agencies to mitigate hazards, protect assets, and provide for public safety (Kimbell et al., 2008). Fire behavior is attributable to three main factors; fuels, weather, and topography. To effectively address fire behavior, managers must be able to manipulate fuels around uncontrollable but predictable weather conditions. Fuel conditions that are outside a normal local range may be designated as hazardous fuels due to potential fire behavior and top the priority list for treatment actions.

In order to make well-informed and effective decisions about land holdings, a vast amount of data is required. Planning documentation for proposed actions such as the National Environmental Policy Act (NEPA) environmental assessments (EA) or environmental impact studies (EIS) require hours of research and writing, planning, and hard evidence to complete. The intensive effort required to accomplish hazardous fuels reduction goals can be daunting. Fire and fuels management officers (FMO) and their assistants are mandated (USDA Forest Service, 2009) in their job descriptions to:

Plan, coordinate, and direct a complex fire management program on a forest area that poses diverse, unusual, or conflicting problems, such as planning for critical fuel treatment programs that have a wide variety of natural and activity-generated fuel types found over steep, broken terrain in areas of high public interest.

With this in mind, prioritizing specific tracts within thousands if not millions of acres requires complex data and geographic information systems (GIS) to assemble all pertinent data into a meaningful depiction of conditions on the ground. At present, consistent fuels data are available as layers from the LANDFIRE project, that cover the majority of the US at a 30 meter resolution (Schmidt et al., 2002). The LANDFIRE project is a comprehensive coverage dataset addressing the ecological departures from historical conditions of vegetation, fuels, and fire regime layers (Rollins, 2009). These layers function best at small-scale but can prove inconclusive at the stand level, where treatments and actions are applied. Consequently, there is considerable room for improvement of fuels layers at project scales. Although many quantitative analyses are available as large-scale samples for limited parcels, they continue to incur intensive time and money investments for anything above localized field collections. An ideal fuels layer would have full coverage of high resolution data that depict metrics taken from direct measurements of landscape elements.

This study assesses airborne laser altimetry to estimate surface fuel loadings in mixed-conifer forests of western Montana and to project that relationship across a landscape to produce a spatially explicit, consistent fuels map. Surface roughness is used in an attempt to quantify fuel loads, and different classification methods are explored to try to characterize the landscape according to fuel model precedents. Laser altimetry is considered as a potential solution to the problems inherent to measuring, inventorying, and managing fuels.

The relationship between surface roughness and fuels was first explored by Seielstad and Queen (2003) in closed canopy forests of west-central Montana. They found that it was possible to differentiate between Fuel Model 8 and 10 (Albini, 1976) using several different surface roughness metrics including obstacle density (OD) and standard deviation of the ground height distribution (GHD). The fuel component with the greatest impact in this relationship was determined to be coarse woody debris (CWD). It was hypothesized that in closed canopy forests, CWD is the dominant patent reflective surface underneath a dense overstory. It was also suggested that a relationship between roughness and fuel loads might

be established in more diverse fuel complexes (Seielstad and Queen, 2003). These results and assertions were developed in monoculture stands of lodgepole pine (*Pinus contorta*) with definitive differences between FM8 and FM10 fuel types. The statistical reliability and accuracy were very high using OD to characterize the fuelbed in closed-canopy monoculture stands. Therefore, it seemed logical that a similar relationship might hold within closed canopy, mixed-conifer stands with varying fuel models and fuel loadings more typical of lower elevation mixed-conifer forest types.

The research presented in this thesis, then, is based on an airborne laser altimetry dataset acquired in 2005/2006 for The University of Montana's Lubrecht Experimental Forest. The University of Montana's National Center for Landscape Fire Analysis (NCLFA) contracted Horizons Inc., a photogrammetry and remote sensing firm, to acquire the data. Lubrecht was an ideal study site for further fuels research using LiDAR due to its species and structure diversity as well as having a wealth of existing data. The Lubrecht acquisition presented an opportunity for a sensitivity analysis of the relationship between fuels and surface roughness and allowed for further exploration of surface roughness methods and fuel model classifications.

1.1 Importance of Quantifying Fuels for Fire Management

The importance of fuels in an ecosystem cannot be overstated. The accumulation of fuels beyond their historical loads presents future issues with fire management that compound with time. Addressing fuels is not only an issue of scale and time but subjective calls of severity and complexity. Each fire season demands that some type of action in the field be taken, whether mechanical treatments, harvests, or prescribed burns are applied to the landscape. Disturbances will always return to an area and the risk currently being run by the agencies is that wildfire will occur before accumulated fuels can be dealt with. A successful strategy is one where management can seize the initiative and act on the best possible terms rather than having wildfire make the decision for them.

The influx of civilization into forested lands adds a heightened sense of urgency to the problem. Policy and management actions can be derailed when one has to take personal property into account. This grey area between privately owned properties and publicly managed lands is called the Wildland Urban Interface (WUI) and is perhaps the most pressing interaction between humans and the fire environment. About 60% of new homes in

the 1990's, over 8.4 million, were built within the WUI (Harbour, 2008). That trend continues as figures are projected into the future. With these homes comes the infrastructure to support them and an ever-increasing human presence within areas that will burn. This complicates matters as the public puts increasing pressure on the agencies to suppress fires. Fire and Aviation Director for the Forest Service, Tom Harbour states, "Until fuel loads on landscapes are reduced to a level that can safely accommodate some natural wildfire, any cooperative wildland fire framework will remain reactive and potentially ineffective" (Harbour, 2008). To be pro-active, hazardous fuels reduction projects must be undertaken during the off-seasons. Where prescribed fires can be used in remote areas to reduce fuels, the risk associated with losing control of prescribed fire necessitates using mechanical means of fuels reduction in the WUI (Reinhardt et al., 2008). It is critical then, to be able to identify the areas of greatest concern and deal with them in the appropriate manner. Past management practices were effective in dealing with the immediate problems faced in their time. Continuation of these same practices may only exacerbate the problem and prove to be ineffective at dealing with the different dynamics in present day forest management.

1.2 Resulting challenges for fire managers

In the arena of fuels and fire the main challenges for land managers outside of operational duties are to identify, prioritize, and mitigate hazardous fuel concentrations in a timely fashion. Wildfire has been identified as an issue that must be dealt with, the 2010 Forest Service budget requested a \$134 million increase over 2009 to fully fund the average ten-year suppression costs (US Forest Service, 2010). Operational suppression actions are necessary but reactionary; to proactively deal with the problem at hand, managers have to develop plans for hazardous fuels that are based upon sound information. To identify areas of concern at a meaningful scale, the only viable option is to use some sort of remote sensing. Prioritization will mean landscape analysis that can depict and quantify hazardous areas. Mitigation at this scale will require management actions that reduce fuel loads and restore structure to manageable levels in specific areas of the landscape where it is most effective and economical.

CHAPTER 2. BACKGROUND

2.1 Introduction

Forest fuels are most commonly defined by their physical characteristics or their relationship to various disturbances, among others. The relationship between fuels and fire behavior is crucial for fuels assessment, and tends to be the driving force in current fuels management. This includes consideration of classes of individual pieces of fuel, characterization of fuel complexes and accurate assessment of fuel loads. Remote sensing methods and datasets, specifically LiDAR, can be an important link to accurately assessing canopy and ground fuels. In the past, LiDAR data detailing surface roughness has been used to estimate fuel loads in monoculture forests. If these same techniques can be used to estimate fuel loads in mixed conifer stands, fire managers could have access to accurate, landscape level fuels assessments where most fires occur.

From a fire standpoint, fuels are defined as all biomass in a landscape that can contribute to fire behavior (Pyne et al., 1996). The majority of fuels are dead woody material of various diameter and composition that have either fallen to the forest floor or in the case of grasses and shrubs, dead material that has accumulated during the annual life cycle of the plants. These materials accumulate and decompose, adding to surface litter and duff layers as a function of time. How these different types of fuels react and contribute to fire behavior depends on many different factors. Size, shape, placement, type, terrain, and weather are a few of the necessary attributes in determining how fuels will affect fire behavior. How fuels will burn can be identified as the fire environment. The fire environment is often broken down into fire regimes and fire behavior within these can be altered by terrain, weather, and previous management actions. In this chapter I will give background on how fuels are classified and organized and how they are represented according to the expected fire behavior they can produce. I will finish off the chapter with methods of remote sensing and more specifically, airborne LiDAR applications to detect and measure fuels.

2.2 Effects of terrain and weather on fuel flammability

The fire environment is very dynamic and the two influential features that directly affect fire behavior are terrain and weather. Terrain affects pre-heating of fuels, how much solar radiation fuels receive, and serves as a barrier to atmospheric conditions. Weather influences fuel temperature, moisture content, relative humidity, winds, and atmospheric stability. Weather also includes thunderstorm activity that serves as a source for ignition, moisture, and erratic winds, all which influence fire behavior.

In regard to fire behavior, terrain can be broken down in to slope, aspect, and elevation (Agee, 1993). Steeper slopes present fuels higher up to pre-heating from an advancing flaming front. Slope also determines how much of the sun's radiation is absorbed, a function of tangency to the incoming rays. Grade of slope determines how exposed fuels are to upslope winds within the immediate slope wind sheath. The aspect of terrain dictates at what time of day solar radiation will heat the fuels and reduce relative humidity. Elevation of terrain influences dominant species and temperature. The size, shape, and orientation of terrain determine macro and micro-climatic conditions within the fire environment. Winds are channeled through landscapes by terrain and highly influenced by surface friction and heating and cooling of the surface (Schroeder and Buck, 1970). Precipitation often falls heavier on windward slopes as air masses are lifted over the terrain and reduce their moisture holding capacity (Whiteman, 2000). In a broad sense, terrain is the vessel in which the chemical reaction of fire occurs. It is a mostly static facet of the fire environment and critical to understanding and predicting fire behavior.

Weather is the most dynamic factor present in the fire environment and elements of weather that affect fire behavior are: temperature, relative humidity, atmospheric stability, winds, and thunderstorms. High temperatures lower the moisture content of fuels through evaporation, and in live fuels transpiration is accelerated (Waring and Running, 1998). Related to temperature is relative humidity (RH), a ratio of how much water a parcel of air can hold to how much it has (Schroeder and Buck, 1970). RH's below 100% indicate that the air is unsaturated, allowing a moisture gradient to exist between fuels and the air. As RH's begin to lower, fuels release their moisture into the air parcel. Wind compounds this relationship by mixing the air and replacing saturated air with warmer, drier air from lower elevations. During combustion, wind mixes the air around a fire providing a fresh source of oxygen and delivers the heated air to fuels in front of the advancing flame front, pre-heating

them and lowering their immediate RH. Atmospheric stability in the fire environment denotes convective activity that can influence fire behavior (Haines, 1988). Stable lower atmospheric zones suppress vertical convection and mixing of air parcels. Conversely, unstable lower atmospheric zones promote convection and have been correlated to an increase in fire activity. Atmospheric instability creates conditions for the development of thunderstorms, producing lightning that leads to further ignition of fuels. Strong, erratic winds are produced at the ground level from thunderstorms and can cause extreme and unpredictable fire behavior.

Terrain and weather are independent factors of the fire environment that cannot be controlled. Management actions and plans have to be worked around these elements. Fuels are the dependent factor in the fire environment and a proper assessment of the current state of a fuel bed is compared to where it should be sustainably is the subject of fire regimes.

2.3 Fire regimes

Fire regimes are characterizations of how fire disturbance events have shaped an ecosystem (Agee, 1993). For landscape and large scope planning, the most commonly used system is one that broadly denotes the severity of the most common type of event to occur. Severity is a subjective qualifier in this case and uses fire effects on the dominant species to determine a high, medium, or low severity (Agee, 1993). The second descriptive aspect of fire regimes is the frequency with which an event will occur. Mean fire-return intervals indicate this frequency and are mean times between fire events for given areas.

The importance of fire regimes comes to the forefront when they change dramatically. Many species have developed adaptive strategies in response to generally stable, predictable fire regimes (Barnett, 1999). Fire exclusion has historically removed this stabilizing function from stands that relied on disturbance to maintain their dominant species. An example is Douglas-fir encroachment into ponderosa pine stands (Covington and Moore, 1994) and mountain grasslands (Arno and Gruell, 1986). In some ecosystems, ingrowth of shade-tolerant species into the understory and open areas had historically been kept in check by low intensity, high frequency fires. These fires would burn to their natural extents on a frequent basis and reduce the amount of dead and live fuel in the fuel bed, keeping fuel loads relatively low. Dominant species that had long periods of time to adapt survival mechanisms to these types of events would be vulnerable if a different type of frequency or intensity

disturbance event occurred. Higher than normal fuel loads would accumulate if fire frequency was reduced. This would also increase the probability of a higher intensity event.

Accumulation due to low frequency events coupled with higher biomass loads caused by ingrowth pose a risk of high severity fires that dominant species cannot adapt to. In a stand-replacing fire, shade-intolerant species that may have been dominant would have no foothold to compete with shade-tolerant species and the entire makeup of the stand would change from its historic norm. While stand-replacing events probably happened in the past naturally, they were most likely isolated events that affected a small area. The current risk is that fire regimes are changing on a broad scale, partly due to human actions, and that stand-replacing fires in the future won't be isolated events but ones that change the composition of entire forests in a short number of years.

2.4 Effects of fire suppression on fuels and fire management

The term, "Fire suppression" has perhaps incorrectly become synonymous with "fire exclusion." Fire suppression is a management strategy that is not always successful where fire exclusion is an ecological term that denotes a complete absence of fire disturbance. Management strategies of the past were centered on timber resources and forests were seen as cash crops that needed protection from destructive natural forces. The fires of 1910 greatly influenced a young Forest Service that united its power against a common enemy (Pyne, 2002). Fire suppression became the nationwide management response to wildfires. This response interrupted the natural ecological processes and ecosystem balance that had developed for centuries past. Fire regimes, fuel loads, and the character of the landscape would change over the eighty years that suppression held sway. Initially the strategy worked and devastating fire events were apparently held in check. The unforeseen consequences of a suppression strategy are only now becoming apparent. Tree density has increased, increasing the competition for limited resources. Disease and insect infections are more capable against trees that lack the resources to fight them off. Adaptations that take generations to develop cannot keep up with drastic changes that are now taking place. Fire severity has increased due, in part, to historically higher fuel loads. Historic fire events systematically reduced fuel loads to sustainable levels, allowing species with fire-adapted responses to survive. Current fuel loads exceed the ability of those species to adapt, increasing their mortality and hindering their ability to retain their dominant status. Having fire on the landscape has been

found to be a necessary process and excluding it in the short term only created long term problems at an exponential scale.

2.5 Describing Individual Fuel Components in the Fire Environment

A fuel complex is made up of individual pieces of fuel that contribute differently to fire behavior. In general, smaller diameter pieces of fuel are associated with fire behavior where larger diameter pieces deal with fire effects (Lutes and Keane, 2006). It is important to understand the arrangement and classification of these pieces to get a sense of how they appear naturally and how remote sensing can be used to detect and quantify them. A distinction should be made between surface fuels and aerial fuels as they affect fire behavior differently. It should also be mentioned that fuels appear in strata that become relevant to fire behavior under certain conditions in the fire environment.

Typically fuels are stratified vertically from ground and surface fuels to aerial fuels. Pieces of vegetation with similar physical characteristics are grouped together by similar sampling methods (Brown et al., 1982). Size and shape of fuel particles is relative to the surface area to volume ratio, the higher the ratio, the finer the particle. More surface area per volume means less heat is required to drive off moisture and raise the particle to ignition temperature (Pyne et al., 1996).

The initial stages of fire growth and behavior are entirely dependent on surface fuels and most fire behavior prediction simulations center around these. Only when conditions are present in the surface to transfer fire to the crown are aerial fuels analyzed. Aerial fuels become necessary when this transition occurs and then play a part in determining subsequent fire behavior.

2.5.1 Surface fuels and ground fuels

Ground fuels denote the layer of fuel immediately above mineral soil that contains highly decomposed organic material. Surface fuels include surface litter, herbaceous vegetation, shrubs, and downed woody material. Small, live conifers 10 ft or less in height are generally included in the surface fuels layer due to their contribution to fire behavior. While this layer is assumed to be undetectable by LiDAR because the laser pulses cannot penetrate it, it has a correlation to the larger pieces above it that will decay and contribute fuel to this layer.

Duff and litter Duff and litter are the layers of material above mineral soil that are composed of decaying organic material. Duff is merely highly decomposed litter, but it is important to distinguish between them as they contribute to fire behavior differently and signify different types of fire severity when they burn. Generally, duff is highly compacted compared to litter and therefore is less responsive to changes in relative humidity. Litter's lower bulk density allows air to circulate more freely and reflects the more immediate climatic conditions, meaning litter can and often does, burn independently of the duff.

Remotely sensing the duff layer is questionable, and with an airborne LiDAR dataset, it is out of the question. In order to quantify the duff layer, it would be necessary to penetrate the organic material and retrieve returns from mineral soil, a task that is beyond LiDAR's capacities. Surface litter can, however, be detected but is in such close contact with the underlying duff layer that a ground surface model would not be able to differentiate litter from duff.

Dead fuels and DWD: 1-1000 hour Dead and down woody debris (DWD) is categorized into ranges of diameters but more commonly these categories are known by their moisture timelag class names. Moisture timelag classes identify the midpoint for the range of times fuels of corresponding diameter classes will lose or gain approximately two-thirds of their moisture. These classes are defined as 1 hour fuels, 10 hour fuels, 100 hour fuels and 1000 hour fuels. DWD is commonly separated into fine woody debris (FWD) and coarse woody debris (CWD) because they function differently in forest ecosystems (Lutes and Keane, 2006). The 1-100 hour timelag classes make up FWD and the 1000 hour classes are CWD. For this study the distinction is made between FWD and CWD for their suitability as hard targets for LiDAR pulses.

1 hour fuels correspond to pieces of fuel with diameters of 0 to 0.6 cm which react to ambient air moisture changes within 2 hours or less. Common examples are grasses, lichens, herbs, and the topmost needles of the litter layer (Bradshaw et al., 1984).

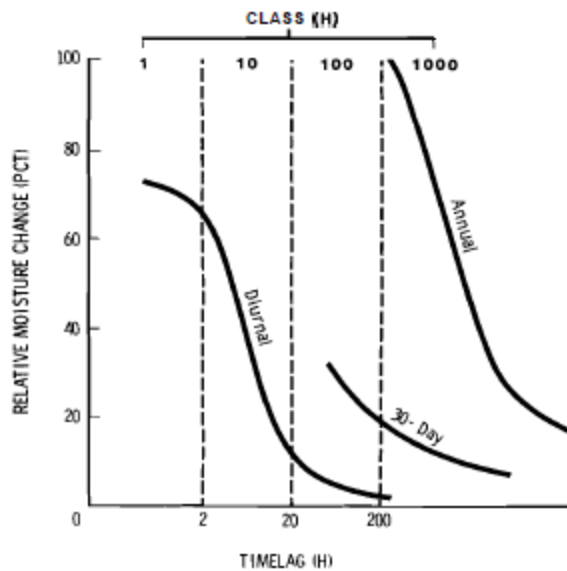


Figure 1. NFDRS 1978 change in relative moisture of various sizes of dead fuels over time (h) (Bradshaw et al., 1984).

Fuel particles such as dead twigs and branches of 0.26 to 1.0 inches in diameter constitute the 10 hour timelag series. Coarser pieces, 1 to 3 inches in diameter are classified as 100 hour fuels. Logs or branchwood over 3 inches comprise the 1000 hour, CWD series (Figure 1).

Live fuels Live fuels provide an excellent target for LiDAR pulses due to their leaf structure, and in the fuel beds of mixed-conifer forests are assumed to be shrubs, herbs, or small trees and saplings. The stems and branchwood of live fuels have a low surface area to volume ratio and do not significantly contribute to fire behavior, therefore while detectable, they are not considered in fuel load calculations. The foliage of live fuels represents the greatest amount of available fuel, depending on its moisture content. In conifer forests, tree needles present a very high surface area to volume ratio meaning they can become part of the available fuel load when temperatures rise and the RH lowers. Smaller trees and saplings can provide a continuous fuel load throughout the entire canopy and are known as ‘ladder fuels.’ When live fuels in the fuel bed become available to combustion, they not only increase the fuel load dramatically, they also provide pre-heating and a source of ignition for the upper strata of the canopy.

2.5.2 Aerial/Crown fuels

Aerial fuels are considered the foliage of mature trees above the fuel bed. They are still classified as live fuels but require an active surface fire for ignition. Once aerial fuels are ignited, they can burn independently of the originating surface fire and can provide an ignition source for surface fires away from the original source. Fires which propagate through the canopy are important to fire behavior and fire effects but are not a part of this study.

2.5.3 Quantifying Fuels

Definitions of common terms Fuel load calculations are comprised of all timelag classes of fuels to determine an estimate of the quantity of fuel present in the fuel bed. Fuel loads are directly related to fire intensity and residence time and have a bearing on fire severity (Lutes and Keane, 2006). Estimations of fuel loads are currently based upon field data gathered from intensive large scale collections or broad, small scale collections. One issue with measuring fuels is that weather conditions change their availability for combustion. The following terms are used to describe fuels: available fuels, potential fuels, total fuels, and biomass. Available fuels and potential fuels are values used to determine fire behavior where total fuels and biomass deal with fire effects and ecological characteristics.

Available fuel Available fuels are the biomass within the fire environment that can burn under the climatic conditions present at the time of a select fire event (DeBano et al., 1998). They will change with differences in RH and temperature and are computed for a single event only. This has pertinence to fire behavior predictions and inputs into fire spread simulations use available fuel.

Potential fuel Potential fuels are vegetation and materials which may burn during an intense fire. This value is generally less than the total fuel and represents the worse-case scenario for fire behavior.

Total fuel Total fuel is all plant material or phytobiomass, above mineral soil to exclude root systems. Total fuel includes the boles of living trees that are never substantially consumed in a fire event (Pyne et al., 1996).

Biomass Biomass includes all organic material above mineral soil and roots below; it is total fuel plus root systems and is any material that can undergo combustion. Biomass is an important value to know to determine how much material a site can support.

2.6 Methods for estimating fuel loads

2.6.1 Fixed Plot Method

Fixed-area or quadrat methods use rectangles, circles, or other known fixed area shapes to bound plots about a centroid. All fuels within the boundaries that meet the sampling criteria are subject to a range of methods of collection. Common methods are destructive sampling which removes all target pieces of fuel and dries them in the oven to obtain dry-weights to volumetric sampling which merely measures the physical dimensions of target pieces. While highly accurate, the collection of fixed-area plots is time and cost intensive and thus, is generally relegated to research purposes (Sikkink and Keane, 2008; Keane and Dickinson, 2007).

2.6.2 Planar Intercept Method

Planar intercept methods were developed by Brown and were based upon the line intercept method (Brown, 1971). Brown addressed errors due to fuel particle tilt by rotating the sampling plane around its x, y, or z axes. Identical to the roll, pitch, or yaw of an aircraft, the planar intercept is oriented perpendicularly to the predominant axis of the vegetation. Fuel volume estimates are sums of all fuel particle intercept areas times the length of the fuel bed. Estimates that are angle-inclusive in their area calculations are more accurate in their predictions, but tend to under-estimation of total volume (Brown, 1971).

2.6.3 Fuel Load Method (Lutes)

The Fuel Load (FL) method was proposed by Lutes and Keane as the sampling protocol for the FIREMON fire effects monitoring scheme (Lutes and Keane, 2006). The planar intercept methods developed by Brown are used to sample DWD. FL uses multiple planes for sampling and may go up to seven planes of different azimuths. This method was designed to reduce overestimation of loads and provide a greater sample size to offset high variability

(Lutes and Keane, 2006). Where Brown's methods and FL differ are the small live tree, herb, and shrub estimations.

2.6.4 Photo Series Methods

The photo series methods use photographs of sites that were subsequently sampled using Brown's methods to obtain fuel loads. These photos are then used by field personnel of varying skill levels to quickly assess a landscape, match the most similar photo, and assign an estimate to the area. Obviously there is a great amount of subjective assessment with this method and the photographs may not adequately capture all diameter classes present in the fuelbed.

2.7 Fuel Models

Fuel complexes are mathematical descriptions of fuels for use in fire behavior models. There are a variety of methods for determining fuel models ranging from field based visual estimations using thirteen simple classifications to databases of thousands of different customizable classifications (Anderson, 1982, Deeming and Brown, 1975, Scott and Burgan, 2005, Keane and Dickinson, 2007, Ottmar et al., 2007). Regardless of the methods used, the intent of fuel models are to predict how a landscape will burn and what the primary carrier of fire will be (Scott and Burgan, 2005). Fuel models are used as inputs into fire spread calculations and need to be correctly identified in order to provide the best outputs for decision-making. Fuel models are a work-in-progress that have taken thirty-seven years to refine. Their subjective nature requires refinement that continues to this day.

Fuel models were introduced to the land management lexicon in 1972 with Rothermel's work on a mathematical model of fire behavior (Rothermel, 1972) and The National Fire Danger Rocky Mountain Rating System (Deeming et al., 1972). The purpose of fuel models was to either mathematically describe physical conditions of a fuel bed as inputs for fire spread and behavior models or to classify potential severity conditions of a landscape (Anderson, 1982). The limitations of models relegate them to aids in decision-making and not self-supporting evidence. These models were knowingly subjective and the authors repeatedly stressed that results should be cross-referenced with on-the-ground observations (Brown et al., 1982). The research into how to mathematically describe fuels found two veins of thought, the first was a short-term solution to use them as inputs for fire spread models to

provide decision-making tools for managers (Brown et al., 1982). The second encompasses the need for long-term predictive tools used to aid in addressing a growing problem of hazardous fuel conditions (Ottmar et al., 2007).

2.7.1 Classic 13

The most common fuel models still in use for immediate predictive purposes are the 13 ‘classic’ fuel models developed by Albin (Albin, 1976) and verified by Anderson (Anderson, 1982). They met the need to estimate fire spread for the fire behavior officer in the field. The impetus behind creating a basic 13 was to expedite predictions in the field on emerging fires and make the system as user-friendly yet accurate as possible. A weakness that makes fuel models subjective is the assessment of humans as to which model best represents the present conditions. It is important to note that fuel models are ultimately defined by fire behavior, specifically spread rates, rather than fuel type. Fuel particle properties are held constant; it is the depth and loading by size classes that change from model to model. At the same time the 13 models were gaining a foothold, 20 parallel models were developed for long-term planning purposes.

2.7.2 NFDRS (20)

The National Fire-Danger Rating System (NFDRS) was the culmination of many efforts to quantitatively evaluate landscapes in order to provide the best available science to decision-makers. NFDRS fuel models differ from the 13 classic models by how they are used. The System’s main objective was to produce viable information for pre-suppression planning (Deeming and Brown, 1975). Weather observations as well as live fuel components are coupled into the model to yield indices for determining seasonal severity. The first two fuel models were made available in 1964 with a closed canopy and open area model. Nine models were formulated for the NFDRS in 1972 when Rothermel’s fire spread model made more detailed models a viable option. Refinement and computerization of the NFDRS process solidified its use by all federal agencies and settled on 20 final fuel models.

2.7.3 New Classics (40)

In 2005, 40 new models were proposed to address the deficiencies the original 13 presented when used during off-peak fire seasons. Predictive applications for Rothermel’s model required new parameters for moisture content, humidity levels, and higher specificity

for surface fuels. The desire to simulate management actions and fuel treatments led to more choices of fuel models to provide a variety of planning options. Model categorization focused on similar fire-carrying fuel type, distinguished by fine fuel load, fuel type, and extinction moisture (Scott and Burgan, 2005).

2.7.4 Fuel Characteristic Classification System

The Fuel Characteristic Classification System was created from the need to have a single fuel model set that incorporated all the attributes currently used as inputs into various models. Most of the previous model sets were geared towards specific software applications and were not comprehensive enough for multiple uses (Ottmar et al., 2007). FCCS is an attempt at a comprehensive, open-ended format of fuel models that function on general as well as specific uses and are provided as templates to be customized or as is. Regional workshops that included land managers, researchers, and policy makers identified the most sought after needs and requirements. It is this type of information that can drive policy and actions taken on public lands and further reinforces the need for accurate inputs and outputs from models and applications.

2.8 Mapping of fuels

2.8.1 Field and passive forms of remote sensing

Field surveys were the first form of fuels mapping involving many workers and numerous amounts of man-hours (Hornby, 1935). While successful, they required more workers and human-hours than most managers could afford. The need to reassess fuels periodically often makes this method impractical for modern day fuels management. Aerial photo interpretation (Lee, 1941) was an advancement in fuels mapping that is still a viable method, but it is also time consuming and subjective. Natural color photography improved stand delineation (Lund, 1969) and infrared photography captured spectral reflectance characteristics of vegetation (Bertolette and Spotskey, 1999) that aided in interpretation of vegetation types. Satellite-based multispectral imagery including SPOT-HRV and Landsat MSS and TM have been used to classify landcover and vegetation for decades. Imagery from the latter sensors has frequently been used with digital elevation data to produce fuel-oriented vegetation maps (Shasby et al., 1981, Chuvieco and Congalton, 1989, De Wulf et al., 1990, Salas and Chuvieco, 1995, van Wagtenonk and Root, 2003). However, because optical

sensors are passive forms of remote sensing they cannot penetrate the canopy and therefore can only derive surface conditions as a surrogate of the canopy (Keane et al., 2001). An alternative approach put forth approximately 12 years ago was ecological gradient modeling, which uses gradients of natural characteristics to predict environmental settings that influence vegetation and associated fuel types (Keane et al., 2001). In this approach, optical remote sensing data are used to establish current condition and type of vegetation and applied in conjunction with biophysical characteristics to model fuel parameters. The need for extensive field data, complex ecological modeling and robust statistical analysis can make gradient modeling impractical for some managers (Arroyo, Pascual and Manzanera 2008), but it remains a viable approach to map fuels across large areas despite its shortcomings.

2.8.2 Active Forms of Remote Sensing

Active forms of remote sensing, such as Synthetic Aperture Radar (SAR) (Saatchi et al., 2007) and LiDAR (Popescu et al., 2003, Mutlu et al., 2008) can provide a structural profile of the canopy as emitted pulses propagate down and reflect off of the canopy. Ground returns can be discriminated from canopy returns to stratify the fuels and iteratively select fuel layers. Canopy metrics, such as canopy base height and crown bulk density can be obtained (Andersen et al., 2005, Riano et al., 2004) as well as surface fuel estimations (Seielstad and Queen, 2003), and surface fuel models (Mutlu et al., 2008). When coupled with optical datasets, these active remote sensing methods offer a more complete picture of a landscape (Erdody and Moskal, 2010).

2.8.3 Why LiDAR presents a different option

Penetrates the canopy The major strength of LiDAR is penetration of the canopy by the emitted pulses. Multiple returns from a single pulse allow stratification of the canopy and provide a dataset that can be used for analyses independent of pre-existing stand delineations. Because LiDAR is an active mode of remote sensing, each emitted pulse can be tagged so as to identify each return with a unique time stamp ID. From this information it can be determined how far down pulses are penetrating and where different stratum of the canopy exist in reference to geolocations. For example, the Lubrecht acquisition used in this study was capable of four returns per pulse, with current systems capable of five or more returns per pulse. The density of information is immense compared to other forms of remote sensing;

a modest dataset with an area of 2km² registers around 5 million returns. Every return has explicit X, Y, and Z coordinates with the intensity of the returns recorded as well. From such dense, georeferenced datasets, several data products can be generated to fulfill many needs an analysis might require.

Full Coverage A benefit of remote sensing and LiDAR specifically is the area covered by the mission. An airborne based sensor can cover an entire management area in a single day. Despite temporal and environmental differences during an acquisition, normalization and calibration can mitigate factors such as: elevation changes, disparity of scan angles, and atmospheric conditions. The time frame in which remotely sensed data is collected can be orders of magnitude smaller than many other methods and as such, minimizes a dynamic environment. The result is an unbiased, even coverage dataset that reflects an instantaneous assessment of the target area.

EMR properties of NIR are well understood LiDAR typically utilizes an airborne laser that emits a wavelength pulse of at or around 1000 nm. The wavelength of 1064 nm is best suited for forestry applications due to the reflectance of vegetation at that spectrum. Visible EMR spans the wavelengths of 400 nm to 700 nm and green, healthy vegetation reflects 500-600 nm wavelengths, the green spectrum, more dominantly. This is why healthy vegetation appears green to the human eye. Visible band EMR is reflected from vegetation due to the palisade layer of leaf structures which contain chloroplasts, photosynthetic cells that absorb light in the blue (400-500 nm) and red (600-700 nm) wavelengths. EMR from the near-infrared (NIR) spectrum (700-1300 nm) is not utilized by vegetation for photosynthesis and passes through the palisade layer to the mesophyll layer, a spongy, air-filled layer used by leaves for respiration. These air pockets within the mesophyll scatter and reflect 40-50 percent of the incident NIR radiation upon it, making healthy vegetation an excellent reflector of the NIR spectrum (Lillesand and Kiefer, 2000). Little of the NIR radiation is absorbed (less than 5 percent) by the mesophyll and the remaining EMR is transmitted through the leaf and propagates down through the canopy. The receiver on the ALS50 sensor array is sensitive enough to register up to four returns from the same initial pulse, even though the propagated portion of the pulse is reduced with each hit. Multiple returns from a single 1064 nm pulse allow a profile of the canopy that cannot be attained otherwise. At

wavelengths above 1300 nm, incident radiation is either absorbed or reflected further emphasizing the utility of the 1064 nm wavelength as a sensor in forestry applications.

2.8.4 Laser Altimetry and forestry applications

The use of airborne optical lasers to scan terrain features was proposed as early as 1964 (Rempel and Parker, 1964). For forestry applications, this would eventually produce Digital Terrain Models (DTM) and Digital Surface Models (DSM). DTM's represent the bare earth and are synonymous with Digital Elevation Models (DEM). DSM's represent the upper-most visible surface presented to the sensor and include vegetation, buildings and other surface features. LiDAR pulses penetrate through multiple canopy layers allowing stratification of vegetation between the DSM and the DTM.

The ability to separate canopy returns and ground returns led to research on measuring forest canopy properties (Andersen et al., 2001). Mapping forest structure for mensuration and inventory purposes was explored using canopy stratification methods (Lefsky et al., 2001). Canopy attributes of canopy height, surface canopy cover, canopy base height, and crown bulk density were derived from LiDAR acquisitions as inputs for fire behavior modeling (Riano et al., 2004, Andersen et al., 2005, Hall et al., 2005). While the majority of studies have examined the upper strata of available fuel, only a few to date have focused on the lower stratum of fuel where surface fires are.

As previously mentioned, Seielstad and Queen (2003) used surface roughness to estimate fuel loadings in monoculture lodgepole pine. Other research has shown that surface fuel models could be estimated using LiDAR datasets and fusing it with multispectral imagery (Mutlu et al., 2008).

2.8.5 Shortcomings of LiDAR

Individual LiDAR pulse entries record explicit x, y, and z coordinates as well as the intensity of the return and scan angle. The coordinate data imparts the location and hence, the structure of the target when compared to adjoining returns. Scan angle may relate to intensity, but no substantial relationship has been determined. Where coordinate data impart structure by comparing a return to all local area returns, traditional remote sensing would indicate that intensity, or spectral reflectance, should relate the character of the return due to its signature.

Currently with LiDAR returns, intensity cannot be normalized to an indicative value. This is because it is impossible to determine how much of the pulse has been reflected, how much has been absorbed, and how much has been transmitted. With multiple returns from a single pulse, each successive return intensity value is compounded by the targets above it as to how much EMR the remaining pulse has propagated further. Despite having a record of reflectance responses for each individual return, these values cannot currently be used to characterize a target.

If a pulse hits a target and there is not enough energy transmitted to register concurrent returns, the pulse number is classified as an “only” return. In an open field there is little doubt that an ‘only’ return is in fact a ground hit as there is no substantial vegetation intercepting the pulse. Also, if an ‘only’ return exists high in the canopy it can be assumed that the target is a solid object such as a branch or a tree bole. Simple target identification becomes less certain when returns come from a fuel bed beneath a canopy where portions of the pulse have been intercepted and a smaller footprint continues down. Terminal hits from these areas are generally classified as ground hits but any number of objects can cause a terminal return underneath the canopy.

CHAPTER 3. METHODS

3.1 Introduction

This chapter describes the methods of data collection and analysis used to generate comparisons of surface roughness to point estimates of ground fuels at Lubrecht Experimental Forest, Montana. I will describe the remote sensing parameters used during the LiDAR mission and then will describe the Fire/Fire Surrogate (FFS) study and its field collection methods. I will explain how I derived surface roughness from raw laser data and then how I aggregated both roughness values and plot data to perform statistical analysis. Regression analyses and a final biomass estimate map will complete this section of the chapter.

The second part of this chapter deals with using a fusion of various remotely sensed layers to perform a landscape classification of fuel models. I will cover the field data for this section which is taken from Lubrecht Resource Inventory Plots (RIP) and a coinciding photo series. Decision trees, A description of Classification and Regression Tree (CART) analysis, and unsupervised classification strategies will conclude the chapter.

3.2 Study Area

The study site is the University of Montana's Lubrecht Experimental Forest in the Blackfoot Valley of western Montana (Metlen and Fiedler, 2006). Lubrecht is an optimal study site for fuels as it represents the predominant terrain, species, and management history of much of western Montana (UM, 2003). Mean annual precipitation averages 18 inches, 44% as snow, and mean annual air temperature is 3.8° C (Nimlos, 1986). Lubrecht has a rich variety of tree, forb, and grass species present that are similar to many other sites in western Montana. It is populated most commonly by ponderosa pine (*Pinus ponderosa*) and Douglas fir (*Pseudotsuga menziesii*), with localized western larch (*Larix occidentalis* Nutt.) and lodgepole pine (*Pinus contorta*) (Metlen and Fiedler, 2006). The forest was managed similarly to areas west of the divide as a source of timber for the Anaconda Mining Company and was heavily logged in the early 1900's. Some isolated pockets of old growth exist, but the majority of the stands are 80-90 year old, second-growth stands. Moderate grazing has helped keep undergrowth down in most of Lubrecht, but no recent grazing has been allowed within the focused study site (Metlen and Fiedler, 2006). Mean fire return interval for the

area is 20 years (Arno, 1980) but the landscape has not substantially burned since the late 1800's (Metlen and Fiedler, 2006).

3.3 Field Data and Resource Inventory Plots at Lubrecht

3.3.1 Field Data of the Fire/Fire Surrogate Study

In this section I will give a brief overview of the Fire/Fire Surrogate Study (FFS) and its field collection methods. Detail about the FFS study is necessary only for the sake of describing the physical characteristics and management history of the focused study sites. The intent is to describe the study and relay a sense of the site's composition and structure after the study was completed. This description will describe conditions in 2002 and not necessarily when the Lubrecht LiDAR mission was flown. It is assumed negligible differences at the site exist between the field collection and the LiDAR mission as no disturbances or management actions other than monitoring had taken place in the three year span. Data collection methods are the main thrust of the FFS section to ensure the integrity of the field data collection.

Research into restoration treatments of understory and surface fuels was conducted at Lubrecht from 2000 to the present under the Fire/Fire Surrogate Study (Fiedler et al., 2000). This project spanned 11 states across the United States and highlighted 13 main study sites where experimental design focused on four restoration treatments. Selection of these 13 sites was based upon their representation of short return interval, low to moderate severity fire regimes. The four treatments called for available management tactics that either used fire directly or mimicked the effects of a natural fire regime. The first treatment was a control unit that was used to test a 'hands-off' management strategy and to provide a baseline for the other three treatments (Control). The second treatment applied mechanical thinning and trampling of slash, testing the most common fuels reduction technique in use today (Thin Only). The third treatment would test a burn only strategy using prescribed fire and subsequent reburns to achieve restoration targets (Burn Only). The last treatment used a combination of thinning and trampling followed by prescribed fire in the subsequent year after the slash and down fuel had cured (Thin/Burn).

Three study blocks with four treatment units for a total of twelve units were established at Lubrecht with each treatment bounded by a 9 ha square aligned on an azimuth. Mechanical thinning operations began on the Thin Only and Thin/Burn units in 2001, implemented

during the winter months when snow accumulation would mitigate soil compaction and disturbance due to the single-grip harvester used. Prescribed fire operations were conducted in the spring of 2002 using a strip headfire technique to emulate natural ground fire progression from the edge of the unit (Metlen and Fiedler, 2006).

Fuels data collection was conducted pre-treatment in 2001 and post-treatment in 2002. Sampling protocol selected 36 gridded points within each treatment, 50 meters apart from each other and 25 m from the treatment unit boundary. Each plot center was identified using an *Impulse LR* laser to measure distance and a hand compass with a declination of 19.5 degrees E to determine the correct azimuth. A standard tape was used for distance in the case of vegetation too dense to allow the use of the laser. Whittaker plots were established at randomly selected points (plots 02, 05, 09, 12, 18, 22, 24, 26, 29, and 33) on the grid center (Fiedler et al., 2000). All points had permanent metal stakes driven flush to the ground to facilitate treatment operations and were spatially located in 2004 using a Trimble Pro XRS GPS unit with differential correction (Fiedler et al., 2000).

The lower forest floor (duff) was indirectly estimated by determining the depth-to-loading relationship for each block. Duff was destructively sampled at 13 randomly selected areas of the 36 grid points by measuring depth at 4 points along the edge of a 1 ft² sample area. Litter layer fuels were measured before and after treatments in two, 1 ft² areas in each of the 36 points to measure fuel loss. Small trees were denoted as either seedlings less than 4.5 ft tall or saplings greater than 4.5 ft tall with a 4 inch breakpoint DBH. Saplings and seedlings were tallied by diameter class, height, and live crown height, with basal area used to estimate volumes (Avery, 1967).

Two opposing 50 ft. planar Brown's transects were used to estimate surface fuels in the 0.25 inch to 3.0 inch diameter categories. Coarse woody debris was sampled using a 20m X 4m strip plot using the Brown's transect as a centerline. Two strip plots were established at odd numbered grid points for a total of 18 per treatment. Only logs longer than 1m and a large end diameter greater than 15cm were sampled. Volumes were based upon diameter of large and small ends rather than tapering functions of species and length.

These field collections represented the best-available representation of field conditions that coincided with the acquisition. The range of values attained from opposing transects captured the high variability of measurements that would be possible from mixed-conifer stands. This high variability of fuel loads was an aspect of fuels that was hypothesized to be

an attainable attribute that LiDAR-derived surface roughness could possibly capture. The focus of this study would not only be on the ability of surface roughness to predict fuel loads, but also on the sensitivity of this determination.

3.3.2 Resource Inventory Plots

In 1998, the University of Montana's College of Forestry and Conservation initiated a field collection of forest stand information which would be updated on a recurring basis to provide a persistent assessment of field conditions that pertained to topographical and vegetation characteristics of Lubrecht. There were 101 fixed plots spaced on a grid approximately 200 acres per plot. Fuels data would be collected as per the FL method described by Lutes and Keane (Lutes and Keane, 2006). Three fuels transects were taken from each plot, oriented 000°, 120°, and 240° true azimuth. Each transect is 60 feet in length taken 15 feet away from plot center to minimize disturbance around the plot center. Digital photos were taken of the plot center at 45 feet and 75 feet along each of the three transects, for a total of six photos per plot. These photos would be used to visually assess fuel models using the Photo Series method.

3.4 Acquisition

The initial Lubrecht LiDAR mission was flown in June of 2005 using a Leica Geosystems ALS50, but scan errors on the eastern section due to improper elevation calibration required that section be re-flown in July of 2006. The 2006 mission replaced all of the 2005 data that had errors and data was validated to ensure data integrity. Terrain elevation minimum and maximum were set at 1140m AMSL and 2070m AMSL respectively. Nominal flying altitude was 2969m AMSL at 140 knots using a 35 degree scan FOV. At the lowest terrain elevation, this gave the widest swath scanned at 1153.36m. Laser pulse rate used was 36.2 kHz at 1064nm with a scan rate of 27 Hz. Using these parameters, our average point density was 0.44 points per square meter.

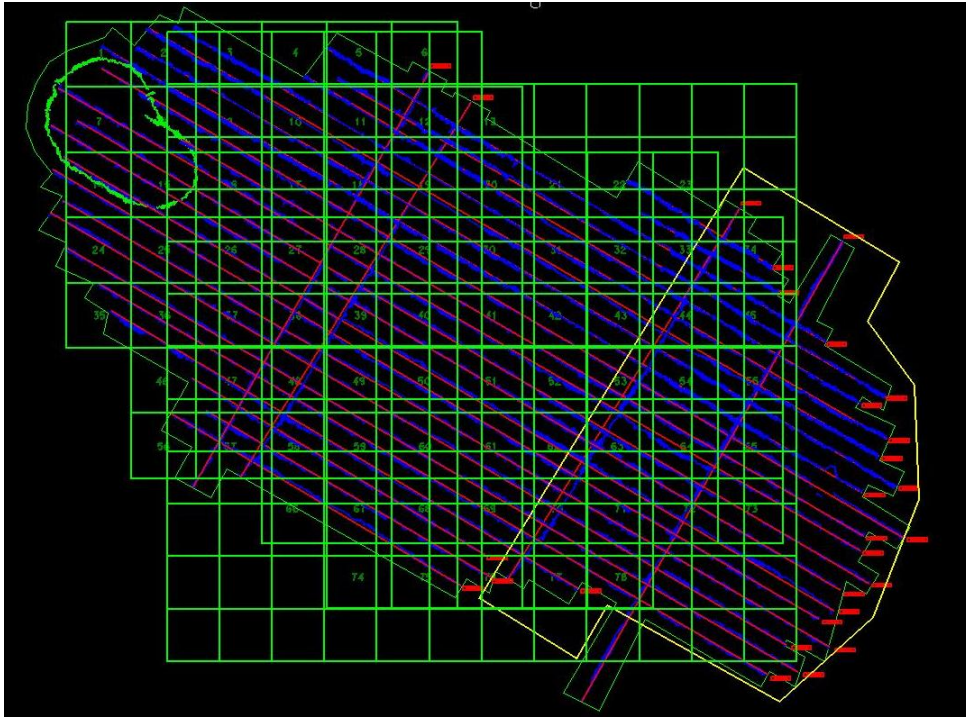


Figure 2. Scan map with tile scheme overlaid for Lubrecht Experimental Forest.

At the highest terrain elevation there was 5.66% sidelap with greater values at lower elevations. Forward overlap was 0.6 meters per scan line. Focal length of the receiver was 62.77mm with a 0.10mr IFOV. The vendor post-processed the data to correct for spatial accuracy and delivered the acquisition in the form of several native LiDAR files.

3.5 Data Pre-processing

All returns recorded during a single flight line swath were stored in the native LiDAR binary format called a LAS file. These individual LAS files are extremely large, spatially covering several kilometers, and require more processing power than most current desktop computers possess. A tiling scheme was designed for the raw Lubrecht LAS files to subset them into sizes manageable by 32-bit operating systems (Chen, 2007). Each tile was 2100m X 2100m with an intentional 50 m overlap of neighboring tile edges of both the X and Y axis to provide continuous data beyond a 2000m X 2000m analysis area. This 50m buffer around each tile could be removed post-analysis to mitigate any edge effects incurred during processing.

3.5.1 TerraScan Surface Model

Ground classification processing was the first step of the analysis and classified points as either bare earth (BE) or canopy (CAN) return types. It was assumed that fine fuel targets reflect insufficient energy to trip the sensor and were thus, indistinguishable from bare earth. Canopy returns were assumed to represent targets that are either solid or present a significant enough surface to constitute a 'hit.' TerraSolid's TerraScan (TerraSolid, 2005) software was used in the Microstation environment to run an unsupervised classification algorithm that assumes the lowest points within a search window are definite BE returns. A triangulated irregular network (TIN) surface is generated from the lowest points and the remaining ground points are queried out using an iterative approach. Ground classification iterations then took unclassified points within the search window and checked them against an angle drawn from the TIN surface to the point in question. With large triangles the 'Iteration Distance' parameter ensures that points aren't incorrectly excluded by restricting their selection until a valid vertex is within the defined proximity (TerraSolid, 2005). If a point exceeded the threshold angle it was assumed to be a canopy point, else it was integrated into the bare earth pool. The process is repeated with an updated TIN consisting of classified BE points. Sources of error during the unsupervised classification involved terrain where the slope was greater than the iteration angle and ground points were misclassified as canopy points. Ends of road culverts or similar features that contain shallow pools of water introduced error-points as the laser pulse returned a z value significantly lower than the surrounding surface. Error-checking and reclassification were done manually with error points being reclassified and stricken from the active dataset. These error points constituted approximately 250 points out of the entire 688 million points of the acquisition and were assumed to have no impact on the integrity of the dataset. Binary LAS tiles were then converted to GIS software compatible point shapefiles for analysis with each point having explicit x, y, and z coordinate attributes that were pertinent to this study. These coordinates are recorded natively in the WGS84 geographic coordinate system. To coincide with existing geographical datasets of Lubrecht, each shapefile LiDAR tile was re-projected into NAD83 UTM Zone 12. This is a source of positional error, however nominal.

3.5.2 Validation

Horizontal accuracy was tested by the vendor during multiple acquisitions at the Missoula International Airport (MSO). LAS shapefiles were visually inspected against aerial imagery in a GIS to validate a general horizontal accuracy. Vertical accuracy was determined by creating a DEM of the BE points for each tile and comparing to ground control.

3.5.3 Error Points

Points with drastic elevation differences were examined in Microstation and the error points were reclassified into a user defined class, separate from the BE or CAN points. Once the error points were removed, the ground classification algorithm was run on the remaining points. Misclassified areas were manually reclassified to BE points. These areas were fairly obvious to detect as they registered only canopy hits; without BE hits, large pockets of the ground surface were missing from the DEM. Generally, these areas coincided with manmade road cuts that were not characteristic of the surrounding terrain.

Initially the CAN points were either classed as ‘low vegetation’ or ‘high vegetation’ but it was decided that early classification beyond ground and vegetation would constrain further analyses. Error points were examined by gathering descriptive statistics on each tile. Drastic height differences were only found on two points and they were assumed to be errors and not addressed further.

3.5.4 Mosaicking and Generating Canopy Height (CH)

Multiple tiles covered the FFS study site and were mosaicked to provide data continuity across the analysis area. Removal of the 50 meter buffer before mosaicking resulted in a seamless edge between tiles. FFS boundaries defined the subset of points used for further analysis. All BE points were used to create a minimum surface from which fuel bed points could be differenced. Circular and square search window options were explored as well as varying sizes to best suit terrain smoothing. Square windows tended to create artificial features due to sharply contrasting edges along a square’s side where the circular edges were ‘softer’ on the terrain. A window that was too large tended to oversimplify terrain differences but smaller windows left areas of no data due to undersampling. A 5 meter circular search window was settled upon as it provided continuous data with the best representation of terrain height. This window was used iteratively on the points using ARCINFO to create a

raster of all minimum surface height values at 1m resolution. The minimum surface raster was converted back into gridded points for the purpose of generating a TIN surface that better interpolates heights between cell centroids. All points from the initial LiDAR acquisition, minus error points, were differenced from the TIN to give height above the smoothed surface and the values stored in a new field termed, 'CH.'

3.5.5 Generating Surface Roughness

All CAN points with CH values less than or equal to 2.0 meters plus all bare earth points were computed for standard deviation from mean CH value using an iterative circular search window originating from the top, left 1m cell within the 2000m tile and continuing to the lower right 1m cell. I determined the best radius of the search window to be 10m using the same logic as the smoothed terrain surface. Windows smaller than 10m had gaps in the data and undersampled the relative vegetation, but larger windows (i.e. 15m, 20m) oversimplified roughness and reduced the range of values for roughness.

Roughness was calculated as the standard deviation of the iteration origin cell CH height from the mean CH height of all points within the search window. Bare earth points would intuitively have a CH of 0, however due to differencing their heights from the smoothed surface step mentioned earlier, most bare earth points' CH value was not equal to 0. The resulting 1m raster represented the laser altimetry derived surface roughness of the 2 meter fuel bed.

3.6 Data Analysis

3.6.1 Analysis of Surface Roughness on FFS

The four treatments of the FFS study were assumed to have different structures that could be identified using surface roughness. The control units would have the most targets in the fuel bed and show a high roughness value. The Thin/Burn units would have the least targets and show as smoother surfaced areas. It was assumed that the Thin Only and Burn Only treatments would contribute material to the fuel bed but due to trampling in the thinned unit and fuel consumption in the burned unit, they would fall somewhere in between the Control and Thin/Burn roughness values. Mean roughness values were produced for each unit and correlated to predicted values for each treatment.

Similar to Seielstad and Queen (2003), I compare roughness to fuels using linear and stepwise regression techniques. Three scales of analysis comprised of 9 ha (300m X 300m; 1 FFS treatment unit), 2.25 ha (150m X 150m; ¼ FFS treatment unit), and 0.07 ha (0.07 ha circular plot; 1 FFS fuels plot) were used. I used the 9 ha treatment unit scale because each unit held clear structural differences due to restorative treatments applied during the FFS study implementation. The 2.25 ha areas represented treatment units divided into four quadrants each with an equal number of plot estimates. The 0.07 ha areas represented individual plots with two opposing 100 ft. long Brown's Transects intended to possibly capture the same fuels measured in the field data. These three scales would allow for appropriate analysis (Waring and Running, 1998) in terms of variability and imprecision of field data in terms of landscape, stand, and plot scales. N-sizes for the 9 ha, 2.25 ha, and 0.07 ha circular plots were 12, 48, and 432 respectively.

As described previously, fuels data consisted of 432 plot-level observations with multiple fuel components described previously in the FFS study. Plot level analysis used each of the 432 observations, 2.25 ha quadrants were represented by mean values from the 9 plots that fell within each of the 150m cells, and 300m cells were represented by the mean of 36 plot observations within each treatment boundary. Within each scale, groups of fuels characteristics were evaluated against roughness. Mean values of roughness and fuel loads for were used for the three different scales by averaging roughness values relative to 9 ha, 2.25 ha, and 0.07 ha zones.

Linear Regression The first statistical analysis was a linear regression model based upon having field estimates as the independent variable and corresponding roughness values as the dependent variable. This analysis was done at the three previously mentioned scales and was done to test the relationship between roughness and CWD developed by Seielstad and Queen (2003). Even at the coarsest scale (9 ha), there was not a strong relationship ($R^2=0.383$; $pvalue = 0.032$); therefore it was decided to test each individual fuel component against roughness using simple and stepwise linear regression methods.

Stepwise Regression Individual fuels data were available from the FFS field collection and included: forest floor mass, forest floor depth, 1 hour, 10 hour, 100 hour, 1000 hour sound, 1000 hour rotten, and small live tree loads. All of these estimates were in

megagrams per hectare (Mg/h) with the exception of forest floor depth, which was in millimeters (mm). Simple linear regression was performed on each component and then all components were used as input for stepwise regression. Stepwise regression was performed on individual fuel components and lacking a decent relationship, combinations of fuel components for total fuel loads were used.

Fuel Combinations Four combinations of single fuel components were tested against roughness using simple linear regression. These combinations were configured as they would most likely appear in the fuel bed and represented Total Biomass in the 2 m-deep fuel bed, Total Dead Fuel, Downed Woody Sound/Rotten, and Downed Woody Sound. ‘Total Biomass’ was defined as dead combustible material of any diameter or integrity that had separated from the tree, plus small live trees, duff, and litter. It included all biomass within the fuel bed, excepting duff. This definition of total biomass closely represents the definition of total available fuel (DeBano, 1998). Total Dead Fuel is identical in make-up to Total Biomass minus the small live tree component. The two downed woody debris (DWD) aggregates contained 1, 10, 100, and 1000 hour timelag fuels, with one of them including rotten logs of 6 inches or more in diameter whose centers were above the duff layer (Lutes and Keane, 2006).

The regressions were bivariate (e.g., Single Combined Fuel Variables with Roughness as the predictor in each of four cases). Several relationships were identified at a coarse scale using the fuel combinations and were projected across the entire acquisition for landscape scale analysis.

3.6.2 Mapping Roughness for Fuels

Once a method of generating roughness from GHD had been established from the FFS area, it was expanded to the entire acquisition area. This required processing each tile for surface roughness, removing the 50m buffer, and mosaicking the tiles together. Surface roughness was coded in Arc Macro Language (AML) script for all 78 tiles. Removal of the 50m buffer was accomplished using a batch file script available in ArcGIS. Mosaicking was done using Leica Geosystems’ Imagine mosaic function. While the mosaic function is normally used for satellite or aerial imagery with overlapping coverage, removal of the buffer left no areas of overlap between tiles. Since the tiles held no sensor information, ‘Most Nadir’

is somewhat misleading because Nadir is the point of an image directly below the sensor. Neither of these discrepancies affected the mosaic output because there is no overlap. The function essentially stitched together neighboring tiles while maintaining edge values.

3.7 Total Biomass and a Fuels Map

As the results below will show, a definitive relationship between fuel loads and roughness could not be attained at a scale that reflected the accuracy and precision LiDAR affords. Thus, a landscape scale relationship was developed and used to assess fuel loads. It would require using the surface roughness values for the entire acquisition area and converting these to biomass values using the regression equation that best expressed the fuels/roughness relationship.

Lacking field data of any roughness metric, validity of landscape surface roughness was done visually, concurrent with easily identifiable features. Known manmade structures such as roads, buildings, and agricultural improvements were identified by surface roughness and were distinct signatures within the entire roughness map. These features proved to be ‘rough’ relative to neighboring points due to the contrasting height differences. Aerial imagery identified stands of low mean height tree regeneration that coincided with higher values of surface roughness. Regeneration has a high target density within the fuel bed and high density of stems per acre. Terrain features such as creek drainages, with a higher probability of denser vegetation, showed high surface roughness where open fields of grasses showed very low surface roughness.

The landscape surface roughness raster was set at a cell size of 1 meter resolution with 268,522,976 cells of valid information. It was resampled to present the mean values for 300m cells representing 3073 cells of valid information. This was done to reflect the appropriate fuels/roughness relationship for predicting biomass. The slope equation of the final fuels/roughness regression; $y = 224.67x - 22.858$ was used where roughness values were ‘x’. This produced a total fuelbed biomass estimate for Lubrecht.

3.8 Classification of Fuel Models

The second phase of this project involved using LiDAR data to predict fuel models as inputs into fire behavior prediction and fire spread software. Layers that can be used as inputs for some prediction models are: canopy cover, crown base height, crown bulk density, digital elevation models, stand heights, and fuel models. A single LiDAR acquisition can produce all of these layers save the fuel model. Currently, no fuel model layers have been created from LiDAR data and they pose the most important input into fire behavior calculations. While most of the other layers define canopy characteristics, fuel models describe surface fuels. As has been mentioned before, ground fuels are what drive fire behavior and propagate fire into the canopy; without a sound assessment of surface fuels, fire behavior calculations cannot be relied on for management decisions.

Photo Series Field Classification The Lubrecht Resource Inventory Plot (RIP) photos were presented to various individuals from the NCLFA who have varied, but good experience with fuels and the Photo Series method of fuel model determination. Fuel models were assigned using Anderson's Aid to Determining Fuel Models (Anderson, 1982). Three separate sets of fuel model assignments were conducted using the same RIP photos. I reviewed the photos on my own to test the fuel model assignment process and gather a separate expert opinion before conducting the two other assignments. Three PhD's of Forestry and a PhD of Forestry candidate were used for the second assessment, all with experience in wildland firefighting and fuels management. The third assessment used a PhD of Forestry and two Master's of Forestry candidates with extensive field fuels work. Each plot was identified by the highest ranking fuel model assignment with a secondary assignment for alternate analysis.

Decision Tree In their previous LiDAR research, Seielstad and Queen indicated that while they were successful in separating FM8's from FM10's to a high degree of accuracy, there were too few examples of FM1 and FM2 to separate them from FM8 based on OD alone (Seielstad and Queen, 2003). They indicated that FM10's could be separated from FM1, FM2, and FM8 by using OD, a surface roughness measurement. They hypothesized further, that FM1's, FM2's and FM8's could be separated by using canopy

metrics that were characteristic and unique to each fuel model. FM1 and FM2 are characterized by more open, grass-type areas where FM8 is closed-canopy timber areas.

For my study, a decision tree was used to classify FM1, FM2, FM8, and FM10 by using values for roughness and canopy cover. The logic follows that FM1 and FM2 should have open canopies and FM1 would be 'smooth' surfaced where FM2 would be 'rough' surfaced. FM8 and FM10 would follow the same logic using closed canopies; FM8 having a 'smooth' surface and FM10 having a 'rough' surface. The median values of roughness (0.24 STD) and canopy cover (61.5 percent) were taken for the landscape layers of Lubrecht and used as breakpoints. Median values were used because outliers existed in both canopy cover and roughness data layers. The output generated a landscape scale layer that held four different attributes for fuel models.

CART Analysis Classification and regression tree (CART) analysis is a powerful data-mining technique, traditionally used for machine-learning, but is now finding favor as a tool for ecology (De'ath and Fabricius, 2000). CART analysis explains the variation of one response variable by examining one or more explanatory variables which can be a mix of nominal or ordinal data (De'ath and Fabricius, 2000). CART analysis is a recurring process that builds 'trees' by separating the response variable into more and more homogenous classes using the best-fit explanatory variable. The best-fit is determined by the highest information gain or simply, the difference in entropy when using a certain explanatory variable (Quinlan, 1993). The analyses used in this project were J48, an implementation of the C4.5 algorithm defined by Quinlan, and Random Forests, a process which builds multiple independent trees from randomly selected attributes and outputs the mode of classification for all trees (Breiman, 2001). The C4.5 algorithm allows for missing values in the dataset which were present in this project where the photo series classification lacked digital photos for 7 plots. Both analyses were computed using the WEKA software package (Hall et al., 2009). Attributes that directly influence vegetation type and understory characteristics were: Species, Elevation, Distance from Stream, Canopy Cover, and Potential Solar Radiation (Krasnow et al., 2009). LiDAR-derived attributes which were added to the classification analysis were: Surface Roughness, STD of Tree Height, BE intensity, and Mean Tree Height. Surface roughness has a relationship with surface fuel loading (Seielstad and Queen, 2003) where it was hypothesized that standard deviation of tree heights and mean tree heights

would give further insight into canopy characteristics not addressed by canopy cover. The response variable used was the photo series classification done by NCLFA personnel that classified 94 plots with 7 missing values.

J48 (C4.5) analysis was computed on a 10-fold cross-validation and also by training the tree on 66% of the response variable and then testing on the remaining 33%. This process was repeated using the Random Forests algorithm with results in Chapter 4.

Unsupervised Classification The third method of classifying fuel models used a fusion of different layers in an unsupervised classification algorithm provided by Leica Geosystem's Imagine software. The traditional use is for landcover classification using different bands of a Landsat image. This project created a 'layer stack', which is a collection of multiple rasters that cover the same geographical area stored as a single data file. Each layer in the stack can be used like an individual band of a Landsat image; the images do not correspond to spectral reflectance, but represent characteristics about an area that can be used to classify individual pixels. The initial layers used in the stack were based upon Krasnow et al's work, and used: aspect, canopy cover, slope, forest type, elevation, distance from stream, maximum tree height, standard deviation of tree height, BE intensity and surface roughness (Krasnow et al., 2009). These first outputs were strongly dominated by terrain and were discarded. The final layer stack was intended to only analyze LiDAR products and had five rasters: maximum tree height, standard deviation of tree height, canopy cover, BE intensity, and roughness.

CHAPTER 4. RESULTS

4.1 FFS Roughness Analysis

CWD Initially, coarse woody debris was tested against roughness at three resolutions with the best relationship observed at the 9 ha cell size. Fuel classes ‘1000 hour sound’ and ‘1000 hour rotten’ were tested individually and then combined for ‘1000 hour sound/rotten’. The combination ‘1000 hour sound/rotten’ produced the highest correlation (Table 1) of the three, with an R-square statistic of 0.383 (p-value = 0.032). At the 0.05 confidence level, these findings are significant, indicating that a relationship likely exists. However, most of the variation observed in fuel loads is not explained by roughness. This result is somewhat different from another study using similar methods (Seielstad 2003) which noted a much stronger correlation between CWD and roughness in lodgepole pine. For my study, ~60% of variance in CWD could be explained by factors other than roughness, and such a vague relationship using CWD alone was disappointing for estimating fuel loads on the ground. It was desired to explain a larger percentage of roughness ($r^2 > 0.60$) at a higher confidence interval (.001) and I concluded that roughness in Lubrecht did not adequately predict CWD.

Table 1. Linear regression of CWD Sound and Rotten vs roughness (9 ha scale).

<i>Model (n=12)</i>	<i>R-Square</i>	<i>p-Value</i>	<i>SEE</i>
1000 hour Sound (Mg/ha)	.122	.122	.0624
1000 hour Rotten (Mg/ha)	.351	.042	.0536
1000 hour Sound/Rotten (Mg/ha)	.383	.032	.0523

Assessment of Timelag Classes using Stepwise Regression Stepwise linear regression was subsequently used to identify and evaluate individual timelag class contributions to the roughness/fuels relationship. Additional fuels variables such as Forest Floor Mass, and Small Live Tree were also included in this analysis. Mean aggregated values of field fuels estimates were used at 9 ha and 2.25 ha, while at the plot level (0.07 ha) total values were used. Pearson correlation was applied to examine inter-component

relationships (Table 2). Remaining components that met the significance threshold of 0.05 were identified by the highest partial correlation values.

Table 2. Pearson correlation and significance between individual fuel components.

		1 Hour	10 Hour	100 Hour	1000 Hour Sound	1000 Hour Rotten	Forest Floor Mass	Small Live Tree
Pearson Correlation	1 Hour	1.000	.454	-.100	.053	.157	.256	.000
	10 Hour	.454	1.000	-.126	.138	.174	.332	-.021
	100 Hour	-.100	-.126	1.000	.166	-.059	-.019	-.023
	1000 Hour Sound	.053	.138	.166	1.000	.003	.086	.003
	1000 Hour Rotten	.157	.174	-.059	.003	1.000	.186	-.005
	Forest Floor Mass	.256	.332	-.019	.086	.186	1.000	.123
	Small Live Tree	.000	-.021	-.023	.003	-.005	.123	1.000
	Sig. (1-tailed)	1 Hour	.	.000	.019	.138	.001	.000
10 Hour		.000	.	.004	.002	.000	.000	.328
100 Hour		.019	.004	.	.000	.110	.347	.317
1000 Hour Sound		.138	.002	.000	.	.479	.036	.479
1000 Hour Rotten		.001	.000	.110	.479	.	.000	.462
Forest Floor Mass		.000	.000	.347	.036	.000	.	.005
Small Live Tree		.499	.328	.317	.479	.462	.005	.

The best stepwise analysis was at the 9 ha scale with an r-square of 0.862 (p-value = 0.037) using Forest Floor Mass plus 1 Hour Material (Table 3). While Forest Floor Mass was a recurring factor at all three scales, inter-correlation between fuel components was high, indicating that it is difficult to distinguish between any one fuel component using roughness with our datasets. Surprisingly, 1000-hr fuels (CWD) were not picked out by the regression.

Table 3. Stepwise regression (roughness – fuels) results at three scales.

Stepwise Regression at 9 ha

<i>Model (n=12)</i>	<i>R-Square</i>	<i>R Square Change</i>	<i>p-Value</i>	<i>SEE</i>
Forest Floor Mass (Mg/ha) ²	.770	.770	.000	0.0319
Forest Floor Mass (Mg/ha)²	.862	.092	.000	0.0261
1 Hour Material (Mg/ha)				

Stepwise Regression at 2.25 ha

<i>Model (n=48)</i>	<i>R-Square</i>	<i>R Square Change</i>	<i>p-Value</i>	<i>SEE</i>
Forest Floor Mass (Mg/ha) ²	.640	.640	.000	.0407
Forest Floor Mass (Mg/ha) ²				
Small Live Trees (Mg/ha)	.692	.052	.000	.0381
Forest Floor Mass (Mg/ha)²				
Small Live Trees (Mg/ha)				
1 Hour Material (Mg/ha)	.737	.045	.000	.0356

Stepwise Regression at 0.07 ha

<i>Model (n=432)</i>	<i>R-Square</i>	<i>R Square Change</i>	<i>p-Value</i>	<i>SEE</i>
Forest Floor Mass (Mg/ha) ²	.150	.150	.000	.0870
Forest Floor Mass (Mg/ha) ²				
Small Live Trees (Mg/ha)	.201	.051	.000	.0844
Forest Floor Mass (Mg/ha)²				
Small Live Trees (Mg/ha)				
1 Hour Material (Mg/ha)	.231	.030	.000	.0829
Forest Floor Mass (Mg/ha)²				
Small Live Trees (Mg/ha)				
1 Hour Material (Mg/ha)	.239	.008	.000	.0826
100 Hour Material (Mg/ha)				

Intuitively, it would be a stretch to consider 1 hour fuels contributing to a relationship with roughness in any sense as they prove to be difficult targets for laser altimetry. Likewise, forest floor estimates are based upon depth of material (below ground) which is beyond the capacity of LiDAR data to detect. Rotten logs are more feasible targets and due to the management history of the area, may account for a majority of CWD. The crux is that most fuels classified as rotten have a low profile on the surface, nominally contributing to roughness. The only viable fuel component attributable to laser altimetry left in the model is small live trees, which contributes little to the overall relationship (r-square change of .052). The lack of a sound relationship between roughness and any single fuel component reinforces the notion that roughness is caused by a multitude of features that cannot yet, be distinguished with the field data available for Lubrecht. In short, the reflective characteristics of the fuel bed/forest floor are still not well understood with respect to laser altimetry.

Combinations of Fuel Components Lacking strong relationships with individual fuel components that LiDAR could reasonably be expected to detect, I came to the conclusion that fuel estimates should be combined as their components occur in the field. Consequently, I tested linear regression at the three previously described scales ranked the four variables in order of descending significance as Total Biomass, Total Dead Fuel, DWD Sound/Rotten, and DWD Sound Only (Figure 4). Results show the best relationship (Figure 3) existed at coarse grain (9 ha) where Total Biomass had the highest r-square of 0.730 (p-value < .001). A color-coded breakdown of the 9 ha regression shows that the treatments used in the Fire-Fire Surrogate Study are easily represented by surface roughness (Figure 4). Total Dead Fuel was also predictable to a lesser degree, but both DWD aggregates showed no indication of a relationship with roughness. Looking at larger scales (Table 4, Figures 5,6) yielded r-squares of .568 (p-value < .001) at 2.25 ha 0.094 (p-value < .001) at 0.07 ha Total Biomass. Regression analyses results were ranked by R² values for all three scales (Figure 4).

Table 4

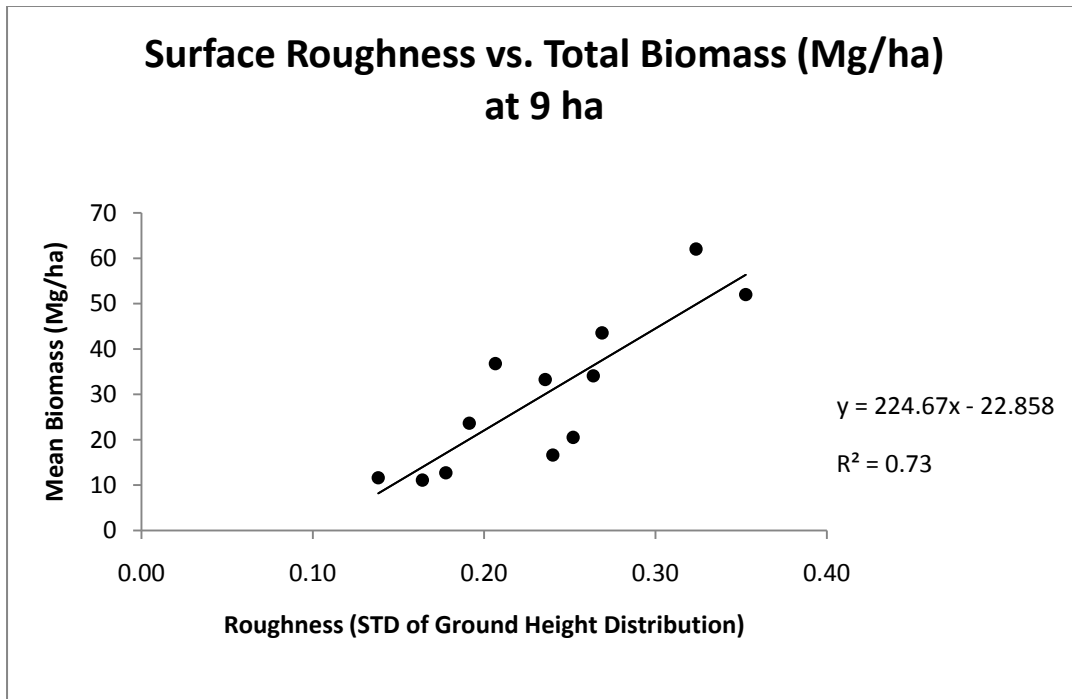


Figure 3. Linear regression plot of the highest correlation between fuel components and surface roughness.

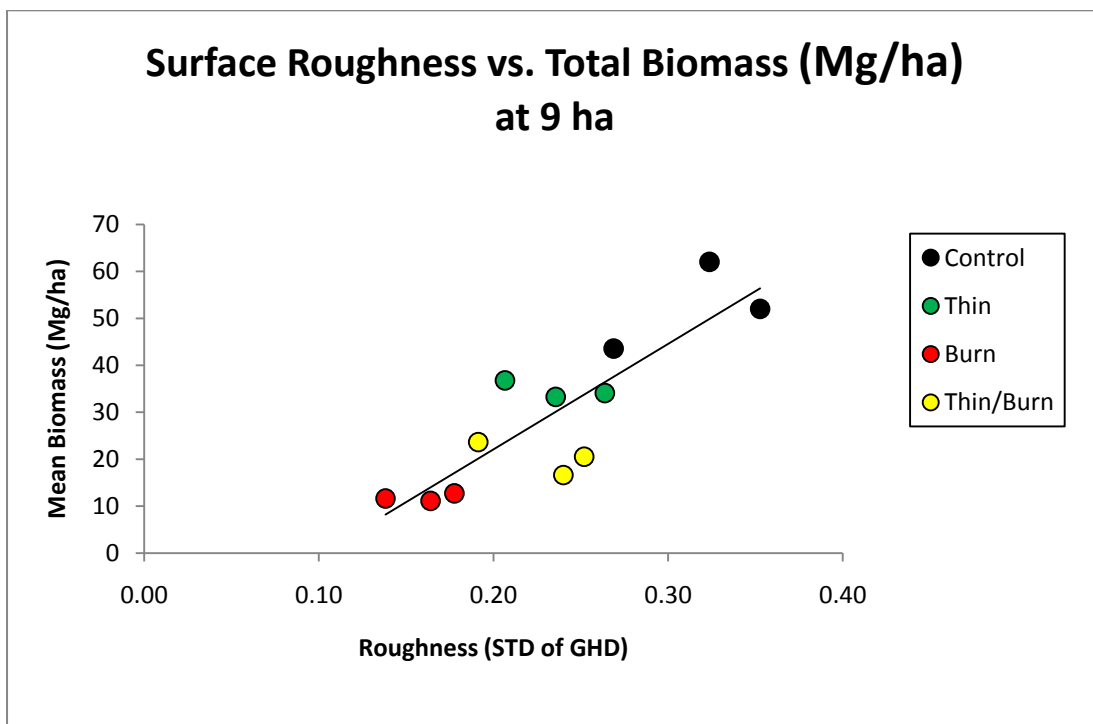


Figure 4. Color coded regression showing different treatment structures and loads with corresponding roughness values.

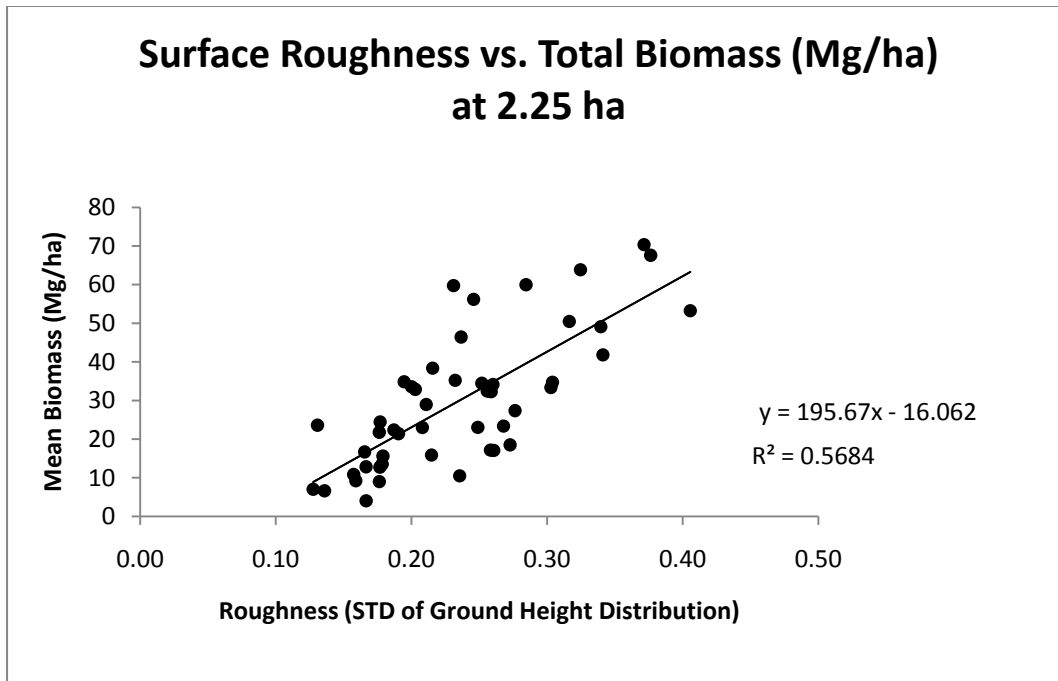


Figure 5. Linear regression of Biomass vs. Roughness at 150m X 150m scale (n= 48).

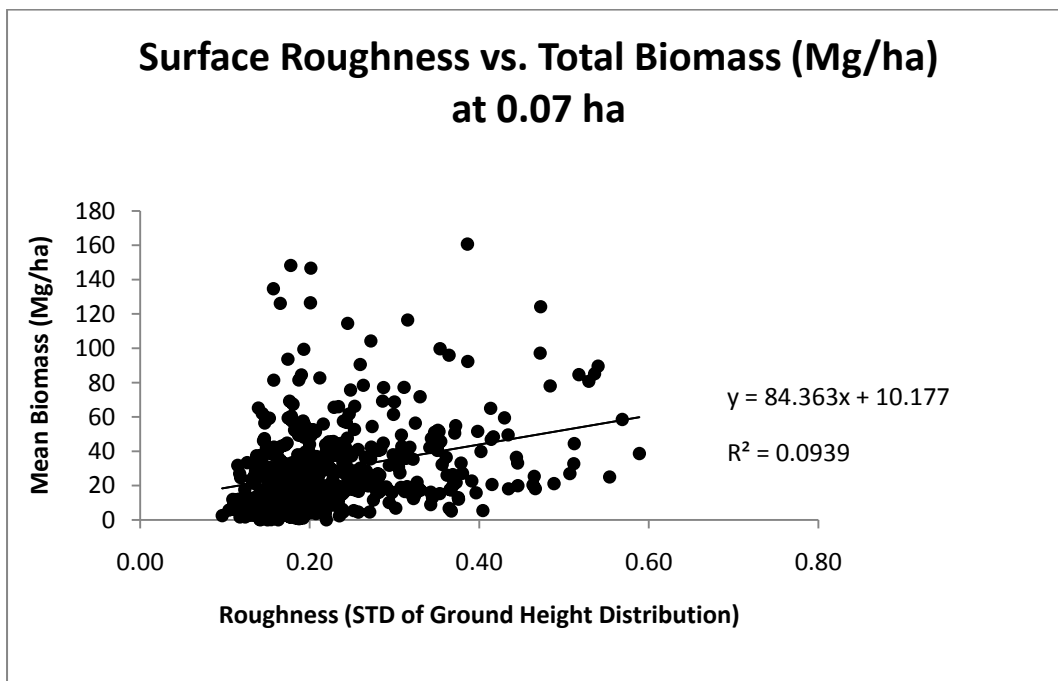


Figure 6. Linear regression analysis of roughness vs. plot level fuels data. Plot is heavily heteroskedastic, indicating high variance of fuels and roughness.

Table 4. Regression Analysis for Aggregated Fuels Estimates vs. Roughness

<i>9 ha</i>	<i>n</i>	<i>R-Square</i>	<i>p-Value</i>
Total Biomass	12	.730	.000
Total Dead Fuel	12	.718	.001
DWD Sound/Rotten	12	.311	.060
DWD Sound	12	.053	.473
<i>2.25 ha</i>	<i>n</i>	<i>R-Square</i>	<i>p-Value</i>
Total Biomass	48	.568	.000
Total Dead Fuel	48	.530	.000
DWD Sound/Rotten	48	.165	.004
DWD Sound	48	.042	.165
<i>0.07 ha</i>	<i>n</i>	<i>R-Square</i>	<i>p-Value</i>
Total Biomass	432	.094	.000
Total Dead Fuel	432	.063	.000
DWD Sound/Rotten	432	.004	.192
DWD Sound	432	.001	.537

4.2 LiDAR-derived Surface Roughness Values

As described previously, surface roughness values were imputed for the entire Lubrecht/Elk Creek area to produce a roughness map showing a maximum value of 1.47 and a minimum value of 2.2×10^{-7} (Figure 7). Intuitively, sections of flat-terrain and agricultural use are relatively smooth. Watershed drainages with variable terrain and greater bio-diversity register higher roughness values. Known areas of high density regeneration also show high surface roughness, and the FFS treatments show a gradient of roughness defined by detailed biomass/fuels estimates. From these roughness estimates, total biomass was calculated on a 9 ha grid by averaging roughness to that grain and applying the 9 ha, Total Biomass regression equation ($y = 224.67x - 22.858$). A histogram of roughness at 9 ha cell size indicates a bimodal distribution, right-skewed (Figure 8). Bimodal distribution is indicative of two separate classes of roughness; lower roughness is representative of close proximity, ground returns where the dominant mode represents positive vegetation/fuel returns.

Total Biomass (Figure 9) predicted for each 9 ha grain indicates a maximum of 211.11 Mg/ha (92.89 T/ac) and a minimum of -22.858 Mg/Ha (-10.06 T/ac). The minimum positive biomass value was 0.043 Mg/ha (0.019 T/ac). Mean biomass was 30.52 Mg/ha while standard deviation was 32.52 Mg/ha. As expected, areas of low biomass are coincident with non-forested areas. High biomass coincides with creek drainages and heavy timber. Total Biomass in the fuel bed for the 23,931 ha Lubrecht Forest is 972,306 Mg.

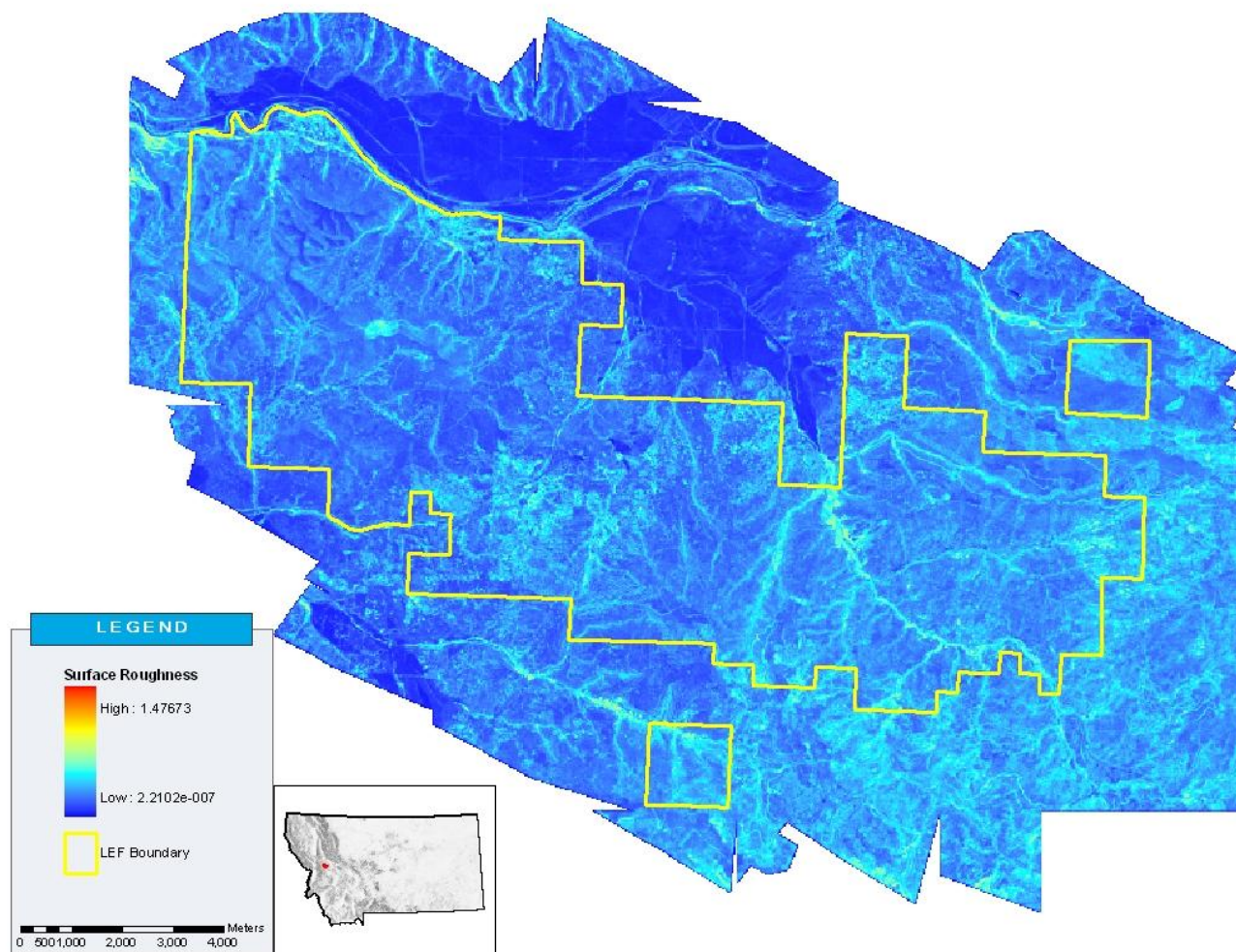


Figure 7. Surface roughness for 2006 acquisition at 1 meter cell size. Blue to red gradient with low roughness as blue, high roughness as red.

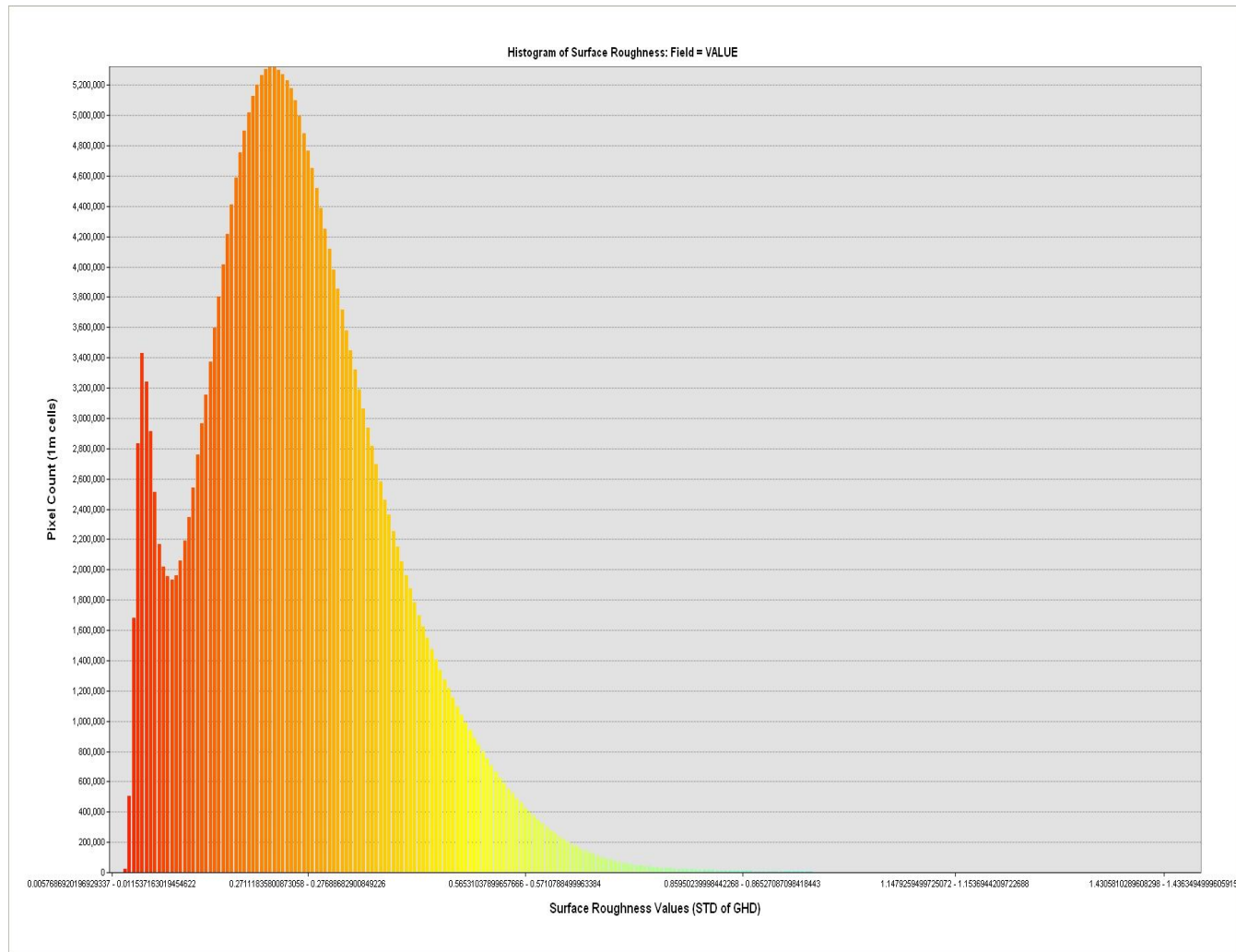


Figure 8. Histogram of Surface Roughness for the Lubrecht Acquisition.

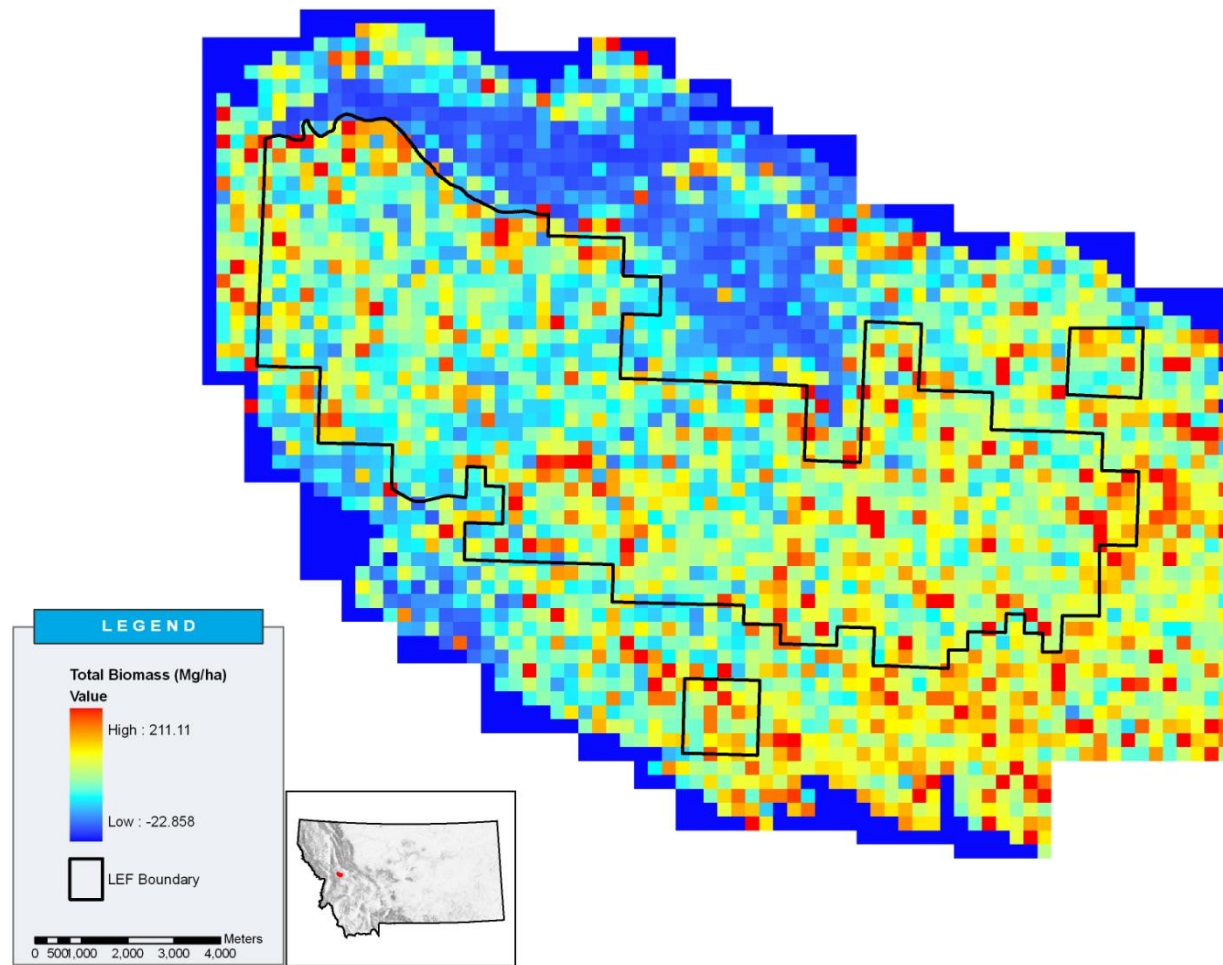


Figure 9. Total fuel bed biomass estimates for 2006 acquisition at 300m cell size

4.3 Fuel Model Classification

As described previously, fuel model classification was performed using the Photo Series method, a Decision Tree, CART analysis, and Unsupervised Classification. The Photo Series classification was conducted to establish a ‘ground truth’ of subjective classifications that reflected the most widely used, standard operating procedure of fuel model classification. Since no definitive data source indicated fuel model classifications for Lubrecht, this classification would also be compared to the LANDFIRE project to assess different ‘ground truth’ data. The RIP collection represented the most current field conditions at the time of the LiDAR acquisition. The Decision Tree approach was a simple straight-forward approach to test assumptions about the physical settings of fuel models. It pivoted around two variables and tested the ability to discern fuel models using percent canopy cover and surface roughness. It would act as an indicator of the further possibility of determining fuel models using multiple LiDAR-derived products. CART analysis was used to expand the notion that decision trees that were regression-based could identify and homogenize the response variables based upon multiple attributes. Unsupervised classification offered a classification technique that was independent of subjective verification. This technique identifies values of each attribute layer and groups classes based upon similar characteristics (Lillesand and Kiefer, 2000). Multiple variables were included in this analysis. They are: roughness, ground return intensity, canopy cover, maximum tree height, standard deviation tree height, elevation, slope, aspect, tree species, potential solar radiation (from slope, aspect, and latitude). These variables were originally described by Krasnow et al., except for surface roughness, bare earth intensity and tree heights (Krasnow et al., 2009).

4.3.1 RIP Photo Series classification

RIP Photo Series used 97 of the available 101 plots (photos were not available for four plots) to classify fuel models. The RIP classification resulted in 37.6% of Lubrecht as a FM2, 23.8% as FM8, 14.9% as FM5, and the remaining classified 16.8% as FM1, FM9, or FM10 (Figure 10). 6.9% of the plots were other fuel models or unassigned due to a lack of photos for classification.

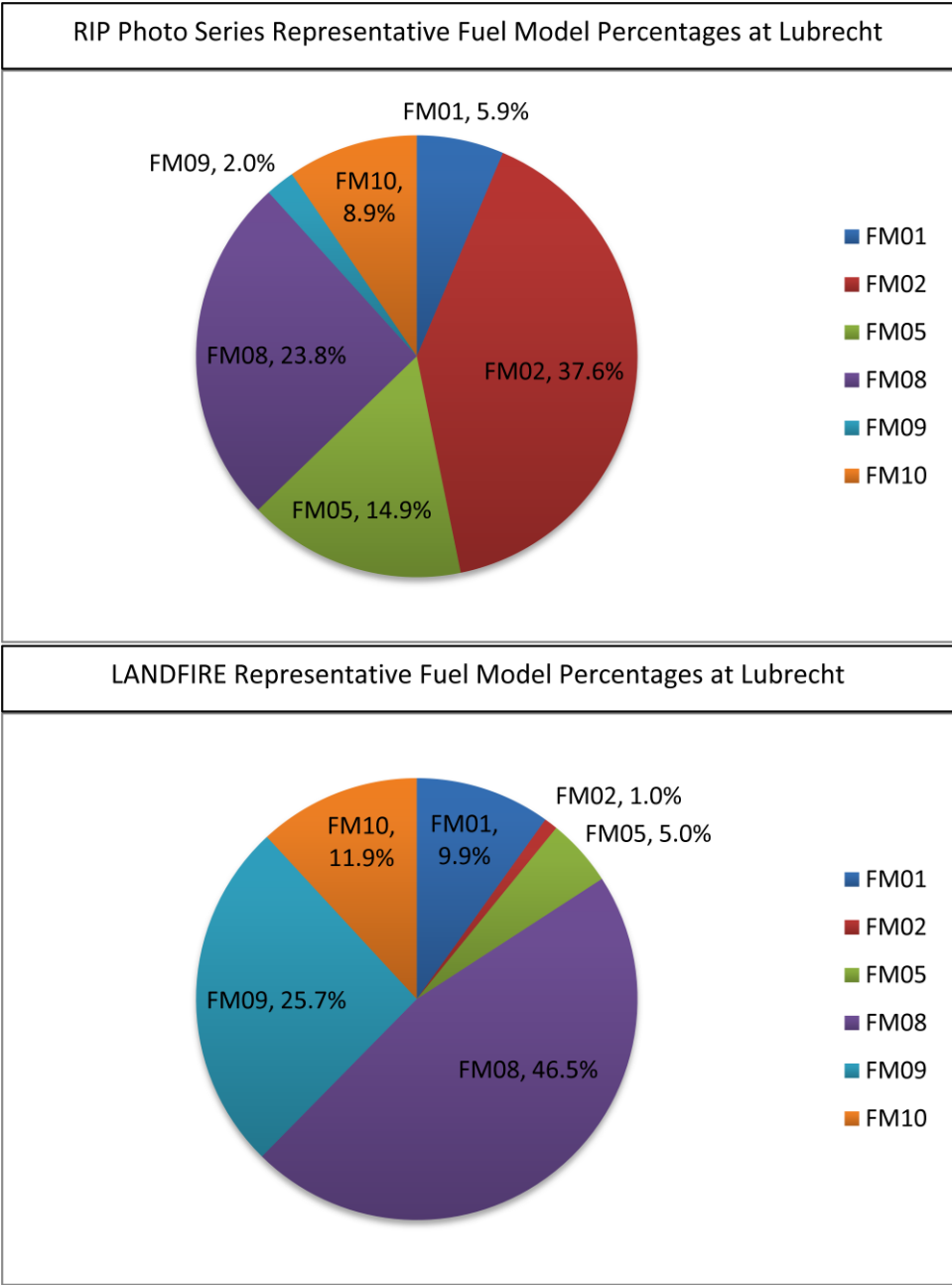


Figure 10. Representative fractions of fuel models in Lubrecht Experimental Forest for Resource Inventory Plots and Landfire classifications.

In my professional opinion and using my field experience at Lubrecht, the RIP classification over-represents FM5 and I would expect as much FM8 if not more, than FM2. I think FM9 is represented fairly well due to a lack of 100% ponderosa pine stands in Lubrecht. However, LANDFIRE probably overrepresents FM 9 and under represents FM2.

4.3.2 Landfire as an independent fuels assessment

Comparisons with the LANDFIRE project were used to evaluate an independent assessment of fuels at Lubrecht. LANDFIRE indicates different proportions than the RIP classification (Figure 10). FM8 is the dominant fuel model in the LANDFIRE classification (46.5%). FM2 is practically non-existent where FM9 is a quarter of Lubrecht. I believe these two classifications are over-represented based upon my field experience and the fact that LANDFIRE has a heavy influence of terrain affecting its classification. A comparison of LANDFIRE to the RIP classification is shown in Table 5.

Table 5. LANDFIRE confusion matrix of four fuel models using RIP photo classification.

Photo Series	LANDFIRE Classification				Totals
	FM01	FM02	FM08	FM10	
FM01	4	0	1	0	5
FM02	3	0	20	3	26
FM08	1	0	9	1	11
FM10	1	0	2	4	7
Totals	9	0	32	8	49
					Accuracy
					34.69%

While LANDFIRE covers the entire Lubrecht acquisition area, this comparison was restricted to the areas the RIP photos could assess. The LANDFIRE project used combinations of biophysical settings to determine fuel models which, in the case of Lubrecht, tend to mirror terrain features (Figure 11).

It was important to cross reference the RIP classifications with LANDFIRE classifications to get a sense of agreement or disparity between the two sources of ‘ground truth’ available to the study. LANDFIRE would be subjectively compared to the Decision Tree, CART analysis, and unsupervised classification with restrictions placed on LANDFIRE concurrent with the limitations of other techniques.

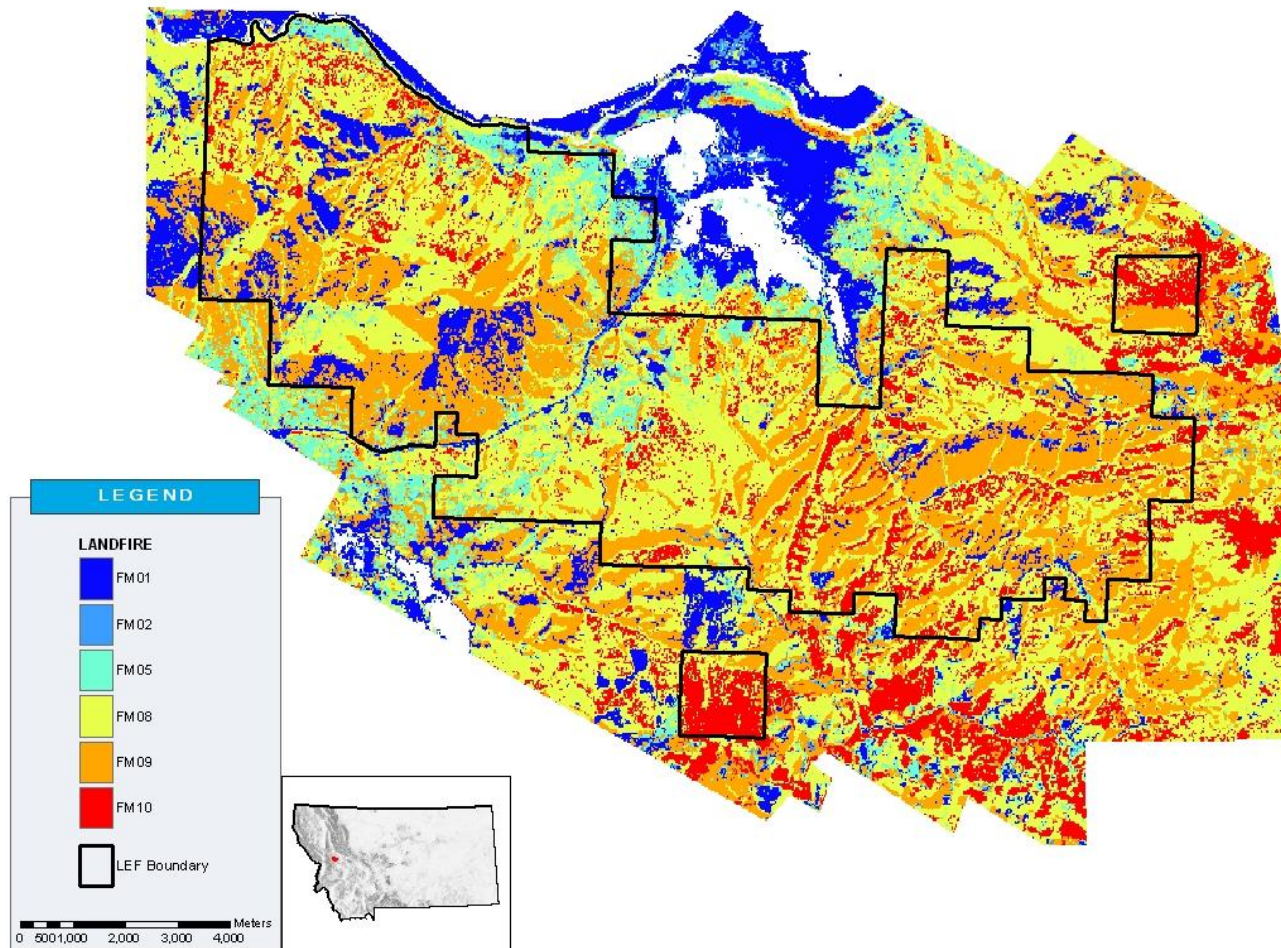


Figure 11. LANDFIRE coverage of Lubrecht showing six fuel models at 30 meter cell size. Open areas were classified as non-forested areas.

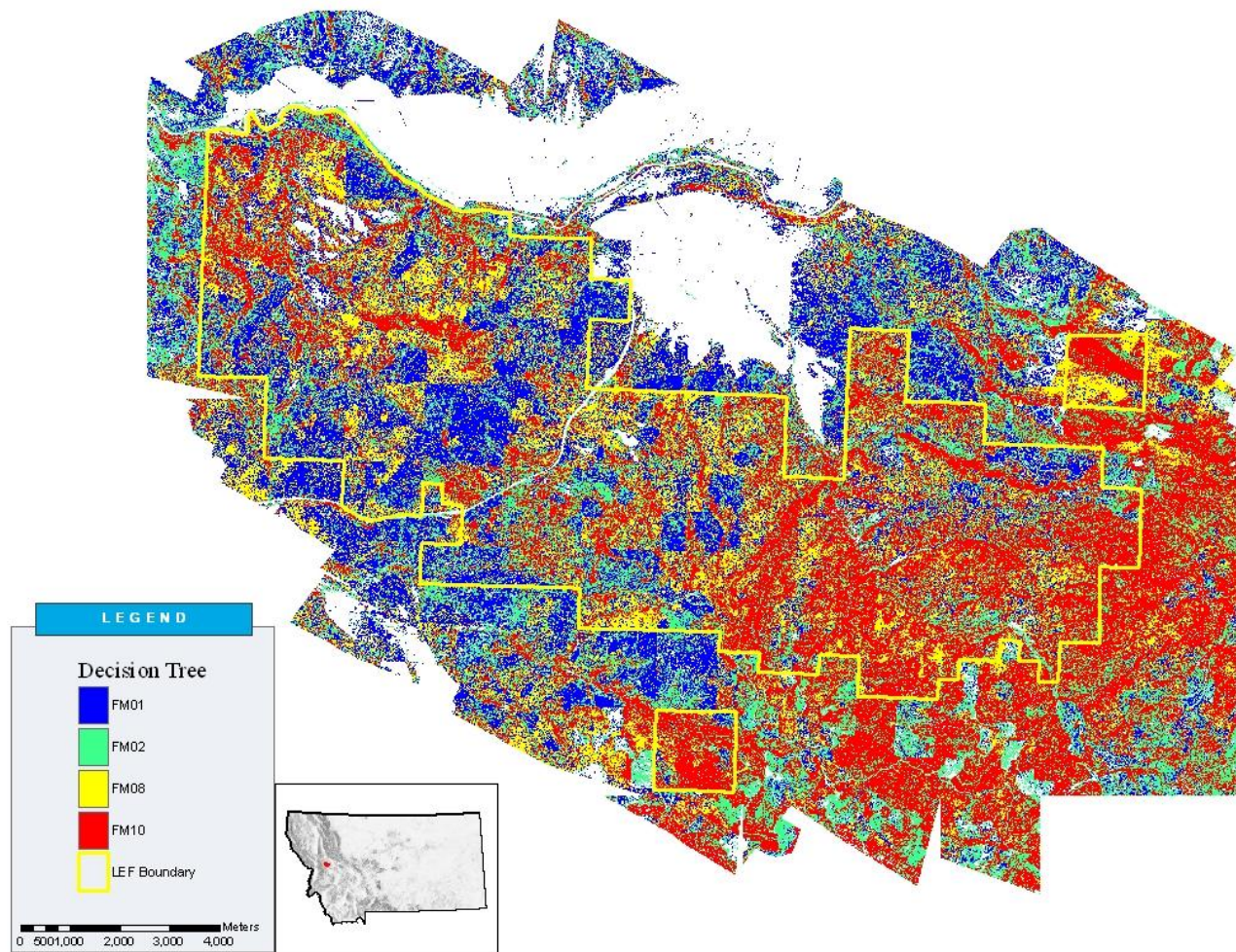


Figure 12. Decision Tree output showing four fuel models within the Lubrecht Experimental Forest at 10 meter cell size.

4.3.3 Decision Tree

The Decision Tree method used median values for canopy cover and roughness and returned values for FM1, FM2, FM8 and FM10 (Figure 12). The Decision Tree method was referenced to the RIP classification (Table 6). An accuracy of 33.77% left many classifications in question and misclassification of FM2 and FM10 indicated a serious flaw in the approach. If we were to assume that the RIP classification was 100% correct, the Decision Tree method under-represented FM1 and FM10. It was an indicator that while 33.77% accuracy showed some promise, the Decision Tree was flawed in using canopy cover to separate even basic fuel model classes (Grass, Shrub, Timber, Slash).

Table 6. Confusion Matrix of Decision Tree vs. RIP Photo Series.

Photo Series	Decision Tree Classification				Totals
	FM01	FM02	FM08	FM10	
FM01	5	1	0	0	6
FM02	12	7	6	13	38
FM08	4	5	6	9	24
FM10	0	0	1	8	9
Totals	21	13	13	30	77

Accuracy
33.77%

4.3.4 Decision Tree and LANDFIRE comparison

LANDFIRE identifies both FM5 and FM9 in Lubrecht (Figure 11) but for a direct comparison to the Decision Tree approach which has only four fuel models, LANDFIRE output was restricted to FM1, FM2, FM8, and FM10. The Decision Tree was referenced to the RIP photo series classifications and LANDFIRE as a baseline investigation into the effectiveness of classification schemes. LANDFIRE coverage of the same area (Figure 11) and decision tree output were cross-referenced (Table 7).

Table 7. Cross-reference of LANDFIRE and Decision Tree Output.

		LANDFIRE Classification				
Decision Tree	FM01	FM02	FM08	FM10	Totals	
FM01	3751	265	10611	1272	15899	
FM02	1971	311	11150	1660	15092	
FM08	534	45	9574	3324	13477	
FM10	640	103	19749	9157	29649	
Totals	6896	724	51084	15413	74117	

Omission		Comission		Accuracy
FM01	54%	FM01	24%	31%
FM02	43%	FM02	2%	
FM08	19%	FM08	71%	
FM10	59%	FM10	31%	

Accuracy in this case is more an indicator of agreement between LANDFIRE and the Decision Tree. Considering 25% of LANDFIRE classification (FM9) at Lubrecht was eliminated, a higher correlation would be expected since FM8 and FM9 are very similar from a remote sensing standpoint and can be mistaken for each other. Accuracy of both LANDFIRE and Decision Tree comparisons to the RIP Photo Series is around 34%, indicating a moderately better than chance classification method.

4.3.5 CART Analysis

CART and RIP Photo Series Classification Four analyses were computed for fuel model classification. An implementation of the C4.5 algorithm named, ‘J48’ and a technique described by Breiman (Breiman, 2001) called ‘RandomForest’ were used. A 10-fold cross-validation and percentage split of 66% training/33% testing methods were used for both J48 and RandomForest. Initial model results showed that the first node split based upon, ‘Species’. While ‘Species’ allowed the greatest information gain statistically, the level of precision of the species layer disqualified it as a dominant attribute. The model showed improvement in true positive and true negative results after the attribute, ‘Species’ was removed.

RandomForest with percentage split testing produced the best results with 14 (46.67%) correctly classified instances and 16 (53.33%) incorrectly classified instances (Table 8). The kappa statistic was 0.2079, showing the highest correlation of the four methods and rated as ‘Fair’ agreement (McGinn et al., 2004). Mean Absolute

Error (MAE) was 0.2167 and Root Mean Squared Error (RMSE) was 0.3353. FM2 had the highest success rate, correctly identifying 10 of 13 observations. Seven FM2 observations were misclassified as FM8 by RandomForest analysis and as will be discussed in Chapter 5, may have more to do with the accuracy of the RIP Photo Series classifications than the RandomForest technique.

RandomForest using 10-fold cross-validation correctly classified 36 (38.30%) instances and incorrectly identified 58 (61.70%) instances (Table 9). Kappa statistic was 0.1288, indicating slight correlation above chance. MAE was 0.2287 and RMSE was 0.3651. While not the most accurate of the four techniques, this method classified a greater population (101) than the percentage split (30). FM2 was correctly identified most often with this method as well. FM2 and FM8 were the most accurately predicted fuel models and showed the highest amount of crossover. Accuracy for Random Forest analyses was similar to the LANDFIRE and Decision Tree classifications (34.69% and 33.77% respectively) again, perhaps an indicator that the Photo Series is flawed.

Table 8. Confusion Matrix of RandomForest Analysis on RIP Photo Series using percentage splits. Correctly identified classes marked in Red.

Classified as:						Field Observations
FM1	FM2	FM5	FM8	FM9	FM10	
0	0	0	0	0	0	FM1
0	10	1	1	0	1	FM2
0	0	2	1	1	1	FM5
0	7	0	1	0	0	FM8
0	0	0	0	1	0	FM9
0	1	1	1	0	0	FM10

Table 9. Confusion Matrix of RandomForest Analysis on RIP Photo Series using 10-fold cross-validation. Correctly identified classes marked in Red.

Classified as:						Field Observations
FM1	FM2	FM5	FM8	FM9	FM10	
1	4	1	0	0	0	FM1
2	20	6	9	0	1	FM2
1	8	3	1	1	1	FM5
2	10	1	11	0	0	FM8
0	1	0	0	1	0	FM9
0	2	3	4	0	0	FM10

J48 testing with percentage splits correctly classified 13 of 30 instances with a kappa of 0.1918, an indication that the agreement between the model and actual classes was marginally above chance. MAE was 0.1928 with RMSE at 0.399. J48 analysis with cross-validation correctly classified 34 of 94 instances. Kappa statistic was 0.106, indicative of a correlation nominally above chance. MAE was 0.2149 with an RMSE of 0.435.

CART and LANDFIRE classification The same four CART techniques, J48 with percentage splits, J48 with 10-fold cross-validation, RandomForest with percentage splits, and RandomForest with 10-fold cross-validation were used to predict LANDFIRE fuel model classes. RandomForest using 10-fold cross-validation produced the best results (Table 10), correctly identifying 43 (42.57%) of 101 observations. Kappa statistic was 0.1314, slight correlation above chance, with MAE of 0.2124 and RMSE of 0.3557.

Table 10. Confusion Matrix of RandomForest Analysis on LANDFIRE using 10-fold cross-validation. Correctly identified classes marked in red.

Classified as:						LANDFIRE Classification
FM1	FM2	FM5	FM8	FM9	FM10	
4	0	0	4	2	0	FM1
0	0	0	1	0	0	FM2
0	0	2	1	2	0	FM5
1	0	2	27	14	3	FM8
3	0	1	12	9	1	FM9
0	0	0	9	2	1	FM10

RandomForest using percentage splits correctly identified 13 (38.24%) of 34 observations. Kappa was 0.0377, MAE was 0.2216, and RMSE was 0.3586 (Table 11). J48 using 10-fold cross-validation correctly identified 32 (31.68%) of 101 observations and J48 using percentage splits correctly identified 8 (23.53%) of 34 observations. Both Kappa values were negative for the J48, indicating no agreement and a predictive power less than chance.

Table 11. Confusion matrix of RandomForest Analysis on LANDFIRE using percentage splits. Correctly identified classes marked in red.

Classified as:						LANDFIRE Classification
FM1	FM2	FM5	FM8	FM9	FM10	
0	0	0	0	1	0	FM1
1	0	0	0	0	0	FM2
0	0	1	0	1	0	FM5
0	0	0	9	5	1	FM8
0	0	0	6	3	0	FM9
0	0	0	6	0	0	FM10

4.3.6 Unsupervised Classification

Unsupervised classification resulted in six classes being populated of the 15 potential classes assigned (Figure 13). I subjectively assigned fuel models to classes using the RIP photos and aerial imagery. RIP photos were used to determine the five best representations of each of the six fuel models. The representative plots were sampled from the unsupervised classification to determine the majority class populating each plot area. Aerial imagery was used to identify areas such as open, grassy fields that presented critical fuel model characteristics. Other known fuel models, such as the FFS units, were used in conjunction with the RIP photos to cross-reference. IR imagery of the area was also used to help identify classes.

Two classes which showed influence from canopy cover, BE intensity, and roughness were assigned to the grass fuel models, FM1 and FM2. FM1 was assigned to the class which had an open overstory and predominantly grass understory. FM2 was the transitional class between FM1 and timbered areas. The dominant factor differentiating FM1 and FM2 was canopy cover. FM1 had little or no canopy present (mean value of 1.3%) where FM2 has some canopy present (mean value of 13.8%). FM2 had a slightly higher mean intensity (192.2 vs. 176.4) than FM1 and a greater mean roughness (0.25 vs. 0.11) than FM1.

FM5 was assigned to a class that was separated from a structurally similar FM2 by mean canopy cover (FM5 = 74.1%; FM2 = 13.8%), mean intensity (FM5 = 146.1; FM2 = 192.2), roughness (FM5 = 0.30; FM2 = 0.25).

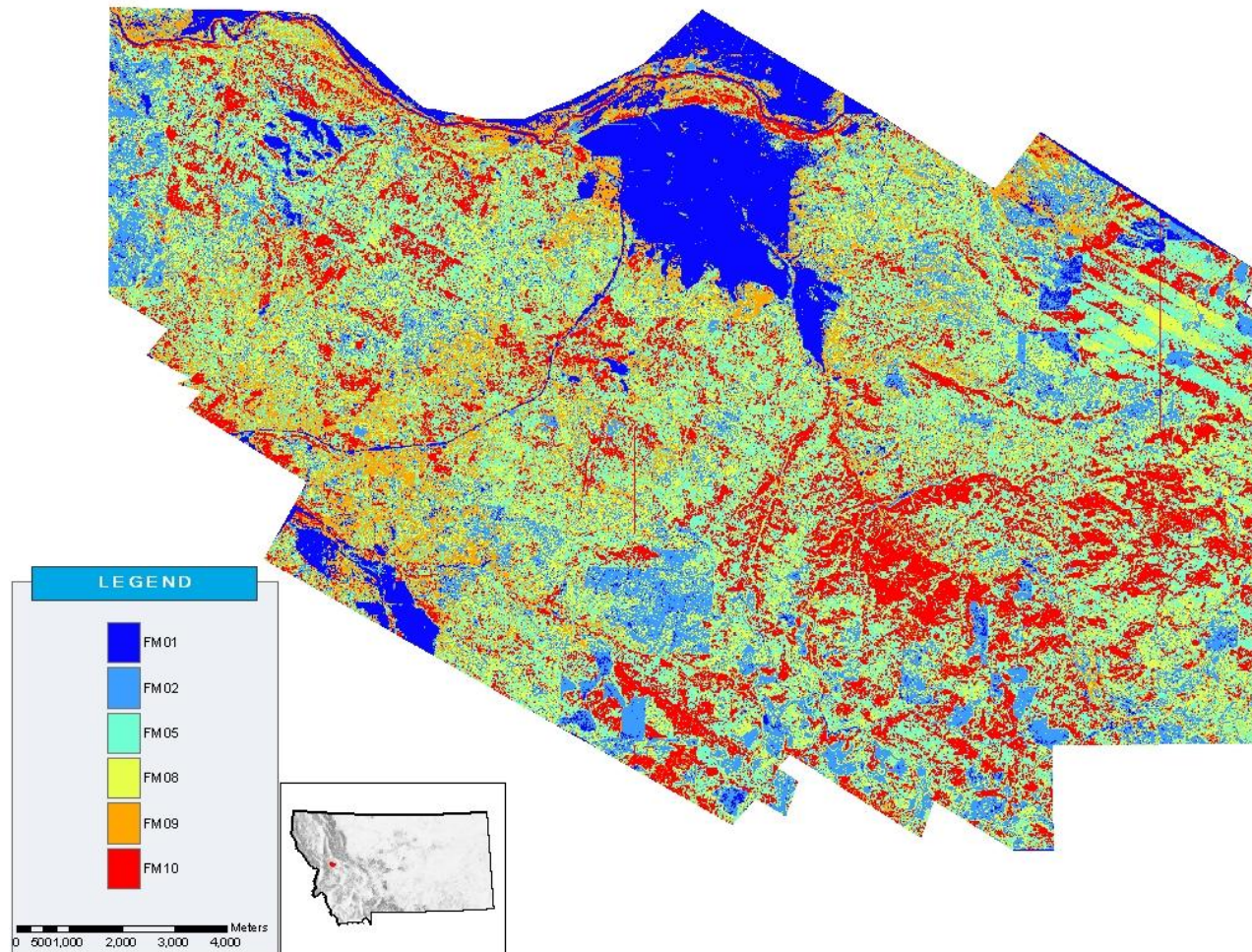


Figure 13. Unsupervised classification of five LiDAR-derived layers resulting in six fuel model classes.

The remaining three classes were assigned to fuel models through a process of elimination and were assumed to be timber fuel models due to the fairly continuous canopy identified with the aerial imagery. It was assumed that since FM8, FM9, and FM10 present increasing fuel loads in the timber group, that they could initially be separated by roughness (class8 = 0.25, class9 = 0.28, class10 = 0.30). The standard deviation of roughness for each class overlapped so much that roughness alone could not separate the classes. Mean BE intensity provided greater separation from the three classes (class8 = 147.8, class9 = 176.6, class10 = 109.7) and standard deviations showed minimal overlap at the tails of the distributions. Mean canopy cover also differentiated the three classes (class8 = 25.6%, class9 = 53.4%, class10 = 84.2%) with minimal overlap at the tails. Timber fuel models were assigned based upon the best available indicator. It was assumed all timber fuel models would have a high canopy cover compared to other general classes. It was also assumed that FM8 would have a low roughness, high intensity return with a moderate canopy cover. Conversely, a FM10 would have high roughness, low intensity, and high canopy cover. FM9 was assumed to lie somewhere between the FM8 and FM10 classes, but identical in structure to FM8. Majority classes taken from the RIP plot areas were used to assign FM8 and FM9. These assignments were subject to the accuracy of the RIP classifications as well as how dominant the majority of the circular area was. Neither maximum tree height nor standard deviation of tree height had any influence on the classification based upon mean values and standard deviations. This was expected as they were included only to detect regeneration which will be expanded on in Chapter 5.

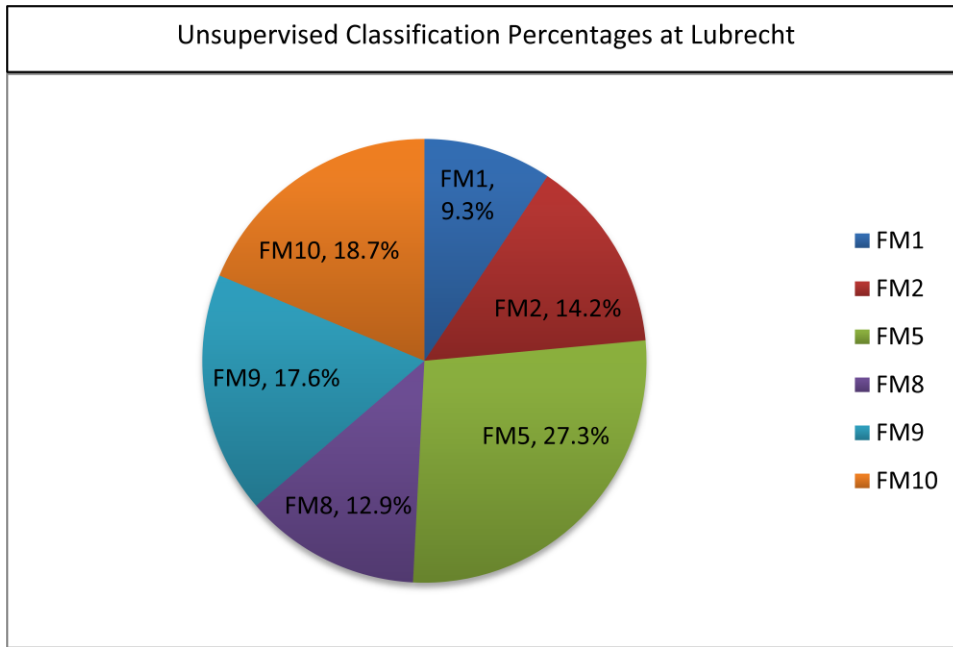


Figure 14. Fractional percentages of fuel models for Lubrecht using Unsupervised Classification.

Because the Unsupervised Classification was assigned fuel models using majority representation of the RIP classification, it would need to be referenced to the other ground truth, LANDFIRE, to independently assess its accuracy. Comparing the Unsupervised Classification to LANDFIRE (Table 12), FM1 performed extremely well. The error of omission is likely due to four non-combustible classes in LANDFIRE being removed for direct comparison. The timber fuel models (FM8, FM9, and FM10) have quite a bit of cross-over and it should be noted that they don't agree exactly on which fuel models are present, but they generally agree on where they are located. FM5, as previously mentioned, is probably over-represented in the Unsupervised Classification. This is made apparent when there are only 4072 cases of agreement on FM5's. The bulk of the Unsupervised FM5's were classified as timber fuel models by LANDFIRE (highlighted total of 68261 cases). Again, it is hypothesized that regeneration within the timber fuel models is structurally and qualitatively identical to FM5 from a LiDAR standpoint.

Table 12. Confusion matrix of LANDFIRE vs. Unsupervised classification.

Unsupervised Classification	LANDFIRE Classification						Totals
	FM01	FM02	FM05	FM08	FM09	FM10	
FM01	12657	1225	892	1734	745	314	17567
FM02	9086	867	3469	16579	7451	1095	38547
FM05	1864	360	4072	33060	23385	11816	74557
FM08	5224	958	4220	11915	10311	2182	34810
FM09	3964	587	3856	23444	13538	2632	48021
FM10	345	132	1580	20003	13225	15702	50987
Totals	33140	4129	18089	106735	68655	33741	264489

Omission		Comission	
FM01	38%	FM01	72%
FM02	21%	FM02	2%
FM05	23%	FM05	5%
FM08	11%	FM08	34%
FM09	20%	FM09	28%
FM10	47%	FM10	31%

Accuracy

22%

Kappa

8%

4.4 Classification method summaries

4.4.1 Fuel model prediction methods and RIP Photo Series

Fuel model prediction using a CART, implementing the RandomForest algorithm with percentage splits of training/test data (CART¹) produced the highest accuracy (46.67%) in predicting the RIP Photo Series classification (Table 13). This accuracy is somewhat skewed due to only 30 total observations used and one class (FM2) representing more than half the total observations (18). CART analysis with RandomForest using 10-fold cross-validation (CART²) used 94 observations and represents the most accurate, statistically sound prediction method. The Decision Tree resulted in 33.8% accuracy but only predicts four fuel models. Where it may better perform is as a first pass examination of basic fuel model groups (grass, brush, timber, slash). Unsupervised classification had the second lowest accuracy (20.21%) that centered around misclassification of FM5, possibly an issue of tree regeneration misidentified as brush, which will be discussed in Chapter 5. LANDFIRE produced the lowest accuracy at predicting

the RIP classification (18.09%). Again, accuracy in this case is more a measure of agreement than the predictive powers of LANDFIRE.

Table 13. Summary of Decision Tree, CART, Unsupervised Classification, and LANDFIRE methods used to classify RIP Photo Series.

RIP Classifications	Classification Methods				
	Decision Tree	CART ¹	CART ²	Unsupervised	LANDFIRE
FM01	23.8%	0.0%	16.7%	100.0%	44.4%
FM02	53.8%	55.6%	44.4%	42.9%	0.0%
FM05		50.0%	21.4%	13.2%	0.0%
FM08	46.2%	25.0%	44.0%	50.0%	20.5%
FM09		50.0%	50.0%	0.0%	0.0%
FM10	26.7%	0.0%	0.0%	24.1%	40.0%
Overall Accuracy	33.8%	46.67%	38.30%	20.21%	18.09%

CART¹ Used RandomForest with percentage split.

CART² Used RandomForest with 10-fold cross-validation

4.4.2 Fuel model prediction methods and LANDFIRE

CART analysis implementing the RandomForest algorithm using 10-fold cross-validation (CART²) to predict LANDFIRE fuel models produced the highest accuracy (42.57%) of four methods (Table 14). As previously noted, this method uses a sound population of observations and of the methods used, presents the best method used to predict LANDFIRE classes. CART analysis with RandomForest using percentage splits (CART¹) and Decision Tree methods produced better accuracy than the Unsupervised classification but, as mentioned previously, have limitations on number of observations and fuel models. Unsupervised classification, while only having an accuracy of 22.21%, used a cell by cell sensitivity analysis for 264489 individual cells and was the most comprehensive method of analysis. Disagreement between the Unsupervised classification and LANDFIRE centered around FM5 and the timber fuel models (Table 12). The regeneration issue discussed later may address the FM5 disparity. Disagreement between timber fuel models is to be expected when a major determining factor between FM8 and FM9 is species composition. FM10 is also expected to be significantly different given LiDAR's ability to penetrate high canopy closure areas and assess roughness where LANDFIRE relied more on

gradient modeling and biophysical settings to derive accumulation and fuel loading levels. These surface characteristics are the main attribute that separates FM8 and FM10.

Table 14. Summary Table of Decision Tree, CART, and Unsupervised Classification methods used to classify LANDFIRE.

LANDFIRE	Classification Methods			
	Decision Tree	CART ¹	CART ²	Unsupervised Classification
FM01	23.6%	0.0%	50.0%	72.0%
FM02	2.1%	0.0%	0.0%	2.2%
FM05		100.0%	40.0%	5.5%
FM08	71.0%	42.9%	50.0%	34.2%
FM09		30.0%	31.0%	28.2%
FM10	30.9%	0.0%	20.0%	30.8%
Overall Accuracy	31.00%	38.24%	42.57%	22.21%

CART¹ Used RandomForest with percentage split.

CART² Used RandomForest with 10-fold cross-validation

CHAPTER 5. DISCUSSION

In this chapter I discuss the work flow of the project the results. I will address the different points of the project in the same order they were presented in Chapter 4.

5.1 Data/Acquisition

The LiDAR acquisition used for this project was an aggregate dataset using data from 2005 and 2006. On the eastern half of the 2005 data, pre-flight high terrain elevation calibration was done incorrectly which resulted in heavy ‘pitting’ of the DEM. These error points were severe enough in certain areas to require a second mission to be flown in 2006. The newer acquisition covered several tiles on the east and southeast areas of Lubrecht and the issue of ‘pitting’ was resolved. The temporal discrepancies between 2005 and 2006 were assumed to be insignificant because annual fuel accumulation should be nominal in one year time span absent significant disturbance. There was no documented disturbance and the acquisition pre-dates significant mountain pine beetle activity in the area. Consequently, it was also assumed that the aggregate dataset was continuous across the entire study area and 2005/2006 data were merged for analysis.

The average LiDAR point density was 0.44 points per square meter for approximately 28,000 acres. Common resolutions for a study area of this size are 10m and 30m cell sizes. In general, I performed neighborhood analyses at 10m cell size and resampled to coarser resolutions. While this is a rich dataset compared to other remotely sensed data at Lubrecht, it is still a low density acquisition compared to other LiDAR datasets. The relatively high resolution of this dataset allowed for analysis at multiple scales and delineations and was optimal for a study of surface roughness and fuels.

5.1.1 Integrity of BE/CAN Classification

The unsupervised classification of Bare Earth points using TerraScan software is a robust technique that has been used on many LiDAR datasets. Each run needs to be calibrated for unique acquisitions in regards to the steepest allowable iteration angle. In short, the algorithm iterates between angles of slope for neighborhoods of points. The majority of issues with this project’s calibration dealt with misclassification of BE points due to steeper than expected terrain (e.g., near-vertical terrain in road cuts and in rocky outcrops. Two sources of error, auto-

misclassification and manual misclassification, are accepted in this project. Sources of misclassification within the unsupervised classification are attributable to, terrain features, rocks, and manmade structures. Rock outcroppings and manmade structures were sparse such that they had little impact on the final dataset. Terrain features that obviously affected larger areas were manually reclassified by several individuals of varying technical expertise. For example, one entire uphill slope of a roadcut was classified a vegetation, but when the imagery was referenced, it showed bare soil. No ground hits were present on the slope, an area of about 1/10 an acre, and the analyst had to essentially reconnect the ground across the slope. This required determining which vegetation points were actually ground points by making a judgment call based upon visual arrangement. The method of manual re-classification done with this project certainly introduced some uncertainty due to the subjective nature of reclassification based upon operator judgment. While these errors are acknowledged, they represent a small fraction of the entire dataset and were accepted as having little impact.

5.1.2 Transformations Applied to Data

Geographic transformations from the native GCS to UTM projection had a minute affect on positional accuracy. Normally a transformation would have little influence but due to the high degree of accuracy and precision that a LiDAR dataset affords, these minor fluctuations in position affect large scale measurements greatly. The scales at which the analyses of this project were conducted were at a far coarser scale than the introduced positional errors could affect. The assumption that positional differences of centimeters or even meters did not significantly change outputs, especially when one considers central tendency, low-pass filters were applied to the data before arriving at the final outputs.

5.2 Surface Roughness

High variations in roughness complicate matters when trying to relate it to fuels that are already highly variable. It is accepted that slight positional error exists with LiDAR data as well as the fuels data. When high variations in roughness are produced, as they were with the Lubrecht data, there is no hard and fast way to determine what on the ground caused the roughness. The roughness raster produced was at 1m resolution (using a 5 meter radius neighborhood), a fine scale for most datasets. The difficulty lies in associating ground fuels with

the values presented on the raster. The finest scale available from the fuels data was the 30m plots, which a 1m resolution raster samples on average, 703 times to produce a single value for a 30m diameter circle. When fuels were correlated to a single roughness value derived from 703 individual cells, there was such a large range of roughness values represented that a single quantifiable estimate was more a matter of chance. Without the ability to assign a small range of roughness values to a small range of fuel loads, the only sound assessment that could be made with the relationship present was qualitative, an attribute that is dubious at best at finer scales. Finer scale analyses are also more susceptible to variation and outliers due to the smaller populations of values they draw upon. I concluded that I could not reasonably analyze fuels at a 1m resolution or even within a 30m diameter area when I also factored in the assumption that not all roughness present in my data was caused by surface fuels.

Two Brown's transects do not characterize actual fuels variability in a plot as well as one might like. Again, a greater number of transects at different azimuths would better capture the true mean fuel load and stabilize some of the variability. Co-location issues between transects, plot center coordinates, and LiDAR accuracy make it unclear whether the problems come from the field data or the LiDAR data or both. In sum, as with many LiDAR studies, relating remote measurements to field estimates poses many challenges. Based on simple observation that roughness usually corresponds to identifiable features on the ground (downed trees, logs, regeneration, rocks), it is my belief that the roughness metric might do a better job of identifying fuels than field transects. However, we don't have the data to support this inference.

5.2.1 Fuel Bed Parameters

2m Threshold Fuel bed depth presents an issue in the analysis when a large percentage of the total available fuel is a live, small tree component. We used 2 meters as a base depth for surface fuel beds as defined by Albin and also Anderson (Albin, 1976), (Anderson, 1982). At Lubrecht, where CWD is not often the driving force between roughness and fuel load, 2 meter fuel beds may have incorporated more of the canopy/ladder fuels. While ladder fuels are still a component of total available fuel and an interesting facet to look at from a fire behavior standpoint, fuel bed depths need to be evaluated for each acquisition in order to draw a distinction between surface fuels and canopy fuels.

Most of the fuel models present in Lubrecht average a 0.3 – 0.6 meter depth of fuel bed, significantly different than two meters. The two meter fuel bed depth was used in this project because of Anderson and Albini's definitions (Anderson, 1982), (Albini, 1976) as well as the precedent set forth by Seielstad and Queen (Seielstad and Queen, 2003). Using a 2m fuel bed at Lubrecht expands the range of the ground height distribution which affords less sensitive comparisons between roughness signatures. It may be useful to reexamine roughness using a 1 meter of smaller fuel bed, although sample size issues and expected low variability in roughness could confound analysis.

Dead vs. Live The lack of any significant fire events in Lubrecht has resulted in a large amount of regeneration in the fuel bed. Currently there is no way to separate live targets from dead ones using LiDAR. This makes it more difficult to identify the drivers of the roughness/fuel load relationship when it is considered that live regeneration can have the same surface roughness as other fuel components.

5.2.2 Other Causes of Roughness

Generating surface roughness from a LiDAR dataset requires using the Z values to find the standard deviation from the mean Z value, in our case, elevation above Mean Sea Level in meters. As surface roughness goes, the greater the standard deviation, the rougher a surface while the smaller standard deviation represents a smoother a surface.

The information from a LiDAR dataset is fairly rudimentary. It is essential to keep in mind that roughness merely represents relative height differences of individual returns and currently no LiDAR return attribute can qualify a target based on its reflectance as something like multi-spectral imagery can. What we have from LiDAR is explicit x, y, and z coordinates, reflectance intensities, and a chronology of when returns are received, but no valid qualitative measurements. In my study, I focused on using the z coordinate, or height values of the returns and at that, I examined the magnitude of height variations. Many things can cause height differences within a landscape that aren't fuels (e.g. man-made features or terrain features). Roughness anomalies other than surface fuels add complexity to the landscape that must be taken into account before surface roughness alone can be used to assess fuel loads (Figure 15).



Figure 15. Digital photo of RIP plot 81, identified by the Unsupervised Classification as FM10.

Since both man-made and terrain sources of roughness exist in nearly every landscape, it is accepted that they will produce incorrect assessments of fuels if they are included in roughness. Most man-made sources of roughness, such as road edges and borrow pits, can be identified well enough using a GIS and buffering these features for manual inspection and error-correction, but this is time-consuming and technically intensive. Unless a distinct terrain feature is known or identified, natural terrain differences blend in and are indistinguishable from vegetative biomass, especially underneath a canopy. In this study it was assumed that terrain roughness existed but contributed to overall roughness slightly. Man-made features in the FFS study were assumed to be non-existent due to lack of infrastructure throughout the study site.

Deciphering what ‘smooth’ and ‘rough’ mean depends on what kind of surface we are considering. For this study, we are looking at the fuel bed which includes bare earth hits. While we are equating a ‘rougher’ surface to indicate that there is more surface fuel present, at the root level a ‘rougher’ surface can only indicate that there are greater micro variations in elevation. This is true when numerous objects provide a contrast in height but sharply contrasting terrain creates areas of high standard deviation that represent a genuine ‘rough’ surface without necessarily having combustible fuels. During an unsupervised classification similar to the TerraScan algorithm, enough mis-classified terrain features can render the roughness map useless due to the high percentage of incorrect areas. Again, one of the strengths of laser altimetry derived roughness is its cost-effectiveness. Manually checking areas erodes LiDAR’s strength and thus, a reasonable set of parameters needed to be developed to classify large areas without over-extending a budget.

Roughness derived from terrain is usually caused by abrupt changes in elevation. Sinkholes, rock outcroppings, or narrow drainages can provide returns whose elevation exceeds the previously mentioned iteration angle used to classify points as either bare earth or canopy. Rock outcroppings may be classified correctly as bare earth but due to the lack of surrounding vegetation, the relative height differences can indicate roughness that would be incorrectly identified as fuel using the roughness to fuel relationship.

Man-made objects and features can inherently have abrupt elevation changes that contribute to roughness. Buildings, mine shafts, and infrastructure features affect roughness the same way terrain features do by exceeding the iteration angle. The highest man-made contribution to roughness observed in Lubrecht was forest roads and their associated objects. Steep road cuts

into the uphill slope had been classified as vegetation in several areas. Culverts and bridges presented contrasting elevations on the sides of roads that were misclassified as canopy or errors.

5.2.3 Variability of Surface Roughness

The high variability of fuels on the ground shows its complexity in several ways. A natural patchiness in the Control unit of the FFS study and the overall patchiness of Lubrecht was identified by the roughness raster. The variability is high in many areas, indicated by an almost ‘salt and pepper’ appearance of the raster values. While a low-pass filter can homogenize an area, this reduces the accuracy and precision LiDAR has been championed for. It is unclear at this time which component of the fuel bed accounts for the higher areas of surface variability. Regression analysis in this study is contrary to Seielstad and Queen’s findings that coarse woody debris drives the relationship. Coarse woody debris alone shows a weak relationship at Lubrecht and the total available fuel load is highly dependent on small live trees and the Forest Floor Mass contribution. The loose correspondence to roughness that Forest Floor Mass has is important to note because while it is not a measureable fuel component using laser altimetry, it may be related to an ecological function that is. The depth of fuel on the forest floor is partly a function of the overstory’s contribution of down material. One possible explanation is that sites which can support greater amounts of vegetation will naturally have higher amounts of accumulation and depth of forest floor mass. Standard deviation of ground height distribution is higher at these sites due to more targets in the fuel bed. The auto-correlation is hypothesized to be a function of biophysical settings that produce greater volumes of forest floor mass at sites that contain higher populations of viable laser targets.

5.2.4 Sidelap/ Data Density Biases

Sidelap of scanned swaths created strips within the dataset with twice the normal point density. Certain areas within the acquisition had three and four passes made with the sensor. This increased overall density, but resulted in areas with very high density. This point density introduces a bias by providing a richer cross-section of the target area. Sidelap can clearly be seen in certain areas of the surface roughness map and it trends towards higher roughness values. These sidelap artifacts were assumed to be isolated enough to have little effect on the landscape scale of the project. Fine scale analyses in areas of known sidelap would need to identify areas of

higher point density and appropriately decimate them to possibly some central tendency point density.

5.2.5 Mosaicking

Removal of 50m Buffer Removal of the 50 meter buffer around each tile was intended to eliminate processing errors incurred due to a lack of data beyond the tile edge. The overlap into adjoining tiles meant that the buffer area was trimmed back so all tiles could be seamlessly connected together during the mosaic process. The final mosaic showed no drastic variations in

values as the seam edges were encountered and appeared to have worked quite well.

Seam Errors/Interpolation Most tiles were seamless in the final mosaic. However, several border tiles of the acquisition area had slight gaps or distinct seams present. While these tiles had buffer areas, they lacked data points along the left edge of the tile. This is important when the raster of roughness is created, based upon the lowest, most-left point of the tile. That point acts as the initial centroid for the grid array to be built upon. When there is no data, the adjoining grids don't align. When the buffer is removed, it removes a row or column of cells that are not completely within the tile border.

A second source of seam errors occurred throughout the mosaic. In this case, the data was continuous but the magnitude of

adjoining cells of the neighboring tiles contrasted. Because each tile was processed individually, the ranges of roughness differed from tile to tile. The magnitude differences on the edges of seams were artifacts of the mosaic process where a common histogram could have been used to

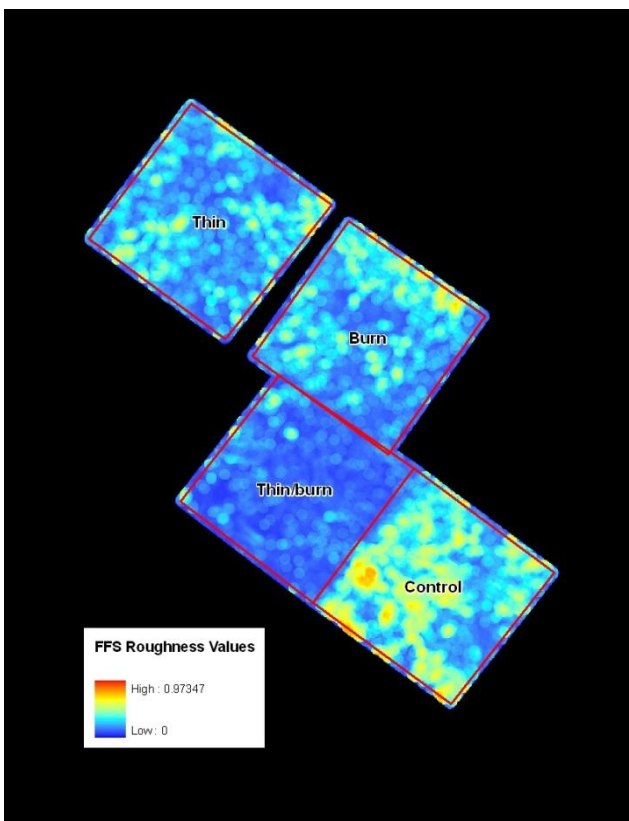


Figure 16. Block 3 of the FFS study site showing roughness raster. Areas of high roughness are coded red with areas of low roughness blue

normalize all the tiles. This was not done to retain the roughness values as a measure of surface roughness instead of producing an arbitrary value which relates only to the histogram.

5.2.6 Validation of Roughness Map

It is interesting to note that intuitively, roughness rasters correlate to surface fuels as one would think. Initial assessment of roughness (Figure 16) shows the untreated control unit having greater roughness and hence, higher probable fuel loading as one might assume about an untreated, undisturbed stand. The Thin/Burn unit also correlates with intuition by showing a relatively smooth surface with little fuel, as to be expected from a unit that has undergone mechanical thinning and subsequent burning. Supporting a quick assumption about a fuels/roughness relationship, the Thin only and Burn only units are of varying degrees of roughness in between (Figure 17).

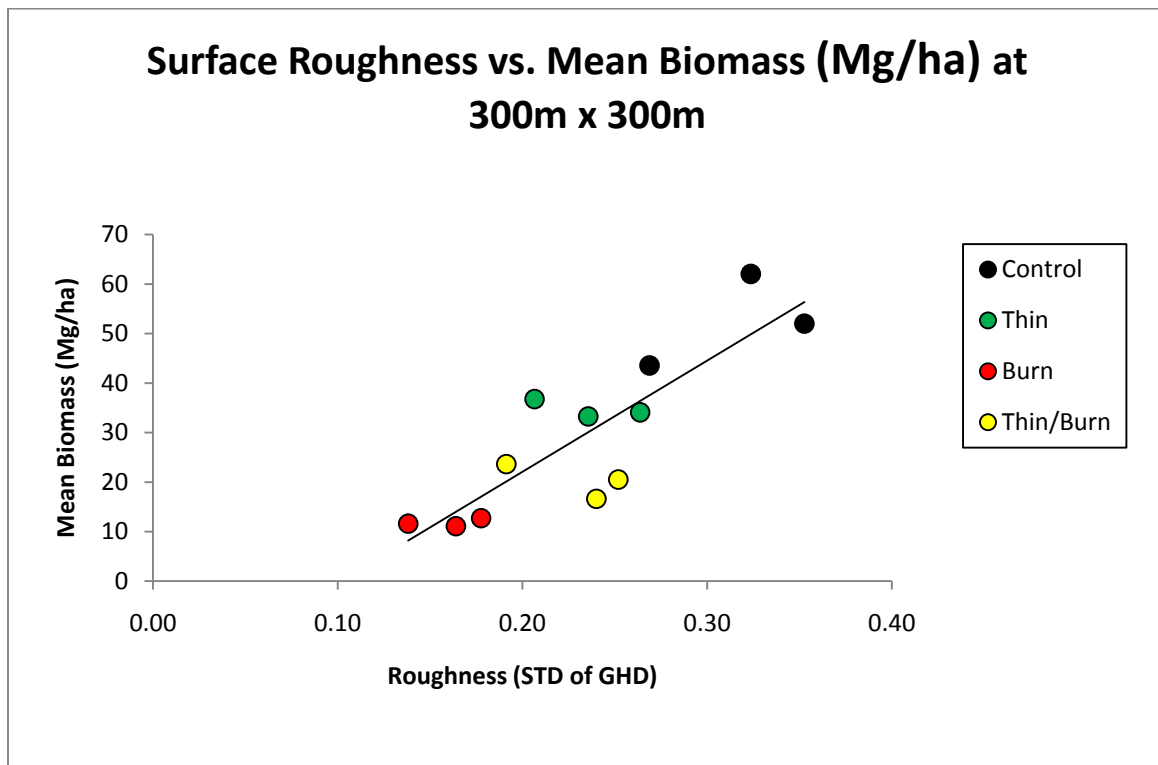


Figure 17. Color coded linear regression of mean surface roughness vs. mean biomass at 9 ha resolution.

The Thin unit should by all rights, have a higher fuel load on the ground due to slash being trampled and left in place. Thin only units on average, have a higher fuel loading than units that were burned but still less on the ground than the control units.

A possible explanation could lie in the live fuel component removed during the thinning process, still present in the control units, that contributes to roughness in acute areas.

Over time, the burn only units would be expected to undergo an accelerated attrition and accumulation of dead fuel just starting to present itself when the LiDAR mission was flown. The field collection of fuel loads was completed in 2002 where the LiDAR acquisition was taken initially in 2005. The three year period between the two may contribute to some disparity between roughness and field estimates. Patchy openings in the canopy created by restoration treatments would allow pioneer species to flourish and enhance roughness that may have been less when the field samples were taken. It is accepted that field estimates of fuel loads might be lower than LiDAR estimate simply due to the fact that the time elapsed allowed for ingrowth of open areas.

5.3 FFS Plot Data

The high variability of estimates from the field data collected at Lubrecht for the FFS study further complicates any direct assumptions about fuels and laser derived products. While the layout and population of sample sites seems adequate, the dependency on capturing appropriate fuel loadings using two Brown's transects alone in Lubrecht is flawed if the intent is to compare on scales of one to tens of meters. The high variability of total fuels from plot to plot and even within single plot transects highlights the need for more decisive field fuels estimations. At the landscape scale, the only conclusion that can be drawn from such highly variable estimates is that the landscape has highly variable fuel loads. LiDAR data is very precise and lacks the human component of data entry. In my opinion, field data is more subject to error and interpretation and I would be more apt to believe the LiDAR data over the field collection for a clearer picture of what field conditions were. I also believe that a more intensive field collection would align itself better with the laser estimates. The stock I put in the laser altimetry is somewhat anecdotal, but it's clear looking at Figure 16 on the preceding pages and Figure 18 on the next page that surface roughness is capturing conditions on the ground at least in some cases.

5.3.1 Brown's Transects

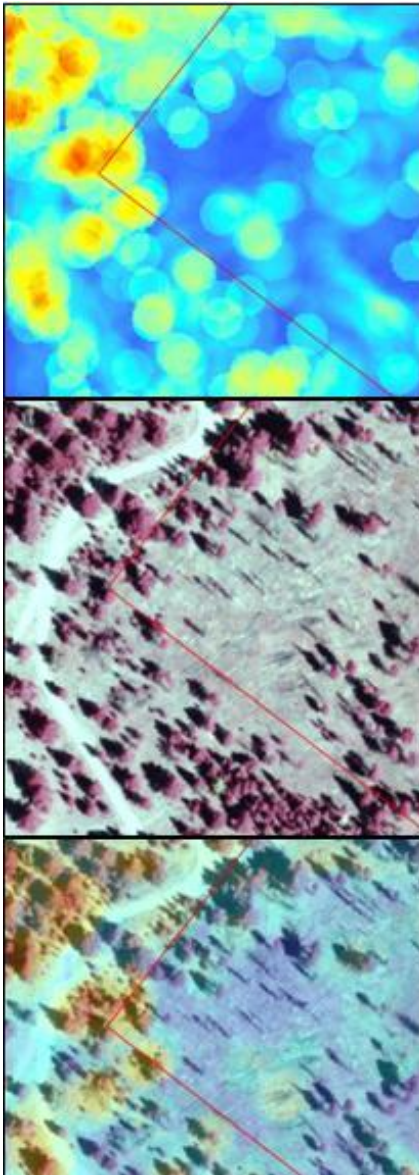


Figure 18. Showing roughness (top), CIR imagery (middle), and overlay (bottom) where roughness identified individual downed tree boles.

The fuels transects taken on each of the FFS plots were indicative of the high variability of fuel loads present in Lubrecht. Many plots had high fuel load estimates for one azimuth while the opposing azimuth held no significant fuel load. The proximity and density of the field collection transects merely highlighted the issue of comparing a different dataset with a highly variable field collection. The variability of fuels and roughness in Lubrecht cannot be understated. Finding the appropriate scale to capture and quantify such variability has proved a daunting task. One perk of LiDAR is that the data has no set scale. As a manager, planning level events may only require small scale analysis, while inventories and projects may require larger scale analyses. The amount of detail will vary and I believe it is best to have the finest scale available to accommodate project scales while retaining the ability to resample for planning scales. It is also good practice to leave as many options open for future use of the data.

The nature of Brown's transects, such as those collected for the FFS study, can lend themselves to a wide range of estimates within a small area. The greatest range of samples taken was sample point 5205 of the FFS study. The first transect reported 9.46 Mg/ha total fuel while the opposing azimuth transect reports 283.07 Mg/ha; all within a 100 ft total sampling plane. 23 plots had one transect which showed some measurement of fuel but no fuel recorded for the second transect, the largest difference being plot 4111 which reported 63.62 Mg/ha for the first transect and 0 Mg/ha for the second transect. The standard deviation of differences between paired transects for all 432 plots was 32.23 Mg/ha which was greater than the mean difference of 22.34 Mg/ha, an indicator of high variability.

What these examples show is the high variability of fuels across the landscape and high variance within sampling points. The Fuel Load (FL) sampling method described as part of the FIREMON project promotes using three sampling planar transects and up to seven if necessary (Lutes and Keane, 2006). Spatial arrangement of transects described in the FL method may provide for a more representative sampling of the non-random orientation of fuels (Lutes and Keane, 2006) that opposing transects can miss. FL protocol suggests positioning the first transect at a 090° true azimuth from the plot center with the second and third transects at 330° and 270° true azimuth respectively from the end of the previous transect.

More is not necessarily better for transects if the design of their layout has faults. Also, time restrictions may not make it possible to collect 7 transects for each of the 432 plots. That being said, more samples of different origins and azimuths in the FFS study may have eliminated the issues of high variance encountered with the two opposing transects. High variability in the fuels estimates makes it difficult to assign a roughness value to a certain fuel load at large scale analyses because of the wide range of loads represented by a single plot.

5.3.2 Positional Accuracy and Precision

Direct measurements of roughness for each return become meaningless if they do not coincide with fuels estimates on the ground. It is not certain that the roughness values indicated by a cell relate to the roughness outside the immediate vicinity. It is also not certain that the roughness values assigned to a cell are coincident with the fuels present. When variability is coupled with positional error, any attempt to directly line up highly variable fuels with their geographically coincident roughness at a fine scale (1m) will fail. The only means available of drawing a conclusive relationship between fuels and roughness is to aggregate roughness up to an area that the fuels data can represent. The smallest area available with our fuels data was the 30m diameter plot, which showed little evidence of a roughness/fuel load relationship. While roughness is indicative of fuels in a landscape absent of other sources of roughness, we cannot say with certainty that at finer scales, roughness represents surface fuels on the ground.

5.3.3 General Sparse Nature of Fuels at Lubrecht

Typical fuel loads for ponderosa pine and Douglas fir stands in western Montana are elusive. Due to fire exclusion and management practices of the last century, a natural range of fuel loads

has been affected by means other than purely ecological. The fuel loads present in the FFS study were thought by several people involved in this project to be somewhat sparse. Compared to fuel loads and fuel models of the Tenderfoot study, the FFS fuels have minimal impact on fire behavior. Measuring, even on the high end, such a sparse fuel load lends itself to the efficacy of roughness as a surrogate for fuels. If meager fuel loads can be detected with a degree of accuracy in mixed-conifer, common fuel loads more prevalent in the northern Rockies would be easier to estimate using LiDAR.

Lubrecht provides an excellent study area but the fuel loads trend towards sparse. At Tenderfoot, coarse woody debris may stack as high as 2 meters and provide a continuous fuel layer throughout the stand. The large range of fuel loads at Tenderfoot may have made detection and segregation more straightforward whereas the small range of fuels at Lubrecht limits the ability to distinguish between differences and variation. While no reasonable fuel model can be discerned from this study, it remains that the relationship between roughness and fuel loads holds at the lighter end of fuel loads and it lends promise towards transitioning surface roughness from a purely academic endeavor to a practical, in-the-field use of laser altimetry when considering the functionality at areas with higher than normal fuel loads.

5.4 Regression Analyses

At this point, it is only safe to say that we can predict total biomass well at a 9 ha resolution, and adequately at 2.25 ha resolution. The relationship between fuels and roughness holds to a lesser degree than Seielstad and Queen's (Seielstad and Queen 2003) findings, and at a coarser resolution. Some errors in estimation are caused by a high variability of both fuels and roughness estimates. This high variability in fuels presented such a range of estimates that no single component could be identified as the landmark estimator that CWD had been for the previous study. At coarser scales, this variability is reduced at the cost of fine scale precision and accuracy that LiDAR datasets could potentially afford to the user. A general mismatch of remote sensing techniques with field data continues to be a problem.

5.4.1 Linear Regression

Linear regression was the most direct statistical analysis for roughness to fuel load comparisons. Seielstad and Queen (Seielstad and Queen, 2003) found that simple linear regression tested their hypotheses more than adequately. One intention of this project was to test the relationship Seielstad and Queen (Seielstad and Queen, 2003) had developed on mixed-conifer forests. The idea was not to re-invent the process but to test proven techniques and methods on a different dataset. Following the linear regression methods offered unbiased insight into the relationship while excluding error and deviation due to methods.

5.4.2 Appropriate Scale

The three scales used for regression analyses were logical divisions of the available data. Plot level was a matter of drawing appropriately-sized circles around plot centers to capture what the Brown's transects represented. On the other end of the scale, the 9 ha areas were defined by the FFS treatment areas with 72 transects per treatment. The 2.25 ha areas were a simple division of each treatment areas into equal quarters, each holding equal numbers of field plots. From my perspective, it would have been better to attempt finer scales but there were no field collections available at anything smaller than the FFS provided. While they were definitely robust, rich data collections for the area they covered, it would be more desirable for similar studies to acquire an extremely intensive field collection over fewer, finer scale plots. A more appropriate study might include a ground-based LiDAR acquisition which would allow extremely fine scale data and multiple fuels transects which were all-inclusive in their estimates. However, even in this case, co-location of the respective datasets might be difficult.

5.4.3 Stepwise Regression

Stepwise regression allowed for multivariate analyses to identify any drivers of the relationship. It also gave insight into how the individual size classes related to each other via a Pearson's correlation. Stepwise regression was a good method for exploring the data. It identified surface fuels as drivers which led us to surmise that some type of auto-correlation had to be occurring in the surface fuels. This was supported by correlation between the size classes.

Realizing that no single fuel component could account for the roughness/fuels relationship led me to begin exploring total biomass, one of the products from this project.

5.4.4 Contributions from Fuel Types

One issue that came up when the FFS field data was related to roughness was dealing with components present in the Total Biomass estimates that are not detectable by laser altimetry. Forest floor fuel loads consisted of newly cast litter and organic material down to mineral soil (Fiedler et al., 2000), sections of the fuel bed not detectable by laser altimetry. This is in direct contradiction to the fact that Forest Floor Mass contributes heavily to the total biomass estimate comprising 44% of the total (Figure 19). In the field study, forest floor mass was destructively sampled and measured by the depth of material underneath a surface the laser would classify as a 'last' return. While 1 hour fuels only contribute 1% to total biomass, in the step-wise regression 1 hour fuels were included in the model with a p-value <0.001, indicating they were significant and improved the model.

The diameters of 1 hour fuels present such small surface areas as targets it was assumed they intercept too little radiation to provide enough reflected energy to register on the receiver. The Pearson's correlation for 1 hour fuels showed significant relationships with 10 hour, 1000 hour rotten, and forest floor mass fuel components (Table 2). It is probable that 1 hour fuels are auto-correlated to other fuel components which are more likely candidates for causing surface roughness and therefore it is not a reflectance issue as much as it is an auto-correlation issue with 1 hour fuels. A possible explanation is that as 1000 hour and 100 hour fuels fall to the surface, they carry many more pieces of 10 hour and 1 hour fuels with them. A single fallen tree bole will register high roughness, but the fuels transect may show a jackpot of smaller diameter pieces if it crosses the crown.

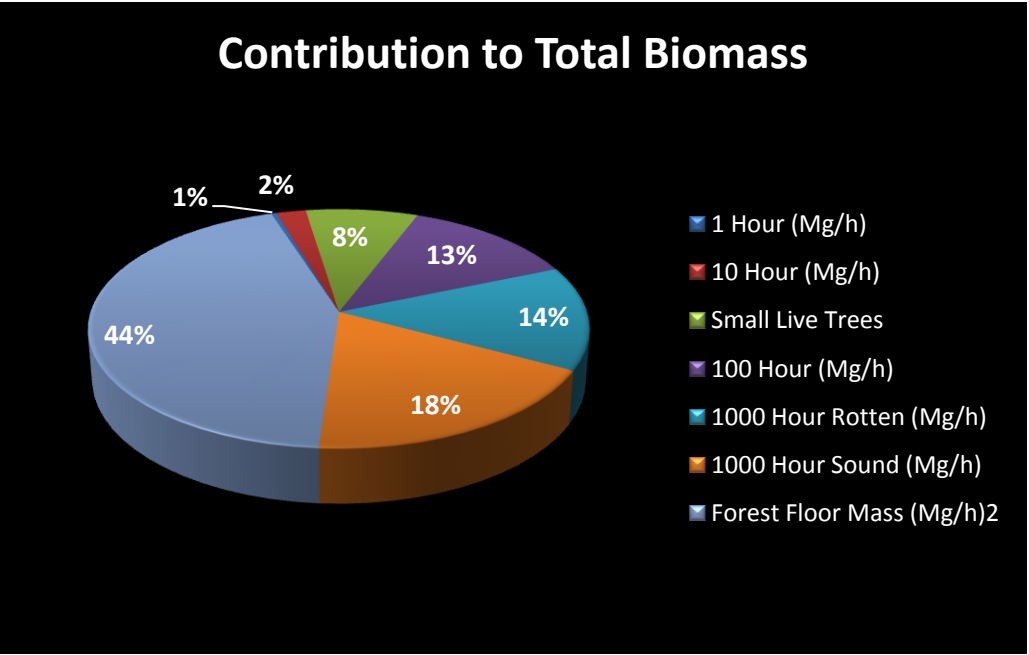


Figure 19. Percentages of single fuel components' contribution to Total Biomass estimate at 300m X 300m scale.

Auto-correlation Forest floor mass may also contribute to the relationship through an auto-correlative function with the coincident vegetation. As shown earlier with the step-wise regression (Table 2) most of the timelag classes are significantly related to each other. This would make sense with a simple observation of downed branches or trees providing many different pieces of fuel of different diameters. Plots with high basal areas contribute greater amounts of material to the litter and duff layers, thus possibly accounting for an improvement of the model by adding a component which is not measureable by LiDAR.

Shrub not captured in field data Shrubs and herbaceous vegetation provide a target which is similar to small, live trees and would contribute to roughness. The field data had no estimates of shrub or herb components that could be compared to roughness. The relationship between roughness and fuels would be diminished when vegetation is present that cannot be accounted for in the field data.

5.5 Biomass Map

Expanding the relationship of roughness to fuels across a larger landscape required the same processing techniques as the FFS data on ten times the number of points. A tiling scheme was established early on in the pre-processing stage to facilitate the limitations of the computer hardware. Raw data points were extracted from flight lines by tile before being classified or processed further. Each tile was 2100 m by 2100 m with the intention of stripping away a 50m border on all four sides to eliminate edge effects. As the data ran out to the edge of a tile, it incurred errors due to sampling from areas of no data that influenced the roughness values. The remaining ‘cores’ of the tiles were mosaicked, creating a final product that was a seamless assessment of roughness across the entire acquisition at the landscape level (Figure 20).

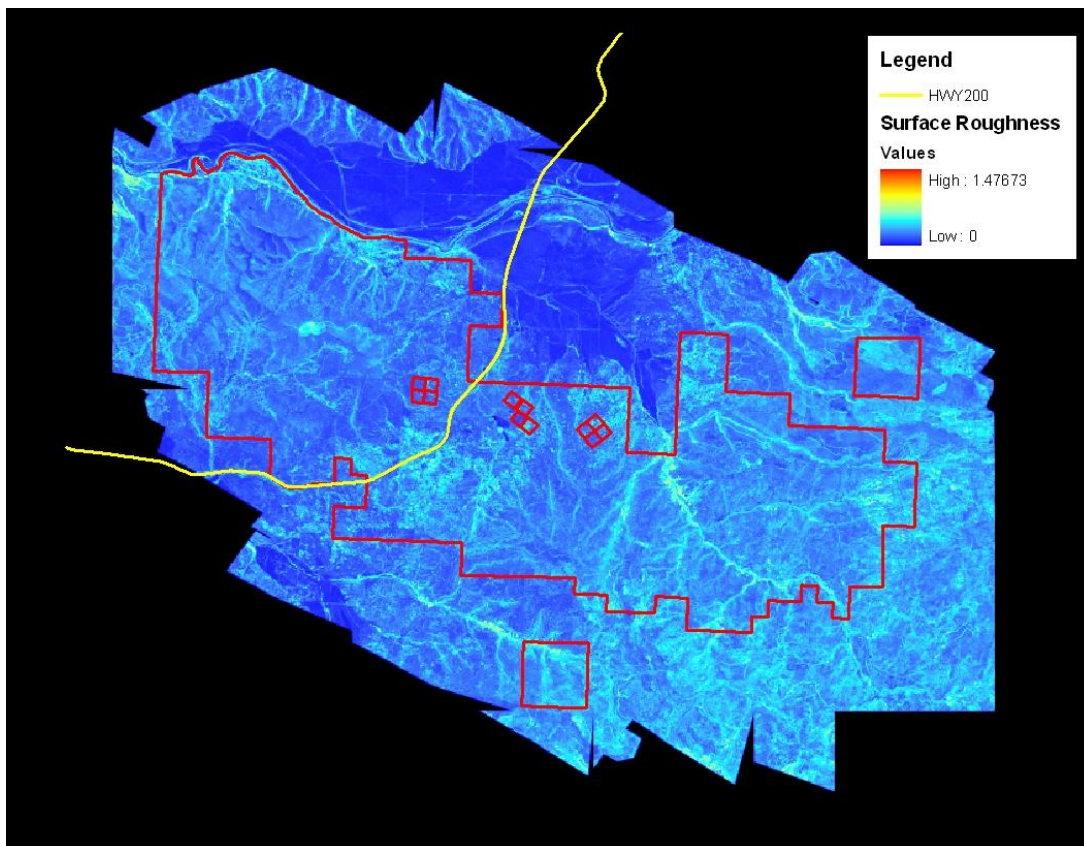


Figure 20. Surface roughness of 2005-2006 Lubrecht LiDAR acquisition.

A total biomass map was created from the roughness map by resampling the 1m cell values of the roughness map up to single 300m cells to reflect the highest resolution fuels could be

predicted effectively at. The regression equation ($y = 224.67x - 22.858$) from the Total Biomass vs. Surface Roughness at 9 ha analysis (Figure 3) was used to calculate fuel values for the 300m cell mean roughness raster (Figure 21). These values reported in were Mg/ha and as each 300m cell represents 9 hectares, the final values were multiplied by 9 to give a fuel load value for each cell in megagrams.

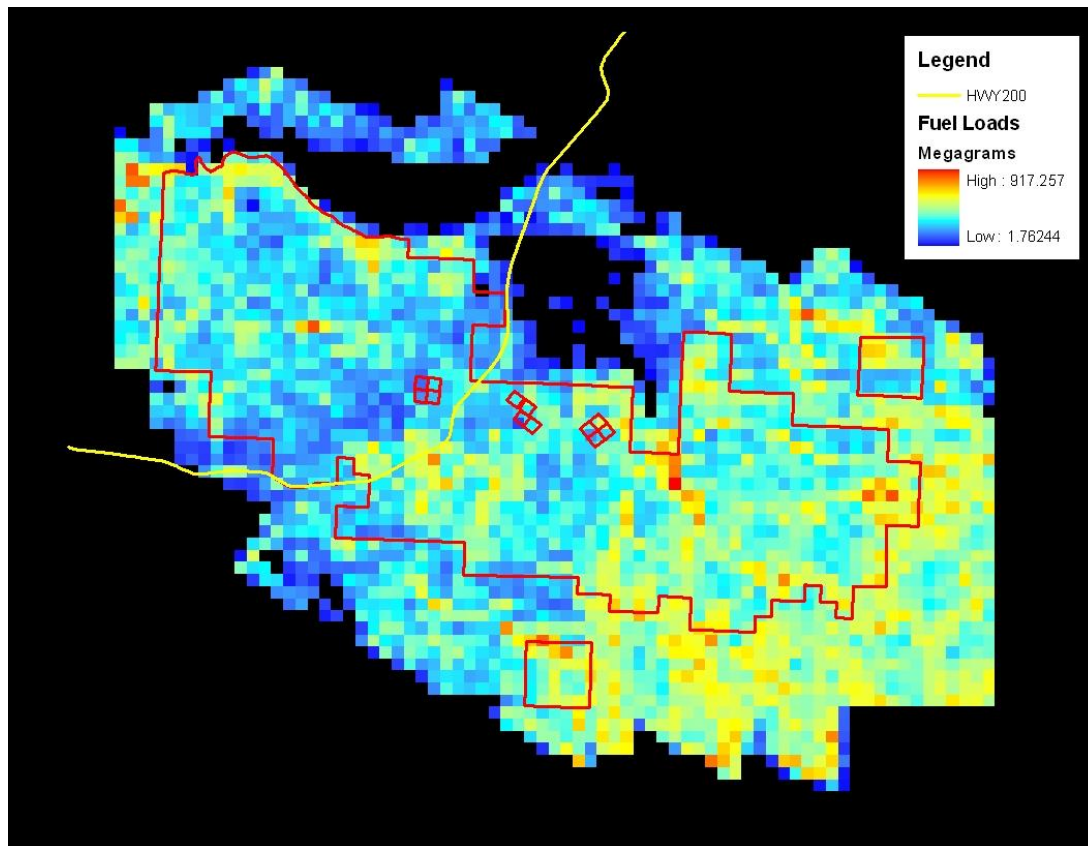


Figure 21. Predicted fuel loads (Mg) for Lubrecht at 300m cell size.

5.5.1 Scale

The resolution of the Total Biomass map is fairly coarse when compared with other remotely sensed datasets. Such coarse resolution can only produce landscape scale outputs from the surface roughness/fuel load relationships, but these are still useful for planning purposes and provide a reasonable characterization of field conditions.

5.5.2 Validity

The Total Biomass map appears to be a reasonable representation of field conditions. The heavier loads in the eastern section of Lubrecht have a high tendency to follow drainages and low areas that can support greater amounts of vegetation. Landmark areas of low loads such as the agricultural areas in the northern section and open, grassy fields or water sources show up as either NoData or very low biomass. Results from this project showed mean biomass values of 30.5 Mg/ha and maximum biomass value of 211.1 Mg/ha. In a similar mixed-conifer ecosystem at the Teakettle Experimental Forest in the Sierra National Forest, Total mean C storage of six different stand structures averaged 289.3 Mg C/ha (North et al., 2009). Species composition and climate may account for higher values in the Sierra study but are comparable.

5.6 Fuel Models

5.6.1 RIP Plots

The Resource Inventory Plots provided an evenly spread dataset for fuel model validation. There were a minimum of two photos per plot and up to nine photos from different azimuths and ranges from the plot center. These proved to be invaluable as a subjective source of plot information. No calls on what fuel models the plots represented were made, allowing NCLFA personnel to make unbiased judgments using the Photo Series method of fuel model assignment.

5.6.2 Problems with Human Subjectivity When Classifying from Photos

Human interpretation was the greatest problem using the photo series method to assign fuel models. Individual focus in the photos changes from person to person and differed with experience levels. Some individuals focused on what they perceived would carry fire through the landscape. Others focused on the structure of the overstory and understory and tried to ‘guess’ how the laser would see the fuels. Another option looked at experience with the perceived fuel load and what the rate of spread might be. It was initially thought to use Scott and Burgan’s 40 fuel models but the variability with just Albini’s 13 fuel models quickly negated introducing other sources of variability.

The group dynamic in which the assignments were held also affected the outcomes. A rotation around the room changed the initial response for each plot. The trend with three people was for the following two to not state their fuel model assignment as much as it was to determine

if they agreed with the first response or not. Thus, it was sometimes more about how much someone bought off on the initial responder's pitch for a certain fuel model. This also brought about another slightly annoying side-effect of a group assignment which was a learning and reasoning mechanism that drove future fuel model assignments based upon previous calls. In what I will call the 'sales pitch' for a certain fuel model it was often said that since the group had assigned one plot a certain fuel model, they must then logically assign the current plot that fuel model as well. While I appreciate logical reasoning, it seemed that both groups quickly limited their options due to some apparent set precedent. The Photo Series part of this project would provide a fascinating social dynamics project on its own and underlines a central issue with clearly identifying fuel models: The only real truth we have when it comes to assigning fuel models is the fire behavior they exhibit while they are burning. With this in mind it certainly fosters a healthy sense of skepticism when assessing scientific studies or even 'Company Lines' that have relied upon on the findings of a 'Panel of Experts.'

The Photo Series assignments were used in the absence of any other source of fuel model ground truth. The results from each method of fuel model classification are difficult to interpret with the underlying knowledge that the 'truth' in this case has variability. If we had had the opportunity of a wildfire in Lubrecht to test our fuel models against, as in the Boulder study (Krasnow et al., 2009), the assignments may have gone through some revisions. Without alternatives, the process was accepted as ground truth with the knowledge that outcomes, either poor or favorable, may have been the results of poor ground truthing.

5.6.3 Decision Tree Approach

Identifying fuel models from just LiDAR data used two layers. The first layer was percent canopy cover classified as either greater or less than the median of 61.455%. The second layer was 1m roughness classified as either greater or less than the median roughness of 0.24. Median values were used to mitigate outliers in both canopy cover and roughness rasters which could not be ground truthed. The concept was that we could identify four groups of fuel model characteristics by either open or closed canopies and whether they have a high or low surface roughness (are rough or smooth). The fuel models present in the LANDFIRE dataset at Lubrecht are FM1, FM2, FM5, FM8, FM9, and FM10. FM1 and FM2 should appear in this scheme as open-canopied, smooth surfaced areas. The break point for inclusion into the canopy cover was

the median value. where areas without any canopy points were classified as NoData. Separating FM1 from FM2 would be a matter of identifying areas of NoData that were smooth as FM1's where FM2 should have some margin of canopy present. FM5 would be differentiated by a higher percent canopy cover with a higher roughness value than the FM1 or FM2.

For closed canopy fuel models, FM8 and FM9 can be separated from FM10 by roughness. FM8 and FM9 will have low roughness values, the difference being FM8 is short-needle where FM9 is long-needle litter. Lacking a species map, I made some assumptions about the structure of FM8 and FM9 in Lubrecht. The first assumption was that FM8 in Lubrecht would be smoother than FM9. This was based upon shade-tolerant regeneration being more prolific in a FM9 due to 80 years of fire exclusion. The second assumption was the depth of forest floor mass would be greater in a FM9, as previously mentioned, a possible auto-correlative effect of biophysical settings. As no species map was incorporated into this classification scheme, roughness values alone were used to differentiate the three timber fuel models, selecting appropriate breakpoint values of roughness. FM10 will be on the higher end of the roughness spectrum and as such, requires a separate breakpoint value. From the initial product I then compared it to an independent classification scheme to identify appropriate breakpoint values.

Photo series were available from a sampling study completed in 2007. This study used 101 fixed plots evenly spaced across the entirety of Lubrecht to assess fuels. Each plot had three fuels transects and at a minimum, two photos taken of the plot centers. Both transects and photos were aligned on a 0, 120, and 240 degree azimuth from plot center. I used Anderson's 'Aids to Determining Fuels Models for Estimating Fire Behavior' to assess the fuel models and categorized them into one of the 13 fuel models available. The main focus was on the ground fuels, characterizing them by what fuel component was the primary carrier of fire. I then extracted the point values for each plot from my initial fuels layer to return a fuel model value that corresponded to each of the 101 plots. Photos were only available for 98 of the plots and the initial validation only produced 26 correct matches. Since there were only four models in the fuels layer, 26 correct matches out of almost 100 plots produced results that were no better than chance. Many plots were identified as a FM2 with the photos that were assigned a FM10 from the fuels layer. When I returned to the photos, it was apparent that a high volume of regeneration had affected the outcome. In a mature ponderosa pine stand the primary carrier of fire on the surface is needle litter and grasses. When Douglas fir begins to infiltrate the stand, as is the case

in Lubrecht due to lengthy fire exclusion, heavy patches of fir seedlings add to the fuel layer. In my decision tree approach of open vs. closed and smooth vs. rough, a FM2 should have a closed canopy with a smooth surface where a FM10 is has a closed canopy with a rough surface. Since the canopy cover layer takes a top-down approach, disregarding height, patches of regeneration add to the canopy cover layer. For uses such as LAI, inclusion of regeneration is appropriate because for LAI one is interested in all strata of the canopy. For determining fuel models, it is inappropriate because all we really want is the dominant strata of trees to gain insight into the probable nature of the surface fuels. Adding to the issue of canopy cover, regeneration also provides targets within the fuel bed that account for higher standard deviation and therefore a 'rougher' appearing surface. The combination of the canopy appearing more closed plus a rougher surface, both due to clumps of regeneration cause the decision tree approach to misclassify FM2's as FM10's. It is critical to distinguish between these two due to contrasting rates of spread; FM2 averages around 35 ch/hour where FM10 averages around 7.9 ch/hour. The fire behavior of these fuel models differs greatly and can dictate suppression methods (Anderson 1982). The possible work-around for this issue is to reduce the pool of points used to determine canopy cover from 2m high and up to possibly the canopy base height. This would eliminate most of the negative effects regeneration has on fuel model classification when deciding between FM2 and FM10.

Another issue that arose was misclassification of FM5's. Since the decision-tree approach only allows for categorization into one of four fuel models, FM5's were either determined to be FM2's or FM10's, depending on the height of the brush. As with the previous regeneration issue, areas of taller shrubs and brush create a higher percentage of canopy closure plus higher roughness which results in a FM10. Classification of FM5's as FM2's was a simple matter of DWD vs. live fuels since both are open canopied, rough surfaced fuel models. Misclassification as a FM2 poses less of an issue than FM10 because FM10's represent the areas of greatest concern when dealing with fuel loading. Nonetheless, it is important to differentiate as many fuel models as possible, especially considering that a FM2 burns can burn at 35 chains/hour where a FM5 burns at 18 chains/hour under similar conditions. One possible method to differentiate between FM5's and FM10's is a reassessment of the canopy closure. As a secondary step in the decision tree, separating out generally open canopied FM5's from FM10's would be possible by

training an unsupervised classification of canopy closure on sample plots of known FM5's and FM10's.

Several FM9's were identified from the photo series that correlates to closed canopy, long-needle conifer stands with generally continuous needle litter being the only carrier of fire. FM8's are short-needle stands with nominal fire behavior under normal weather ranges. Rates of spread and flame lengths are 1.6 ch/hour and 1 foot flame lengths for FM8 and 7.5 ch/hour and 2.6 foot flame lengths for FM9. Again, it's fairly critical from a management standpoint that the two fuel models be distinguished. A high percentage of FM9's identified by the photos were classified as FM8's using the decision tree, understandably so when it is considered that FM8's and FM9's share a closed canopy, smooth surface structure. Since significant fire behavior differences exist between FM8 and FM9, it would be useful to separate the two in a classification scheme. A species layer used in the CART analysis was used before concluding that the current species map was unreliable and removed from the attributes. If a species map were available which had a high degree of accuracy and reliability, it is hypothesized that it could differentiate FM8's from FM9's.

5.6.4 Issues with Decision Tree

Limiting Lubrecht to only four fuel models was considered restrictive when several viable fuel models were excluded. Many FM5's, a few FM9's, and two FM4's were identified using the Photo Series method on the RIP data. Because these fuel models were excluded from the decision tree outputs, they then lend weight to misclassification of other fuel models. The variability of fuels and a degree of complexity of Lubrecht has become the recurring theme of this project. To categorize fuel models into four groups, even at 100% accuracy, doesn't best capture the range of variability on the ground. Lubrecht may be somewhat structurally simple, but when the possible fuel models are considered, the rates of spread and flame lengths tend to stand out. Even though Lubrecht can be simplified into 3 basic fuel models (Grass, Brush, and Timber) the focus of the study is to explore the potential of the techniques and science. If these methods and techniques work well at Lubrecht, they can be applied to more complex landscapes with a greater degree of certainty. While a decision tree approach with four outcomes isn't necessarily decisive science, it certainly acts as an indicator of how other classification methods

may fare. Good progress on simple classification methods allow for more complex analyses that might better reflect the field conditions of a complex landscape.

5.6.5 CART Analyses

Classification and regression trees provided an approach to unsupervised classification methods that re-tooled each run according to the results of the previous ones. CART analyses are used extensively in machine learning projects to mine vast datasets and provide dynamic flow-charts which identify sometimes obscure patterns in the data. For ecological applications, they are ideal because they can deal with nonlinear relationships and missing data.

Validation Two methods of validation were used on both the J48 and RandomForest analyses. The first method was a percentage split which held back a third of the original data and created a tree from the remaining two-thirds. The tree was then tested on the portion held back for validation. The second method was cross-validation which divides the original data into even numbered subsets. A ten-fold cross-validation divided the original data into ten equal parts and developed the tree on nine of them. The tree was tested on how well it predicted the tenth subset. This was repeated ten times with each subset held back for testing. The final tree was developed by using the majority nodes for all ten iterations.

Sampling of Attributes Sampling attributes for individual plots was done by finding the mean value for a 75 foot diameter area around each plot center. This was done to reflect the length of each fuel transect collected for the RIP data. It was assumed that only the viewable area of the most distant photo from plot center could be used to determine fuel models using the Photo Series method. The high variability within Lubrecht makes a mean value more and more suspect as the area of the circle increases. While 75 feet diameter represents the absolute best positional accuracy, the geographic error of this project makes a plausible value more like 150 feet. The range of values for each attribute within a 150 foot diameter circle more than likely encompass a multitude of fuel models. Selection of a single-most likely candidate glosses over the possibility that the correct model wasn't necessarily the most common model, but may have been the most geographically correct one. A FM5 surrounded by FM2 is an example of this type of error.

Selection of Attributes Attributes of the landscape which could determine fuel models were similar to the Boulder study (Krasnow, Schoennagel and Veblen 2009) which used the term, ‘predictor variable.’ Most of the predictor variables were already available from on-going NCLFA LiDAR studies and only a few required further processing to create. The predictors used reflected vegetative and non-vegetative qualifiers for fuel models. The ‘species’ layer was used for the first several iterations, but was eventually dropped because its accuracy and resolution were not verified. While ‘species’ had a large influence on the first node of the tree, it became apparent that the species assignments differed greatly from field observations of the RIP Photo Series. The ‘species’ layer was also too general over large areas which led to highly heterogeneous node breaks after the first node. While species is important for fuel model classification, the available layer’s use in this project proved to grossly overpower equally important factors of fuel models, such as structural and biophysical attributes.

5.6.6 Unsupervised Classification

Validation Validation of the unsupervised classification output used a combination of RIP photos, known areas of fuel models, and IR imagery. FM1 was selected first due to the high signature grassy, open field presented in the output. Not everything in the FM1 class was fuel, since it included highways, water sources, and agricultural areas. FM2 had a tendency to line open areas and was almost a buffer between meadows and timber. FM2’s were differentiated from FM8’s and FM9’s due to the higher reflectance of IR radiation. FM2’s appeared ‘brighter’ on the IR imagery than either of the competing timber fuel models. A larger than expected number of areas were classified as FM5. While there are brush fields present in Lubrecht they are not as prolific as the classified output would suggest. The most likely cause of this is a large amount of regeneration which shares the same structure as brush. The FM5’s aren’t necessarily brush fields, but have the same ladder fuels and share the same structure. There is also a similar amount of live fuels present in the fuel bed which makes the fuel model RH dependent. The timber fuel models appear to have been most influenced by BE Intensity. FM8’s tended to have the highest intensity returns of the three, FM9’s were mid-range, and FM10’s reflected the least amount of radiation. This appears to be a function of mean canopy cover for the three classes as well (FM8 = 25.6%, FM9 = 53.4%, FM10 = 84.2%)

The intensities would make sense for the FM10 due to canopy interception of the pulse as it propagated through to the ground; a partial return pulse would register lower intensity. FM9 may return mid-range intensities due to height differences between dominant trees and regeneration. While the mature trees would define the stand as a timber fuel model, regeneration in the fuel bed would intercept the pulse, albeit for a shorter vertical range than FM10 might. FM8 is assumed to have sparse fuels on the ground and while canopy interception would still degrade intensity, canopy cover is generally more open, allowing pulses to complete the trip unhindered.

Selection of Attributes The attributes used for the unsupervised classification were initially the same as the CART analysis. The first output resembled a hillshade effect and was not unlike the LANDFIRE data. It became readily apparent that with more than one elevation feature in the mix, terrain quickly dominated the results. It was then decided to remove all elevation attributes and focus on LiDAR-derived canopy and vegetation layers. It would be interesting to include ecological layers in further research, which was the idea behind the elevation and distance-from-stream layers.

5.7 Project Summary

Quantifying and characterizing forest fuels will remain an elusive endeavor as long as variable and subjective qualification of both persists. In this project I explored the viability of measuring fuel loads and classifying the landscape using a remote sensing technique with mixed results. It is a promising branch of previous laser altimetry work and tested effective methods in a different forest type. While the current methods need to be re-tooled for fine scale analysis, they return products that can be used at a coarse scale for planning purposes. Future work with surface roughness and fuels will require sound field assessments that can reciprocate the fine scale nature of LiDAR data. Detailed field collections that are exhaustive and all-inclusive should be coupled with ground-based LiDAR at a fine scale and cross-referenced with airborne LiDAR data to explore the relationship between surface roughness and fuels. In my professional opinion, this would address the deficiencies identified in this study and provide a clearer picture of how LiDAR can be utilized by land managers to effectively measure the current fuel loads of a landscape.

Classifying fuels into pre-determined fuel models leaves a great deal of room for error. Even with picture-perfect structure and representation, parcels can only be assigned to a certain fuel model based upon the fire behavior exhibited while they burn. This is a reactive process. Fuel models are used to describe the most-likely fire behavior and most often, the potential worst-case scenario for any given area. Pro-active classification needs to allow for variability that cannot be captured in 13 fuel models, perhaps not even with 2500+ fuel models. Fuel models are defined by the main carrier of fire and are segregated into bins that represent rates of spread and flame lengths. Field experience will show that actual fire behavior will defy many of the best estimates. With this in mind, the efforts spent in classification are not wasted, and perhaps the best strategy for prevention is to assume a worst-case-scenario and plan accordingly. While fine scale fuel model classification cannot currently be done with a high degree of accuracy, coarse scale classification shows promise when correlated to independent land classifications. The high severity, project fire events that land managers spend the most time planning for are not determined at the 1/10th acre or even the 10-acre scale. These events are managed and executed at a landscape scale, a scale that some of these classification methods perform at. The classes presented in the Unsupervised Classification represent different structures and fuel loads that equate to some construct that when burned, will exhibit similar fire behavior. Assignment of fuel models to classes was an academic venture that can be replicated by a land manager using their professional experience and field collections to verify. In my opinion, the classes are valid and remain, they are structurally and characteristically different, despite the fuel model assignments and that is the accomplishment of this project. The accuracy of the fuel model assignments presented in this project may not be 100% accurate, but the same method of assignment using local knowledge of field conditions would allow a land manager to independently assess conditions using the same classes. The variable nature and distribution of the classes make them valuable for fire spread predictions at a planning level. They represent the best possible distinction from each other in a highly variable landscape. The expected fire behavior from a FM8 and FM9 are distinct, but do not greatly affect the outcome of an emerging project fire. The perimeter of such an event will be assessed at the landscape scale, and the findings of this project present a valuable contribution to planning for and dealing with such an event.

CHAPTER 6. BIBLIOGRAPHY

- Agee, J. 1993. *Fire Ecology of Pacific Northwest Forests*. Island Press: Washington, D.C.; 250.
- Albini, F. 1976. *Estimating Wildfire Behavior and Effects*. USDA Forest Service General Technical Report INT-30, 97.
- Andersen, H., R. McGaughey, and S. Reutebuch. 2005. Estimating Forest Canopy Fuel Parameters Using LiDAR Data. *Remote Sensing of Environment*. **94**(4): 441-449.
- Andersen, H., S. Reutebach, and G. Schreuder. 2001. Automated Individual Tree Measurement Through Morphological Analysis of a LiDAR-based Canopy Surface Model. *Proceedings of the First International Precision Forestry Symposium*: Seattle, 193.
- Anderson, H. 1982. *Aids to Determining Fuel Models for Estimating Fire Behavior*. USDA Forest Service General Technical Report INT-122, 28.
- Arno, S., and G. Gruell. 1986. Douglas-fir Encroachment into Mountain Grasslands in Southwestern Montana. *Journal of Range Management*. **39**(3): 272-276.
- Arno, Stephen F. 1980. Forest Fire History in the Northern Rockies. *Journal of Forestry*. **78**(8): 460.
- Arno, S., M. Harrington, C. Fiedler, and C. Carlson. 1995. Restoring Fire-Dependent Ponderosa Pine Forests in Western Montana. *Restoration and Management Notes*. **13**(1): 32-36.
- Arroyo, L., C. Pascual, and J. Manzanera. 2008. Fire Models and Methods to Map Fuel Types: The Role of Remote Sensing. *Forest Ecology and Management*: 1239-1252.
- Avery, E. 1967. *Forest Measurements*. McGraw-Hill: New York, NY, 480.
- Barnett, J. 1999. Longleaf Pine Ecosystem Restoration: The Role of Fire. *Journal of Sustainable Forestry*. **9**(1/2): 89-96.
- Bertolette, D., and D. Spotskey. 1999. Fuel Model and Forest Type Mapping for FARSITE. *Proceedings of the Joint Fire Science Conference and Workshop*: Boise.
- Bradshaw, L., J. Deeming, R. Burgan, and J. Cohen. *The 1978 National Fire-Danger Rating System: Technical Documentation*. USDA Forest Service General Technical Report, Intermountain Forest and Range Experiment Station, GTR-INT-169, 44.
- Breiman, L. 2001. Random Forests. *Machine Learning*. **45**(1): 5-32.
- Brown, J. 1971. A Planar Intersect Method for Sampling Fuel Volume and Surface Area. *Forest*

- Science*. **17**(7): 96-102.
- Brown, J., R. Oberheu, and C. Johnston. *Handbook for Inventorying Surface Fuels and Biomass in the Interior West*. USDA Forest Service General Technical Report INT-129, 52.
- Chen, Q. 2007. Airborne Lidar Data Processing and Information Extraction. *Photogrammetric Engineering and Remote Sensing*. **73**(2): 109-112.
- Chuvieco, E., and R. Congalton. 1989. Application of Remote Sensing and Geographic Information Systems to Forest Fire Hazard Mapping. *Remote Sensing of the Environment*. **29**: 147-159.
- Cohen, J. 2008. The Wildland-Urban Interface Fire Problem, A Consequence of the Fire Exclusion Paradigm. *Forest History Today*, 20-26.
- Covington, W., and M. Moore. 1994. Southwestern Ponderosa Forest Structure. *Journal of Forestry*. **92**(9): 39-47.
- De Wulf, R., R. Goossens, B. Deroover, and F. Borry. 1990. Extraction of Forest Stand Parameters from Panchromatic and Multispectral SPOT-1 Data. *International Journal of Remote Sensing*. **11**: 1571-1588.
- De'ath, G., and K. Fabricius. 2000. Classification and regression trees: A powerful yet simple technique for ecological data analysis. *Ecology*. **81**(11): 3178-3192.
- DeBano, L., D. Neary, and P. Ffolliott. 1998. *Fire's Effects on Ecosystems*. John Wiley & Sons: New York, NY, 319.
- Deeming, J., J. Lancaster, M. Fosberg, R. Furman, and M. Schroeder. 1972. *The National Fire Danger Rocky Mountain Rating System*. USDA Forest Service Research Paper RM-84.
- Deeming, J., and J. Brown. 1975. Fuel Models in the National Fire-Danger Rating System. *Journal of Forestry*. **73**(6): 4.
- Erdody, T., and M. Moskal. 2010. Fusion of LiDAR and Imagery for Estimating Forest Canopy Fuels. *Remote Sensing of Environment*. **114**(4): 725-737.
- Fiedler, C., T. DeLuca, M. Harrington, S. Mills, and D. Six. 2000. *A National Study of the Consequences of Fire*. Fire/Fire Surrogate Study Project: Missoula, MT.
- Haines, D. 1988. A Lower Atmosphere Severity Index for Wildland Fires. *National Weather Digest*. **13**(2): 23-27.
- Hall, M., E. Frank, G. Holmes, B. Pfahringer, P. Reutemann, and I. Witten. 2009. The WEKA Data Mining Software: An Update. *SIGKDD Explorations*. **11**(1):10-18.

- Hall, S., I. Burke, D. Box, M. Kaufmann, and J. Stoker. 2005. Estimating Stand Structure Using Discrete-return LiDAR: An Example from Low Density, Fire Prone Ponderosa Pine Forests. *Forest Ecology and Management*, 208: 189-209.
- Harbour, T. 2008. The Tie that Binds. *Remarks delivered by FAM Director Tom Harbour to the Congressional Fire Service Institute National Advisory Committee*. USDA Forest Service: Washington, D.C.
- Hornby, L. 1935. Fuel Type Mapping in Region One. *Journal of Forestry*. **33**: 67-72.
- Keane, R., R. Burgan, and J. van Wagtenonk. 2001. Mapping Wildland Fuel for Fire Management Across Multiple Scales: Integrating Remote Sensing, GIS, and Biophysical Modeling. *International Journal of Wildland Fire*. **10**: 301-319.
- Keane, R., and L. Dickinson. 2007. *Development and Evaluation of the Photoload Sampling Technique*. USDA Forest Service Research Paper RMRS-RP-61CD, 29.
- Kimbell, A., J. Caswell, M. Bomar, J. Gidner, and H. Hall. 2008. *2008 Direction to Leaders-Federal Fire and Aviation Programs*.
- Krasnow, K., T. Schoennagel, and T. Veblen. 2009. Forest fuel mapping and evaluation of LANDFIRE fuel maps in Boulder County, Colorado, USA. *Forest Ecology and Management*. **257**(7): 1603-1612.
- Lee, H. 1941. Aerial Photography: A Method for Fuel Type Mapping. *Journal of Forestry*. **39**: 531-533.
- Lefsky, M., W. Cohen, and T. Spies. 2001. An Evaluation of Alternate Remote Sensing Products for Forest Inventory, Monitoring, and Mapping of Douglas-fir Forests in Western Oregon. *Canadian Journal of Forest Research*. **31**(1): 78-87.
- Lillesand, T., and Kiefer. 2000. *Remote Sensing and Image Interpretation, 4th Edition*. John Wiley & Sons, Inc.: New York, NY, 736.
- Lund, H. 1969. Appraising and Mapping Fuels with Aerial Photographs. *Proceedings American Society of Photogrammetry and American Congress on Surveying and Mapping: Portland*.
- Lutes, D., and R. Keane. *Fuel Load (FL) Sampling Method*. 2006. USDA Forest Service General Technical Report, Rocky Mountain Research Station, 25.
- McGinn, T., P. Wyer, T. Newman, S. Keitz, R. Leipzig, and G. Guyatt. 2004. Tips for Learners of Evidence-based Medicine 3: Measures of Observer Variability (Kappa Statistic). *Canadian Medical Association Journal*. **171**(11): 1369-1373.
- Metlen, K., and C. Fiedler. 2006. Restoration treatment effects on the understory of ponderosa

- pine/Douglas-fir forests in western Montana, USA. *Forest Ecology and Management*. **222**(3): 355.
- Mutlu, M., S. Popescu, and K. Zhao. 2008. Sensitivity Analysis of Fire Behavior Modeling with LiDAR-derived Surface Fuel Maps. *Forest Ecology and Management*. **256**(3): 289-294.
- Mutlu, M., S. Popescu, C. Stripling, and T. Spencer. 2008. Mapping Surface Fuel Models Using LiDAR and Multispectral Data Fusion for Fire Behavior. *Remote Sensing of Environment*. **112**(1): 274-285.
- Nimlos, T. 1986. Soils of Lubrecht Experimental Forest. *Miscellaneous Publication No. 44*. Montana Forest and Conservation Experiment Station: Missoula, MT.
- North, M., M. Hurteau, J. Innes. 2009. Fire Suppression and Fuels Treatment Effect of Mixed-Conifer Carbon Stocks and Emissions. *Ecological Applications*. **19**(6): 1385-1396.
- Ottmar, R., D. Sandberg, C. Riccardi, and S. Prichard. 2007. An overview of the Fuel Characteristic Classification System-Quantifying, classifying, and creating fuelbeds for resource planning. *Canadian Journal of Forest Research*. **37**(12): 2383-2393.
- Popescu, S., R. Wynne, and R. Nelson. 2003. Measuring Individual Tree Crown Diameter with LiDAR and Assessing its Influence on Estimating Forest Volume and Biomass. *Canadian Journal of Remote Sensing*. **29**(5): 564-577.
- Pyne, S. 2002. *Year of the Fires: The Story of the Great Fires of 1910*. Penguin Publishing: New York, NY.
- Pyne, S., P. Andrews, R. Laven. 1996. *Introduction to Wildland Fire*. John Wiley & Sons. Inc.: New York, NY.
- Quinlan, J. 1993. *C4.5: Programs for Machine Learning*. Morgan Kaufmann Publishers Inc.: San Mateo, CA.
- Reinhardt, E., R. Keane, D. Calkin, and J. Cohen. 2008. Objectives and considerations for wildland fuel treatment in forested ecosystems of the interior western United States. *Forest Ecology and Management*. **256**(12): 1997-2006.
- Rempel, R., and A. Parker. 1964. *An information note on an airborne laser terrain profiler for micro-relief studies*. Proceedings from the 3rd. Symposium of Remote Sensing Environment, 321-337.
- Riano, D., E. Chuvieco, S. Condes, J. Gonzalez-Matesanz, and S. Ustin. 2004. Generation of Crown Bulk Density for *Pinus Sylvestris* L. from LiDAR. *Remote Sensing of Environment*. **92**(3): 345-352.
- Rollins, M. 2009. LANDFIRE: A Nationally Consistent Vegetation, Wildland Fire, and Fuel

- Assessment. *International Journal of Wildland Fire* (CSIRO). **18**: 235-249.
- Rothermel, R. 1972. *A Mathematical Model for Predicting Fire Spread in Wildland Fuels*. USDA Forest Service Research Paper INT-115, 50.
- Saatchi, S., K. Halligan, D. Despain, and R. Crabtree. 2007. Estimation of Forest Fuel Load From Radar Remote Sensing. *IEEE Transactions on Geoscience and Remote Sensing*. **45**(6): 1726-1740.
- Salas, F., and E. Chuvieco. 1995. Aplicacion de imagenes Landsat-TM a la cartografia de modelos de combustible." *Revista de Teledeteccion*. **5**: 18-28.
- Schmidt, K., J. Menakis, C. Hardy, W. Hann, and D. Bunnell. 2002. *Development of Coarse-Scale Spatial Data for Wildland Fire and Fuel Management*. USDA Forest Service General Technical Report RMRS-GTR-87, 50.
- Schroeder, M., and C. Buck. 1970. *Fire Weather...A Guide for Application of Meteorological Information to Forest Fire Control Operations*. US Forest Service: Washington, D.C.
- Scott, J., and R. Burgan. 2005. *Standard Fire Behavior Fuel Models: A Comprehensive Set for Use with Rothermel's Surface Fire Spread Model*. USDA Forest Service General Technical Report GTR-153, 72.
- Seielstad, C. and L. Queen. 2003. Using airborne laser altimetry to determine fuel models for estimating fire behavior. *Journal of Forestry*. **101**(4): 10-15.
- Shasby, M., R. Burgan, and R. Johnson. 1981. Broad Area Forest Fuels and Topography Mapping Using Digital Landsat and Terrain Data. *Proceedings of the Seventh International Symposium Machine Processing of Remotely Sensed Data*. West Lafayette: Purdue University, 529-538.
- Sikkink, P., and R. Keane. 2008. A comparison of five sampling techniques to estimate surface fuel loading in montane forests. *International Journal of Wildland Fire*. **17**(3): 363-379.
- TerraSolid. 2005. TerraScan User's Guide, 169.
- University of Montana. Updated 2003. *Lubrecht Experimental Forest*. <<http://www.cfc.umt.edu/Lubrecht/History/history.htm>> Accessed September 2008.
- US Forest Service. 2010. *US Forest Service Fiscal Year 2010 President's Budget Overview*.
- USDA Forest Service. *Full Job Description-Assistant Fire Management Officer, GS-0401-09*. <<https://www.avuedigitalservices.com>> Accessed March 2009.

van Wagtendonk, J., and R. Root. 2003. The Use of Multitemporal Landsat Normalized Difference Vegetation Index (NDVI) Data for Mapping Fuels Models in Yosemite National Park, USA. *International Journal of Remote Sensing*. **24**: 1639-1651.

Waring, R., and S. Running. 1998. *Forest Ecosystems; Analysis at Multiple Scales*. Academic Press: San Diego, CA.

Westerling, A., H. Hidalgo, D. Cayan, and T. Swetnam. 2006. Warming and Earlier Spring Increase Western U.S. Forest Wildfire Activity. *Science*. **313**(5789): 940-943.

Whiteman, D. 2000. *Mountain Meteorology: fundamentals and applications*. Oxford University Press: New York, NY, 355.